# Hydrodynamics for the integration of fermentation and separation in the production of diesel and jet biofuels

Sousa Pires da Costa Basto, R.M.

**DOI**
10.4233/uuid:2dd874e6-bb94-4e3d-848d-3b54a0bc856a

**Publication date**
2024

**Document Version**
Final published version

**Citation (APA)**
Sousa Pires da Costa Basto, R. M. (2024). *Hydrodynamics for the integration of fermentation and separation in the production of diesel and jet biofuels*. [Dissertation (TU Delft), Delft University of Technology]. https://doi.org/10.4233/uuid:2dd874e6-bb94-4e3d-848d-3b54a0bc856a

**Important note**
To cite this publication, please use the final published version (if applicable).
Please check the document version above.

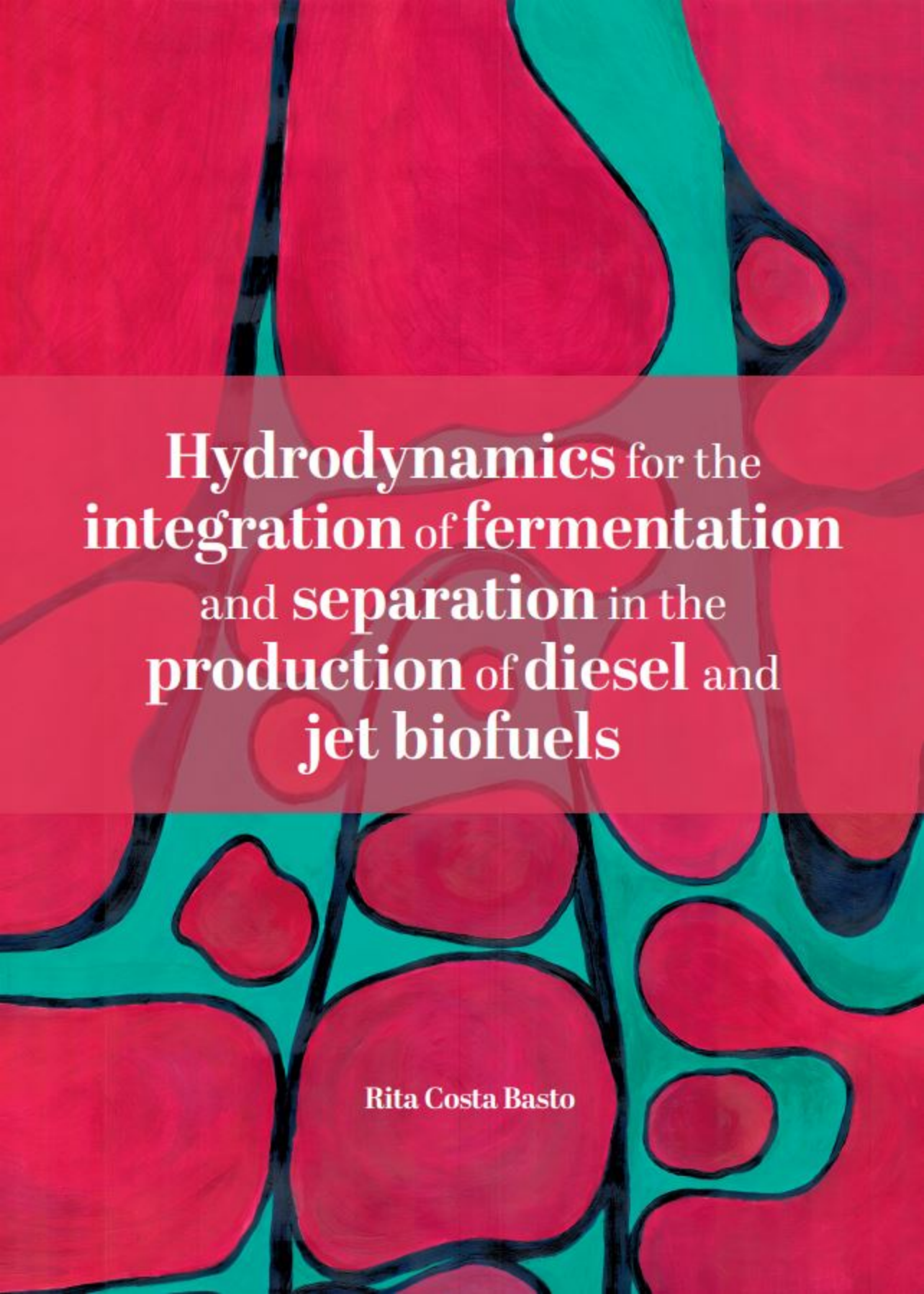

# Hydrodynamics for the integration of fermentation and separation in the production of diesel and jet biofuels

Rita Costa Basto

# Hydrodynamics for the integration of fermentation and separation in the production of diesel and jet biofuels

Dissertation

for the purpose of obtaining the degree of doctor
at Delft University of Technology
by the authority of the Rector Magnificus, prof.dr.ir. T.H.J.J. van der Hagen
chair of the Board of Doctorates
to be defended publicly on
Thursday, 11 January 2024 at 10 o'clock

by

Rita Maria SOUSA PIRES DA COSTA BASTO

Professional doctorate in Bioprocess Engineering.
Delft University of Technology, the Netherlands

Born in Lisbon, Portugal

This dissertation has been approved by the promotors.

Composition of the doctoral committee:

| | |
|---|---|
| Rector Magnificus | Chairperson |
| Prof. dr. ir. L.A.M. van der Wielen | Delft University of Technology, promotor |
| Prof. dr. ir. R.F. Mudde | Delft University of Technology, promotor |

Independent members:

| | |
|---|---|
| Prof. Dr. M.R.M.S. Aires Barros | Instituto Superior Técnico, Portugal |
| Dr. Ir. A.J.J. Straathof | Delft University of Technology, NL |
| Prof. Dr. H.J. Noorman | Delft University of Technology / DSM, NL |
| Prof.dr.ir. J.T.F. Keurentjes | University of Twente, NL |
| Prof.dr.P. Osseweijer | Delft University of Technology, NL, reserve member |

Other Members

| | |
|---|---|
| Dr. Ir. A. Oudshoorn | Delft Advanced Biorenewables BV, NL |

The research described in this thesis was performed at the Bioprocess Engineering Group, Department of Biotechnology, Faculty of Applied Sciences, Delft University of Technology, the Netherlands.

This work was carried out within the BE-Basic R&D Program, which was granted a FES subsidy as well as a TKI-BBE grant (TKI-AMBIC-program TKIBE-01003) from the Dutch Ministry of Economic affairs.

Cover design by: Maria João Proença and Ridderprint BV

Printed by: Ridderprint BV | www.ridderprint.nl
An electronic version of this dissertation is available at
http://repository.tudelft.nl/.

ISBN 978-94-6483-631-8

“Deus quer, o homem sonha, a obra nasce.”

*“God wills, Man dreams, the work is born.”*

*“Mensagem”,* Fernando Pessoa, 1934

This thesis is dedicated to my Father (my compass) and my Mother (my bright star).

# Summary

Over the years, various technologies have been developed to produce and separate advanced biomolecules. These technologies range from complex terpenoids for pharmaceuticals and flavors to commodity chemicals and fuels via the fermentative route. These compounds are often poorly water soluble, phase splitting organic compounds or inhibitory and unstable necessitating addition of an extractive, second liquid phase for product removal. The turbulent conditions in the multiphasic fermentation coupled with the presence of surface-active compounds in the medium create a stable emulsion that is difficult to separate in conventional systems. Technologies such as centrifugation and de-emulsifiers have been used to separate the emulsion and recover the product. However, these type of recovery processes are expensive, drastically increase the final product's environmental footprint and often hamper cell recycling.

Delft Univesity of Technology, in collaboration with the start-up company Delft Advanced Biorenewables (DAB bv), started the Delft Integrated Recovery Column (DIRC) project. This project aimed to leverage the immiscibility of the second liquid phase, i.e. the phase splitting product or external extractant (both labeled as "oil"), to enable in-situ product recovery, cell re-use, and reduce downstream processing steps. The Fermentation And Separation Technology (FAST) integrated bioreactor was developed during the course of this project.

The FAST integrated bioreactor has two main compartments: fermentation compartment – where the "oil" phase is produced and excreted (or added as extractant) to the liquid media, and a separation compartment – where the "oil" phase is recovered as a single phase. The broth significantly depleted from "oil" flows back from the separation compartment to the fermentation compartment via external tubing.

At the start of this research, the pilot FAST integrated bioreactor was under construction at 100 L scale. Then, quantitative insights for further scale-up and "oil" recovery optimization were limited. The FAST integrated reactor encompasses four different phases (gas, liquid medium, "oil" phase, and cells) and has different zones, each with distinct functionalities and requirements that present challenges for the future design and scale-up of this technology.

The primary aim of this thesis is to investigate effective scale-up strategies for the integrated reactor and elucidate the relation between its design features and functionalities to recover and optimize the phase separating products.

To separate the “oil” phase from emulsions in the separation compartment without harming the cells, a method was developed within the DIRC project to use gas bubble/”oil” phase interactions. In Chapter 2 of this thesis, a mathematical model is proposed to describe “oil” phase coalescence due to gas bubbles in a region of high “oil” droplet concentration. “Oil” phase optimization was studied at laboratory scale using a model emulsion. At lab scale, combinations of unfavourable interfacial tension, oil fraction and viscosity of broth lead to poor “oil” recoveries. However, our mathematical model indicated scenarios in which oil recovery exceeded 90% by increasing the surface area to volume ratio of the separation compartment, and thus increasing the “oil” fraction.

The next step was to quantify the impact of adding flocculants using various separation techniques to promote “oil” separation from the emulsion (Chapter 3). Two different flocculants were identified as most promising: $CaCl_2$ and $(NH_4)_2SO_4$. Their time and quantity of addition to the fermentation broth were evaluated against three oil recovery methods: gravity settling, gas enhanced oil recovery (GEOR) and centrifugation. It was observed that flocculants could destabilized all emulsions to promote “oil” coalescence. A 3-fold increase in “oil” recovery and creaming rate was observed when using low concentrations (75 mM) of $(NH_4)_2SO_4$ with GEOR, without altering overall fermentation performance. Addition of $CaCl_2$ was observed to improve “oil” recovery by centrifugation. However, the timing and amount of flocculant addition were critical to maintain fermentation performance and oil recovery. This creates new insights and possibilities for optimizing oil recovery, not only using the integrated FAST bioreactor but also conventional separation methods.

In Chapter 4 of this thesis, experiments were performed to analyse the performance of a pilot scale 100 L integrated FAST bioreactor. Two different systems were selected: dodecane recovery as overlay (extractant) phase in a sesquiterpene-producing *E. coli* fermentation and Oleyl alcohol recovery in butanol producing *Clostridia* fermentation. In the experimental studies at pilot scale, it was investigated how the integrated FAST bioreactor separation performance depends on the oil properties and elements of FAST bioreactor system hydrodynamics (Figure 1 depicts how oil

is separated in the FAST bioreactor). Therefore, theoretical hydrodynamic studies using computational fluid dynamics (CFD) were conducted on the 100 L integrated FAST bioreactor by evaluating geometry and operation conditions of the "oil"/broth separation section. This study allows to better understand and quantify the trends within the integrated reactor and provide guidance on how the integrated FAST design characteristics and liquid recirculation could influence the "oil" separation at larger scale.

In brief, results indicated that FAST "oil" recovery systems with Reynolds numbers (Re) in the recirculation section of the separation compartment exceeding 250, create excessively turbulent flows that negatively impact "oil" separation and cell recirculation. Moreover, steeper angles of the separation compartment will create swirls of the multiphase mixture throughout the separation compartment. To optimize oil separation during scale-up, a geometrical design (and matching operational conditions) that minimizes the distance between the recirculation zone and separation compartment (depicted by "↑" in Figure 1), while maintaining low turbulence and swirls in the recirculation zone, will be preferred.

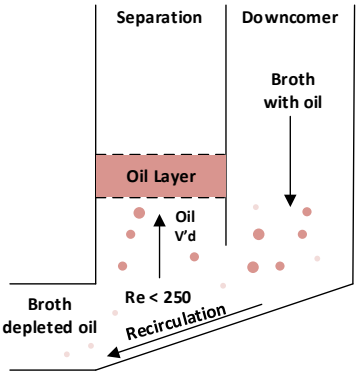


**Figure 1 -** Infographic of the oil separation in the 100 L pilot integrated FAST bioreactor. Red circles represent the "oil", where darker red represent the droplets that separate and lighter red the droplets that recirculate back to the fermentation compartment.

In conclusion, as described in Chapter 5, the data gathered during this research project provided critical insights to guide the design and scale-up of integrated bioreactors. Although more work is needed toward actual implementation of large-scale FAST reactors, we have demonstrated critical relations between droplet sizes, oil fraction and recirculation flow for the (efficient) separation of "oil" from emulsions. The use of different methods, such as GEOR and flocculant

addition, can be incorporated into large scale integrated FAST bioreactors to enhance and optimize oil recovery while maintaining suitable conditions for viable cell recirculation.

This work, while requiring further analysis and demonstration, highlights the potential of the integrated FAST bioreactor as a cost-effective and scalable solution for manufacturing and recovering phase-separating products across a diverse range of application.

# Samenvatting

Al jaren lang is er een immer aanhoudende doorontwikkeling op diverse technologieën voor het produceren en scheiden van geavanceerde biologische moleculen. Deze biologische moleculen worden vervaardigd door middel van een fermentatie proces; hieronder vallen zowel hoogwaardige varianten zoals terpenoïden die gebruikt worden in medicatie en smaakstoffen, als ook de minder complexe varianten zoals gebruikt in chemicaliën en brandstoffen. Deze moleculen zijn vaak fase splitsende organische stoffen en slecht oplosbaar in water, of remmend en onstabiel waardoor een organische fase toegevoegd moet worden tijdens de fermentatie. De tubulente condities in de fermentor samen met de oppervlakte actieve stoffen in het medium vormen een een stabiele emulsie die in conventionele systemen moeilijk te scheiden is. Technologien zoals centrifugeren en de-emulsificeren worden gebruikt om de emulsie te scheiden en het product te winnen. Dit soort opwerkingsprocessen zijn echter kostbaar, milieubelastend en vaak belemmerend voor het terugwinnen van de celcultuur.

De Technische Universiteit Delft (TU Delft) heeft in samenwerking met het bedrijf 'Delft Advanced Biorenewables' (DAB bv) het 'Delft Integrated Recovery Column' (DIRC) project opgestart. Dit project had als doel het scheidend vermogen van de tweede vloeibare fase (i.e. het fase scheidend product of de toegevoegde organische fase, beide gerefereerd als "olie") te bevorderen om in-situ product winning, hergebruik van cellen en reductie van processtappen mogelijk te maken. De "Fermentation And Seperation Technologie (FAST)" geïntegreerde bioreactor is tijdens dit project onwikkeld.

De FAST geïntegreerde reactor heeft twee compartimenten. Een fermentatie deel waar olie geproduceerd en uitgescheiden wordt in het vloeibare medium (of waar olie toegevoed wordt als extractie middel), en een scheidings compartiment waar de olie gewonnen wordt. Het van olie uitgeputte beslag wordt gerecirculeerd van het scheidings compartiment naar het fermentatie compartiment via een externe slang verbinding.
Aan het begin van deze onderzoek was het eerste 100L prototype FAST geintegreerde reactor nog in verbouwing, en quantitatieve inzichten voor de opschaling en optimalisatie van de olie winning waren gelimiteerd. De FAST reactor bevat vier fases: (de gas fase, het vloeibare medium, de olie (met het product) en als laatste de celcultuur. Hiernaast bevat de FAST reactor meerdere

zones, ieder met specifieke eigenschappen en eisen die vertalen zich in uitdagingen voor het ontwerp en opschaling van de technolgie. Het belangrijkste doel van dit proefschrift is om kennis te genereren over hoe de reactor opgeschaald moet worden, en een goed begrip te vormen over hoe de fases behandeld dienen te worden om maximale efficiëntie met de reactor te bereiken bij het winnen van zich in fases opdelende producten.

Om in het scheidingsdeel de olie fase van de emulsie te scheiden, zonder hierbij de cellen te beschadigen, is binnen het DIRC project een methode ontwikkeld die gebruik maakt van gas bel/olie fase interacties. In hoofdstuk 2 van dit proefschrift is een wiskundig model ontwikkeld dat olie fase coalecentie door gas bellen in een gebied met hoge concentratie olie druppels beschrijft. Olie fase optimalisatie was bestudeerd op labschaal met een model emulsie. Op labschaal leidde combinaties van ongunstige oppervlaktespanning, olie fractie en viscositeit van het beslag tot matige olie winning. Echter, ons wiskundige model liet door aanpassingen in de oppervlak tot volume ratio van het scheidings compartiment scenarios zien met een olie rendement van meer dan 90 %.

De volgende stap was om te bepalen wat de invloed is van het gebruik van flocculant om de olie winning uit de emulsie verder te bevorderen (hoofdstuk 3). De flocculanten $CaCl_2$ en $(NH_4)_2SO_4$ zijn hierin het meest geschikt bevonden. Het effect van toediening op varierende fermentatie tijdstippen en in verschillende hoeveelheden was getest op drie olie scheidingsmethodes: zwaartekrachts-scheiding, gas gedreven olie winning, en centrifugatie. Het bleek dat het gebruik van flocculanten alle emulsies kon destbiliseren en zo het olie coalecentie kon bevorderen.
Scheiding kon tot driemaal zo effectief gemaakt worden met toediening van een lage concentratie (75 mM) aan $(NH_4)_2SO_4$ voor de gas gedreven scheiding zonder de fermentatieprestaties te veranderen. Toevoeging van $CaCl_2$ bevorderde de olie winning door centrifugatie. Echter, het tijdstip van toevoeging en de hoeveelheid flocculant waren bepalend om de fermentatie en olie winning op pijl te houden. Deze inzichten kunnen gebruikt worden om olie scheiding verder te optimaliseren, zowel in de FAST reactor als ook in de meer conventionele scheidings technieken.

Hoofdstuk vier van dit proefschrift beschrijft de experimenten die gedaan zijn op de 100L prototype FAST reactor. Hiervoor zijn twee verschillende cel cultures gebruikt waar twee

verschillende organische fasen zijn toegevoegd voor product extractie: een sesquiterpene producerende *E. coli* cel cultuur met dodecaan toegevoeging, en een butanol producerende Clostridia cel cultuur met oleyl alcohol toegevoeging. Met de experimenten op de 100L prototype werd bestudeerd hoe de mate van succes in de scheiding die behaald kon werd beïnvloed door de eigenschappen van de olie en hydrodynamica van de FAST reactor (Figuur 1 laat zien hoe olie wordt gescheiden in de FAST bioreactor). Ernaast werd een hydrodynamische studie uitgevoerd door middel van Computational Fluid Dynamics (CFD) waar de geometrie en proces condities van de scheidingsdeel werden geëvalueerd. Deze studie voordeert het begrijpen en quantificieren van de tendens binnen de reactor, en geeft richtlijnen over hoe het ontwerp en vloeistof recirculatie binnen een FAST reactor de olie scheiding op grotere schaal zou kunnen beinvloeden. In het kort, resultaten gaven aan dat een FAST olie winnings systeem, met Reynolds numbers (Re) in het reciculerings deel van het scheidings compartiment boven de 250, ervoor zorgenden dat er turbulente vloeistofstromen ontstaan met een negatieve uitwerking op de olie scheiding en cel recirculatie. Daarnaast, een grotere hellingshoek in het scheidings compartiment zorgt voor wervelingen door het gehele scheidings compartiment. Bij het opschalen van de reactor is het om die reden belangrijk dat de geometrie van de reactor en de daarbij bij behorende proces condities tot een verkorte afstand tussen de olie druppels en het scheidingsdeel (Weergegeven met "↾" in Figuur 1), en tot weinig recirculatie wervelingen leiden om zo de olie scheiding te optimaliseren.

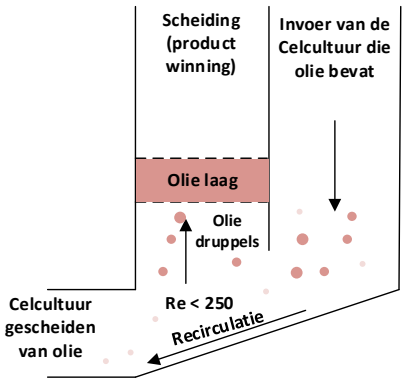


**Figure 1 -** Schematische weergave van het olie scheidings deel van de 100L pilot integrated FAST reactor. De olie druppels zijn weergegeven als rode cirkels. Hierbij zijn de de donker gekleurde en grotere druppels de gene die succesvol gescheiden zijn. De kleinere licht rood weergegeven druppels zijn niet succesvol gescheiden en gaan samen met de celcultuur terug naar het fermentatie deel van de reactor.

Concluderend, de data die vergaard is tijdens dit onderzoek geeft een essentieel inzicht over hoe de geïntegreerde FAST reactor ontworpen en opgeschaald kan worden. Dit is verder uitgewerkt in hoofdstuk 5. Ondanks dat er meer werk nodig is om tot werkelijke implementatie van FAST reactors op grote schaal over te gaan zijn de belangrijkste relaties tussen de grote van olie druppels, de olie fractie en de recirculatie snelheid die leiden tot een efficiente olie scheiding uit emulsies vastgelegd. Daarnaast kunnen de verkregen inzichten in methoden zoals GEOR en flocculant toevoeging gebruikt worden op grote schaal FAST bioreactors om de olie winning te optimaliseren zonder de condities om de cel cultuur gezond te houden negatief te beïnvloeden.

Dit werk, al hoewel nog niet volledig uit geanalyseerd en bewezen, onderstreept dat de geïntegreerde FAST reactor als concept technisch haalbaar is, en een interessant alternatief is dat tegen lage kosten ingezet kan worden voor een breed scala aan toepassingen. Zowel in de productie van hoogwaardige bio chemicaliën op kleine schaal als voor productie op grote schaal zoals die van biologische brandstof of chemische verbindingen.

# Sumário

Ao longo dos anos, várias tecnologias foram desenvolvidas para produzir, através da via fermentativa, e separar biomoléculas, que variam desde terpenóides complexos para uso em fármacos e aromatizantes até produtos químicos de uso comum e biocombustíveis. Estes compostos são frequentemente pouco solúveis em água, são compostos orgânicos que se separam em fases ou são inibitórios e instáveis, sendo necessário por vezes a adição de uma fase líquida extrativa secundária para a remoção do produto. As condições turbulentas na fermentação multifásica, juntamente com a presença de agentes ativos de superfície (surfactantes), criam uma emulsão estável que é difícil de separar nos sistemas convencionais. Tecnologias como a centrifugação e adição de agentes para destabilizar a emulsão têm sido utilizadas para separar a emulsão e recuperar o produto. No entanto, este tipo de processos de recuperação são dispendiosos, aumentam drasticamente a pegada ambiental do produto final e frequentemente dificultam o re-uso das células.

A Universidade Técnica de Delft, em colaboração com a *startup* Delft Advanced Biorenewables (DAB) BV, deu início ao projeto Delft Integrated Recovery Column (DIRC). Este projeto tinha como objetivo aproveitar as características imísciveis da segunda fase líquida (produto) ou do agente de extração externo (ambos designados como "óleo") para permitir a recuperação *in situ*, reutilização celular e potencialmente reduzir a quantidade de etapas do processo de separação do produto. Foi então assim concebido o bioreactor integrado de Fermentação e Tecnologia de Separação (The Fermentation And Separation Technology integrated bioreactor - FAST).
O bioreactor integrado FAST possui duas secções principais: a secção de Fermentação - onde o "óleo" é produzido e excretado (ou adicionado como agente de extração externo) no meio de cultivo; e a secção de Separação – onde o "óleo" é separado e recuperado como uma fase única. O meio de cultivo proveniente da fermentação e significativamente esgotado de "óleo" é recirculado da secção de separação de volta para a secção de fermentação através de tubagens externas.

No início desta pesquisa, o bioreator integrado FAST encontrava-se em construção em escala piloto e tinha o volume de 100 litros. Nessa altura, o conhecimento para dimensionar o reactor

em grande escala (*scale-up*) e otimizar a recuperação do "óleo" era limitado. O reactor integrado FAST engloba quatro fases diferentes (gás, meio de cultivo líquido, "óleo" e células) e diferentes zonas, cada uma com funcionalidades distintas e características específicas, que apresentam desafios para o *scale-up* desta tecnologia.
Portanto, o objetivo principal desta tese é compreender como realizar o *scale-up* deste tipo de reactores integrados e obter mais informações sobre as funcionalidades principais do reactor e a sua conexão com o design de forma a otimizar a recuperação do "óleo".

Um método foi desenvolvido no âmbito do projeto DIRC que utiliza interações entre bolhas de gás e a fase "oleosa" para separar o "óleo" de emulsões na secção de separação sem prejudicar as células. No Capítulo 2 desta tese é proposto um modelo matemático para descrever a coalescência da fase "oleosa" usando bolhas de gás numa região de elevada concentração de gotas de óleo. A otimização da separação da fase "oleosa" foi estudada em escala laboratorial para uma emulsão química que imita a emulsão criada durante a fermentação. A nível laboratorial, combinações de tensão interfacial desfavorável em conjugação com a fração de óleo e viscosidade da fermentação resultaram em baixas separações de óleo. No entanto, o modelo matemático indicou cenários nos quais a separação de óleo excedeu os 90% se se aumentar a relação área superficial/volume da secção de separação, e consequentemente, aumentando a fração de "óleo" nessa zona.

O próximo passo foi quantificar o impacto da adição de floculantes combinadas com várias técnicas de separação para promover a separação do "óleo" da emulsão (Capítulo 3). Dois tipos de floculantes foram identificados como os mais promissores: $CaCl_2$ e $(NH_4)_2SO_4$. O tempo e a quantidade de adição no meio de cultivo da fermentação foram avaliados em relação a três métodos de separação de "óleo": separação por gravidade, separação usando bolhas de gás (GEOR) e centrifugação. Observou-se que os floculantes podem desestabilizar todas as emulsões e promovem a coalescência do "óleo". Um aumento de 3 vezes na separação de "óleo" e na taxa de formação de *creaming* foi observado ao usar baixas concentrações (75 mM) de $(NH_4)_2SO_4$ e o método de separação GEOR, sem alterar o desempenho geral da fermentação. A adição de $CaCl_2$ promoveu a separação de "óleo" por centrifugação. No entanto, o tempo e a quantidade em que o floculante foi adicionado foram críticos para manter o desempenho da fermentação e a separação de "óleo". Esta pesquisa cria novos conhecimentos e possibilidades para otimizar a

separação de "óleo", não apenas ao usar o bioreator FAST integrado, mas também ao usar outros métodos de separação convencionais.

No Capítulo 4 desta tese são referidas experiências que foram realizadas para analisar o desempenho do reactor integrado FAST em escala piloto de 100 litros. Dois sistemas diferentes foram seleccionados: a separação de dodecano usado como fase extra (extratante) na fermentação de *E. coli* para produção de sesquiterpenos; e a separação de álcool oleílico na fermentação de *Clostridia* para produção de butanol. Os estudos experimentais em escala piloto investigaram como o desempenho de separação do bioreator integrado FAST depende não só das propriedades do "óleo" mas também da hidrodinâmica do sistema FAST (Figura 1 demonstra a separação de "óleo" no bioreator FAST). Estudos hidrodinâmicos teóricos foram conduzidos utilizando Fluidodinâmica computacional (CFD) usando a geometria do reactor integrado FAST de 100 litros e as condições de operação para a separação de "óleo"/meio de cultivo.

Este estudo permite compreender e quantificar melhor as tendências dentro do reator integrado e fornecer orientações sobre como as características geométricas do reactor integrado FAST e as condições de recirculação do líquido podem influenciar a separação de "óleo" em grande escala. Os resultados indicam que sistemas em que o número de Reynolds (Re) na zona de recirculação do reactor FAST que sejam superiores a 250, criam fluxos excessivamente turbulentos que impactam negativamente a separação do "óleo" e a recirculação celular. Além disso, ângulos mais íngremes na secção de separação criam redemoinhos da mistura multifásica ao longo dessa secção. Portanto, ao fazer o *scale-up* do bioreactor FAST, um design geométrico (e condições operacionais correspondentes) que reduza a distância das gotas entre a zona de recirculação e a zona de separação e onde os redemoinhos de recirculação são minimizados são as condições ideais para otimizar a separação do "óleo".

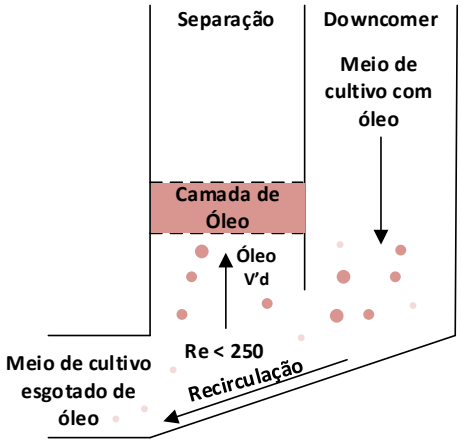


**Figura 1 –** Infográfico da separação do "óleo" no bioreactor integrado FAST em escala piloto de 100 L. Gotas encarnadas são o "óleo", onde as encarnadas escuras são as gotas que são separadas e as encarnadas claras as gotas de "óleo" que são recicladas de volta a secção de fermentação.

Em conclusão: Como descrito no Capítulo 5, os dados colectados durante esta pesquisa cientifica forneceram entendimentos críticos para orientar *scale-up* de biorreatores integrados. Embora a continuação da pesquisa seja necessário para a implementação real de reactores FAST em grande escala, esta tese procura demonstrar relações críticas entre tamanho das gotas, frações de óleo e fluxo de recirculação para a separação (eficiente) de "óleo" das emulsões. A utilização de diferentes métodos, como GEOR e adição de floculantes, pode ser incorporada em biorreatores integrados FAST em grande escala para melhorar e optimizar a recuperação de óleo, mantendo condições realistas para a recirculação viável das células.

Sem olvidarmos que o assunto merece mais aprofundada analise, cremos que este trabalho mostra que o conceito do biorreator integrado FAST é uma alternativa tecnologicamente viável e de baixo custo para a fabricação e recuperação integradas de componentes de separação de fases, com uma ampla aplicabilidade, que varia desde produtos bioquímicos de alto valor adicionado de pequeno volume, até produtos de grande volume, como componentes de biocombustíveis e blocos químicos.

# Table of Contents

# Chapter 1: General introduction

## 1.1 Background and social motivation

The use of fossil resources as crude oil, coal and natural gas in modern society is of increasing concern in the past decade. Increasing global warming, oil spills in ocean's killing millions of animal species and increase of pollution leading to an increase in population illness are examples of how the use of fossil resources have a negative impact in the world. New technologies have been investigated to try reducing or even eliminate the use of these resources (Mainar Causape, Philippidis and European Commission. Joint Research Centre., no date; Cuellar, Heijnen and L. A. M. van der Wielen, 2013; P, 2019). Biobased fuels, chemical building blocks and materials, and high added value specialties as flavors and fragrances are being introduced in the market due to their lower environmental impact. A growing portfolio of biobased fuels (ethanol, biodiesel), chemical building blocks (lactic acid, succinic acid, FDCA, long chain di-carboxylic acids in coatings), and specialty products (amino acids, peptides) are already being produced competitively at commercial scale (Kenneth, 2007; IEA (2021), 2021). They are all well soluble in aqueous solution and are effectively recovered and purified by well-established molecular separation processes.

This is not the case for a growing group of hydrophobic microbial products such as sesquiterpenes (Jackson, Hart-Wells and Matsuda, 2003; Cuellar, Heijnen and L. A. M. van der Wielen, 2013), carotene (van Hee *et al.*, 2006) and long chain polysaturated fatty acids (LC-PUFAs) by fermentation. Farnesene is an example of a sesquiterpene that is already being produced at commercial scale (Lane, 2013), (Warner and Schwab, 2017). This compound is certified for implementation into jet fuel blends up to 10% after hydrogenation to farnesane (Total and Amyris renewable jet fuel ready for use in commercial aviation, 2014), and can be directly used without engine modifications (U.S. Department of Energy - Energy Efficiency and Renewable Energ, 2023). This group of molecular compounds is characterized by phase separation in aqueous solutions due to their hydrophobicity, leading to phase separation as a liquid ('oil') or solid in fermentation broth. Efficient separation of the oily or particulate phase from multiphase mixtures is critical for technological feasibility as well as for reduction of capital and operational costs. Improving process technology for the efficient separation and recovery of the 'oil' or particulate phase from the multiphasic mixture has received significantly less attention than strain development(Cuellar and van der Wielen, 2015; Cuellar and Straathof, 2020). A similar technological challenge is found where water immiscible solvents are added to the fermenter as

second phase for product extraction (Chandran, Kealey and Reeves, 2011; Pedraza-de la Cuesta et al., 2017).

Due to their immiscible properties, liquid-liquid phase split, and selective mechanical separation of the light oily phase would create an easy opportunity for product separation. However, the high mixing in the fermenter together with surface active compounds in the medium, which stabilize the oil/water interface (Heeres et al., 2014), creates an emulsion hampering product separation and recovery.

Several techniques have been already tested and used in different industries (e.g.: chemical, waste treatment, flavour and fragrances) to recover 'oils' from multiphasic mixtures, namely centrifugation, flotation, hydrocyclones and membranes (Cheryan and Rajagopalan, 1998; Fakhru'l-Razi et al., 2009; Behin and Bahrami, 2012; Tabur and Dorin, 2012; Velasco, 2014). However, these techniques add to the capital costs and may require the addition of chemicals during the process leading to a higher environmental impact (Figure 1).

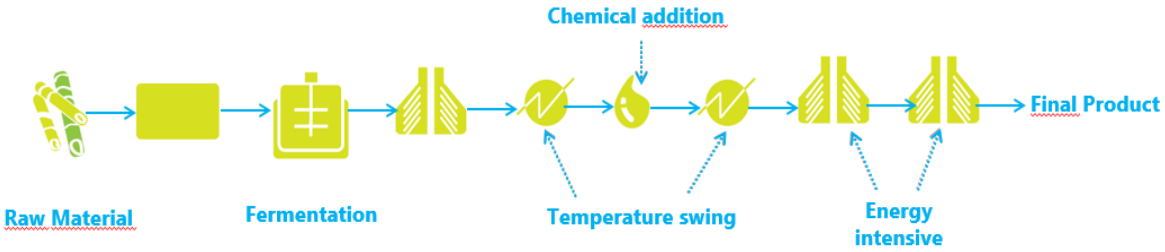


**Figure 1 –** Simplified block scheme, adapted from(Pedraza de la Cuesta, 2019), of the large-scale microbial production process of farnesene based on surfactant addition, temperature change and centrifugal separation (Cuellar and Straathof, 2018).

## 1.2 Integrated Fermentation Accelerated by Separation Technology (FAST) bioreactor

Integration of fermentation and separation of the oil has in one step, been demonstrated to potentially reduce investment costs and environmental impact (Figure 2) (Heeres et al., 2015). The integration of the two processes in one step will also enable cell reuse and continuous product recovery. Compartment integration have been used in processes that require two different conditions and low-cost technologies, such as waste-water treatment processes (e.g.: BASE reactor; Circox reactor; A/O biofilm reactor; airlift loop SBBR) (Heijnen et al., 1990; van

Benthum et al., 1999), or production of biogas from wastewater (DANA - Aqwise) (Integrated Water & Wastewater Treatment Solutions, 2010).

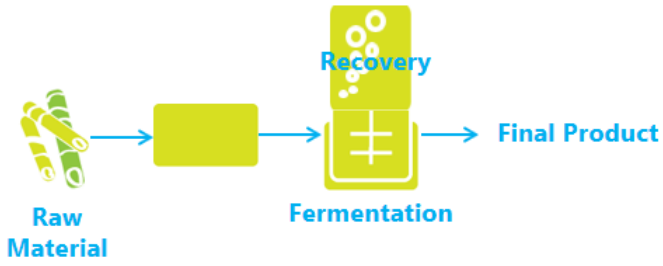


**Figure 2 –** Block scheme of the large-scale microbial production process if integrated reactor was used.

Heeres *et al*. (Heeres, 2016)developed a process using gas flows at relatively low superficial gas velocity to induce coalescence of oil droplets from aqueous systems leading to a continuous oil layer. For integration purposes, this method is beneficial since it uses mild conditions compatible with fermentation conditions, that does not need addition of chemicals potentially toxic for the cells and allows continuous product recovery. This method has already been tested during fermentations by means of an external loop where it was observed that it did not reduce cell growth, and cell viability while separating the oil. It was also observed that recirculating fermentation broth through the column increased the extracellular protein created undesired stable emulsions (Keijzers, 2016; Steinbusch, 2016).

Based on this early work, the integrated Fermentation Accelerated by Separation Technology (FAST) (DAB BV, no date; Oudshoorn et al., 2021) was developed by TU Delft spin-out DAB BV. FAST bioreactor is an integrated reactor that combines the two compartments (fermentation compartment and bespoke separation compartment), each working at different conditions (Figure 3). In the fermentation compartment, the cells produce the hydrocarbon that is excreted to the medium creating an emulsion. In the separation compartment, gas bubbles break the emulsion and form a continuous oil layer during which cells are recycled back to the fermentation compartment (Heeres et al., 2014; Heeres, 2016). Besides, a second phase can be continuously added to the reactor at the same rate as the oil production to facilitate coalescence of smaller droplets and oil separation.

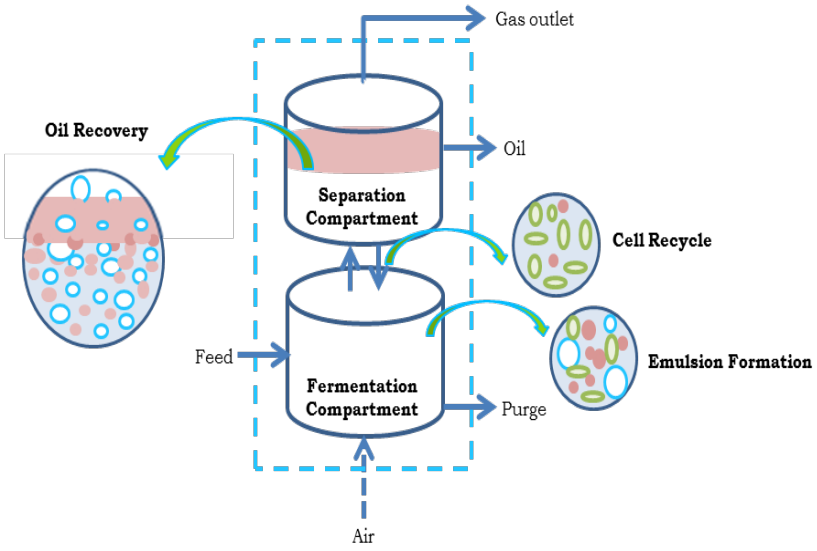


**Figure 3 –** Schematic of FAST bioreactor for the production, separation, and recovery of a clear oil layer (pink colour) with highlights on its main functionalities oil production, separation recovery and cell recycle (gas bubbles – white circles, cells – green circles, and oil droplets – pink circles).

## 1.3 A model-based approach for design and guide the scaling up of an integrated FAST bioreactor

The integrated FAST bioreactor concept with interdependent fermentation, separation, product recovery, and cell recycle, creates challenges for its design, the scale-up and optimization. On one side, bioreactor scale up has two different technological objectives for reducing operational costs (OPEX): (1) optimization of metabolic performance in the fermentation process and (2) optimization of separation and purification (Cuellar, Heijnen and van der Wielen, 2013). On the other hand, there is the objective of reducing capital expenditure (CAPEX) by development and demonstration of an industrial-scale integrated reactor.

Studies have proven that microorganisms respond quickly to heterogeneity of the large-scale environment (Neubauer and Junne, 2010; Wang et al., 2015). Thus, conventional scaling-up of fermentation processes to be economically feasible begins at choosing the correct microorganism and improving the strain to attain high productivities and low susceptibility to contamination (Westfall and Gardner, 2011). Once initial microorganism optimization is done, the optimization of its bioreactor environment needs to be done (Oosterhuis and Kossen, 1984;

Westfall and Gardner, 2011; Wang et al., 2015) with respect to mixing and mass transfer, coping with (local) toxic and inhibitory effects of product and feedstock, and (local) concentrations of dissolved oxygen, carbon dioxide, nutrients availability, pH, temperature, and anti-foam.

Currently scale-up studies are being carried out at lab and pilot scale with the goal to collect data that can be extrapolated for use in large scale. This is complicated for multiphasic mixtures in multiple compartments, while maintaining microorganism performance during transport across compartments. Different technological problems such as foaming, substrate and oxygen depletion zones, heat transfer, bad mixing and inefficient oil separation may arise when increasing the scale of the integrated reactor. If so, there might be a necessity to drastically change the reactor design for industrial scale.

Historically, the scaling up of new process technologies in biotechnology industries was based on trial and error, rules of thumb and experience of the engineers and scientists. These are gradually being replaced by model-based approaches by solving of all micro-balances, using simplified flow models, dimensional analysis and scale down method based on regime analysis) (Noorman, 2011), that increase rate and reduce costs of bioprocess development.

Nowadays, the scale-down approach to study the influence of local gradients of substrate, product, nutrient/carbon compounds and oxygen (Schmidt, 2005; Neubauer and Junne, 2010; Jonge et al., 2011) essentially mimics large-scale conditions in small scale equipment and focus in understanding, optimizing and solving of bottlenecks of a large-scale process at laboratory or pilot scale. Regime analysis is the first step to identify characteristic times of relevant sub-processes in the bioreactor and allows predicting the rate limiting step(s). These times can be obtained by experiment (if available), by using known correlations (Oosterhuis and Kossen, 1984; Noorman, 2011) and simplified models.

Given the system complexity (four different phases, different functionalities, and specific geometry) of FAST bioreactors, engineering correlations and regime analysis alone do not give enough information for the scaling-up of the integrated reactor. Moreover, the difficulty of in-situ and offline measurements during experiments at different scales, the availability and reproducibility of fermentation broth and the lack of know-how of the mechanisms present during emulsification, oil separation and recovery and cell recycle adds extra challenges to this complex problem.

Computational fluid dynamic (CFD) is a tool that is increasingly used for bioreactor development driven by the availability of increasingly powerful computers. This tool has been used in both scale up and scale down to analyze the fluid dynamics and local gradients of carbon, oxygen, pH etc in a bioreactor with accurate temporal and spatial resolutions (Noorman, 2011). Furthermore, CFD has successfully been employed for other unit operation such as separation processes for a better guidance and understanding of equipment design, optimization, and gradient impact on the microorganism with limited experimental work (Schmidt, 2005; Kelly, 2008; Neubauer and Junne, 2010; Noorman, 2011; Sharma, Malhotra and Rathore, 2011; Wang et al., 2015). Hence, CFD is used as a reliable tool to study the hydrodynamics of the system and to gain realistic insights on the multiphase interactions and the different mechanisms at different scales.

Although CFD is a powerful tool and has been applied for many reactor developments successfully, it still has some limitations, specially related to multiphase technology. In this work, we propose a combined model based and experimental approach to evaluate and calibrate the impact of various parameters on oil recovery and thus to guide the design and scale-up of the integrated reactor.

## 1.4 A proposed approach to guide the design and scale-up of an integrated FAST bioreactor

Model-based development of an integrated reactor at large scale with limited or no experiments is a lasting challenge (Noorman, 2011). In literature, no common strategy is reported on how to develop and use models, especially for multi-phase systems. Most phenomena have been studied and described in isolation, for one or a few scales and one- or two-phase flows. Some studies compare results from other models; others use a more qualitative approach while others just assume the model is mimicking the reality.

In this work, a combined, task-based approach is taken, based on (1) the scale-down methodology for the integrated FAST bioreactor based on the physical mechanisms and phenomena underlying the different reactor functionalities, (2) perform smaller scale experimental result (Wang, Wang and Jin, 2006; Haringa et al., 2016) to calibrate important

fundamental parameters for dominant mechanisms in the window of reactor operation, and then (3) the use of CFD to guide scale-up of an integrated reactor combining the different functionalities. To the best of our knowledge, this approach has not been implemented and tested before for integrated bioreactors.

The method allows focus on the macro effects underpinning main functionalities (oil recovery and cell recycle in the FAST bioreactor), describing in (fundamental) detail only the mechanisms that matter. For the FAST bioreactor, the different functionalities to be studied in the integrated reactor are: emulsion formation, liquid recirculation and cell recycle, gas-liquid separation and oil recovery (Heeres, 2016; Pedraza de la Cuesta, 2019). For each functionality several mechanisms can occur: mixing, bubble bursting, flotation, coalescence of droplets, oxygen or glucose limitation by cells, formation of surfactants, etc.. Albeit for each functionality a group of mechanisms might occur, in the end the intention is to highlight the dominant mechanism for each functionality.

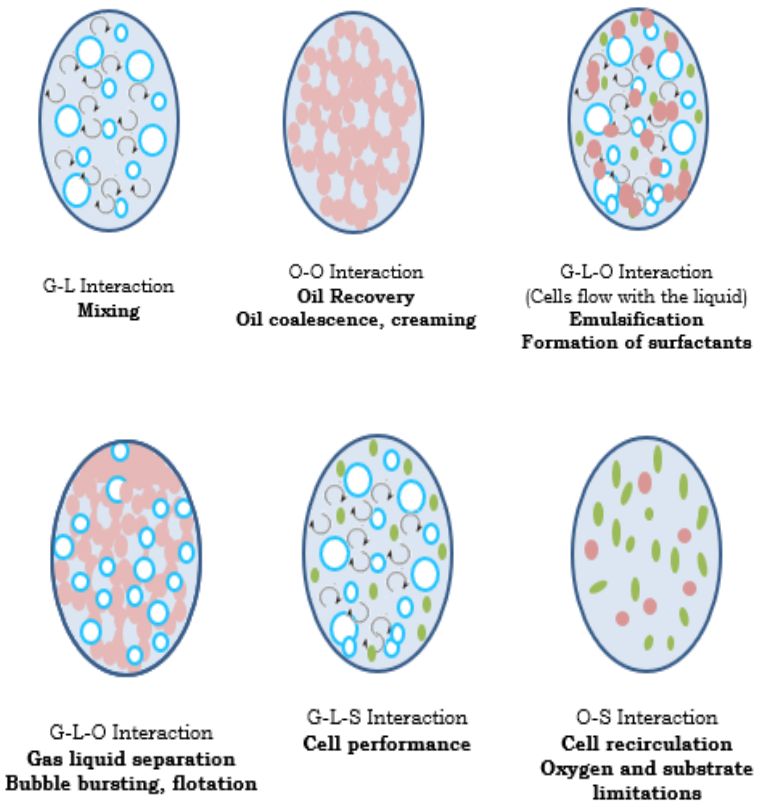


**Figure 4 –** Diagram of the different interactions between phases and the different mechanisms involved. Where G is gas (air – white circles), L is water (medium – blue background), O is organic phase (oil – pink circles) and S is solids (cells – green circles)

A schematic overview applying this a methodology on the integrated FAST bioreactor is shown in Figure 5. The schematic overview shows resulting combination of modelling work using CFD, and experimental work are combined to collect fundamental information and validate the outcomes of each route.

The complexity of the system requires some simplifications. The complex interactions are broken down into simpler sub-processes, for the dominant mechanism for oil recovery, emulsion formation and cell recycle. CFD simulations are used to describe the hydrodynamics in the specific sections of the FAST bioreactor, integrating dominant mechanisms.

Specific attention must be given to the challenge of appropriate *in-situ* and offline measurements at different scales. Some techniques can be used at lab scale to try to achieve some qualitative and quantitative insight on the mechanisms. However, this must be performed using synthetic emulsions to assure reproducibility which is difficult to achieve with actual fermentation broth. Image analysis is one of the main techniques used to record and measure oil gradients and recovery. In addition, equivalent experiments using fermentation broth will be used as qualitative and quantitative benchmarks of the technology. When increasing scales, the tools used become scarcer. They are essentially limited to flow and time measurements and overall hold-ups, allowing trend analysis of model framework and applicability to larger scales.

By following this combined approach, correlations can be drawn between the resulting parameters of the modelling work and experimental work at different scales. Knowing the relevant mechanisms at lab and pilot scale, one can adjust the design of internal structure and dimensions, and operational conditions of the integrated FAST bioreactor to guide optimization of the separation and recovery of oil at production scale.

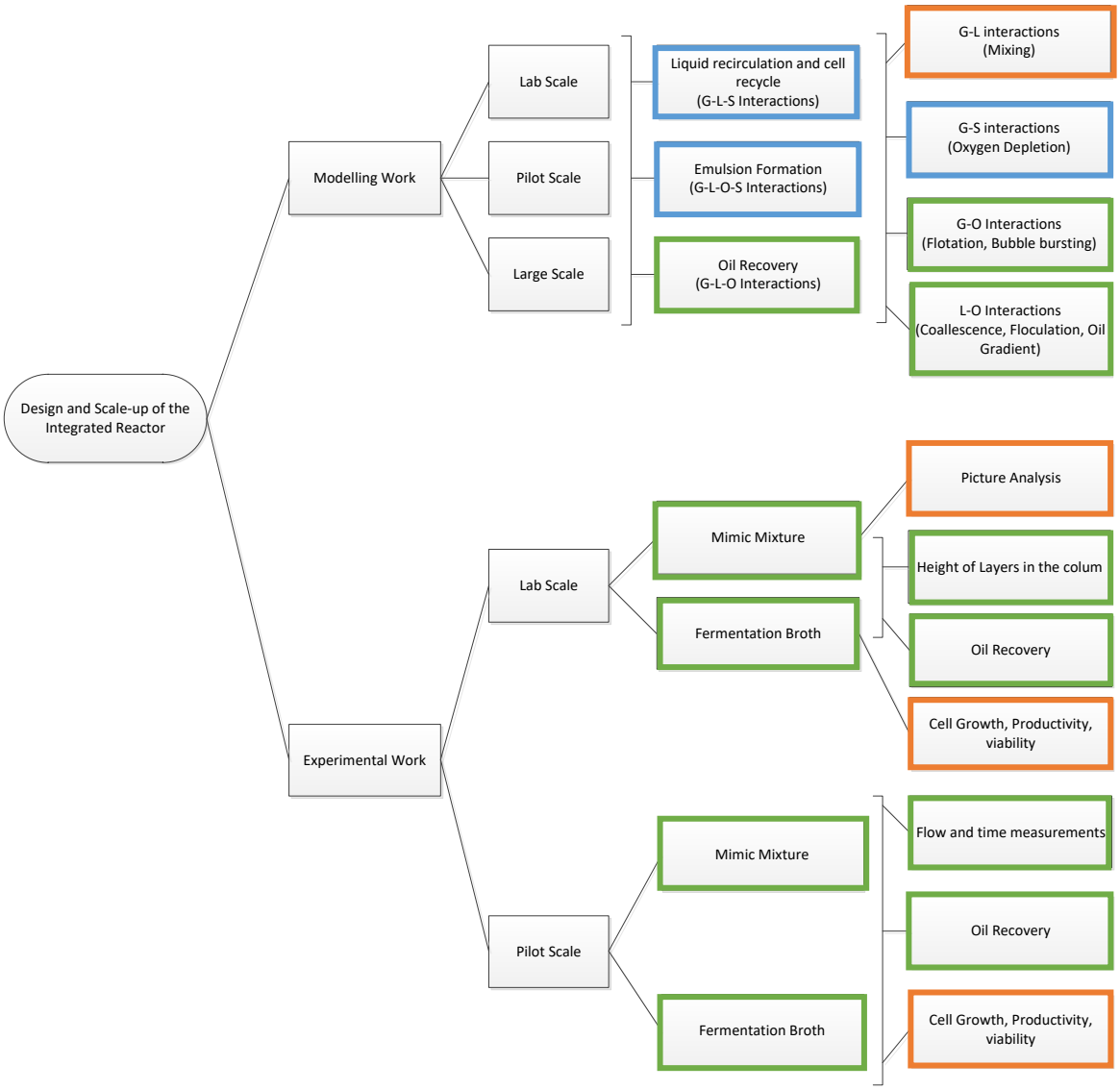


**Figure 5 -** Model based approach for the design and understanding the relevant parameters for scale up of the integrated FAST bioreactor. Where G is gas (air), L is water (medium), O is organic phase (oil) and S is solids (cells). Green squares were addressed in this thesis; Orange squares not reported in this thesis but studied during research; Blue squares are not addressed in this thesis.

## 1.5 Thesis Outline

The work presented in this thesis has the aim to understand design and scale-up rules for the integrated FAST bioreactor and how its main functionality, the recovery of phase separating (oil) products, can be optimized. In Chapter 2, a mechanistic model to describe oil coalescence when a gas bubble is in contact with a region of high oil droplet concentration was developed. This model allowed to improve oil recovery from multiphasic emulsions at lab scale and could be used to guide the design of the integrated reactor at production scale. Next, in Chapter 3, the use of flocculants to improve oil recovery in multiphasic fermentation was tested in three different oil recovery methods: gravity settling, gas enhanced oil recovery and centrifugation. The flocculant time of addition and its impact on multiphasic fermentations have been evaluated by comparing fermentation performance and the oil recovery by the three methods. In Chapter 4, the experimental results of the pilot scale of the FAST bioreactor are presented for a model and for a planned commercial case study of one of our industrial partner DAB BV. A CFD model was created to study hydrodynamics of the integrated reactor at certain conditions and understand for which conditions oil recovery can be promoted. A window of operation was achieved that can be used for the scale up of the integrated reactor. Finally, Chapter 5 summarizes the main conclusions of this thesis and gives an outlook for future research.

## 1.6 References

Behin, J. and Bahrami, S. (2012) 'Modeling an industrial dissolved air flotation tank used for separating oil from wastewater', *Chemical Engineering and Processing: Process Intensification*, 59, pp. 1–8. Available at: https://doi.org/http://dx.doi.org/10.1016/j.cep.2012.05.004.

van Benthum, W.A.J. *et al.* (1999) 'The biofilm airlift suspension extension reactor. Part I: Design and two-phase hydrodynamics', *Chemical Engineering Science*, 54(12), pp. 1909–1924. Available at: https://doi.org/http://dx.doi.org/10.1016/S0009-2509(99)00034-2.

Chandran, S.S., Kealey, J.T. and Reeves, C.D. (2011) 'Microbial production of isoprenoids', *Proc Biochem*, 46(9), p. 8. Available at: https://doi.org/10.1016/j.procbio.2011.05.012.

Cheryan, M. and Rajagopalan, N. (1998) 'Membrane processing of oily streams. Wastewater treatment and waste reduction', *Journal of Membrane Science*, 151(1), pp. 13–28. Available at: https://doi.org/http://dx.doi.org/10.1016/S0376-7388(98)00190-2.

Cuellar, M.C., Heijnen, J.J. and van der Wielen, L.A. (2013) 'Large-scale production of diesel-like biofuels - process design as an inherent part of microorganism development', *Biotechnol J*, 8(6), pp. 682–689. Available at: https://doi.org/10.1002/biot.201200319.

Cuellar, M.C., Heijnen, J.J. and van der Wielen, L.A.M. (2013) 'Large-scale production of diesel-like biofuels - process design as an inherent part of microorganism development', *Biotechnol. J.*, 8(6), pp. 682–689. Available at: https://doi.org/10.1002/biot.201200319.

Cuellar, M.C. and Straathof, A.J.J. (2018) 'CHAPTER 4 Improving Fermentation by Product Removal', in *Intensification of Biobased Processes*. The Royal Society of Chemistry, pp. 86–108. Available at: https://doi.org/10.1039/9781788010320-00086.

Cuellar, M.C. and Straathof, A.J.J. (2020) 'Downstream of the bioreactor: advancements in recovering fuels and commodity chemicals', *Current Opinion in Biotechnology*, 62, pp. 189–195. Available at: https://doi.org/https://doi.org/10.1016/j.copbio.2019.11.012.

Cuellar, M.C. and van der Wielen, L.A.M. (2015) 'Recent advances in the microbial production and recovery of apolar molecules', *Current Opinion in Biotechnology*, 33(0), pp. 39–45. Available at: https://doi.org/http://dx.doi.org/10.1016/j.copbio.2014.11.003.

DAB BV (no date) 'DAB.bio's revolutionary FAST$^{TM}$ biomanufacturing platform'.

Fakhru'l-Razi, A. *et al.* (2009) 'Review of technologies for oil and gas produced water treatment', *Journal of Hazardous Materials*, 170(2–3), pp. 530–551. Available at: https://doi.org/10.1016/J.JHAZMAT.2009.05.044.

Haringa, C. *et al.* (2016) 'Euler-Lagrange computational fluid dynamics for (bio)reactor scale-down: an analysis of organism life-lines', *Engineering in Life Sciences* [Preprint]. Available at: https://doi.org/10.1002/elsc.201600061.

van Hee, P. *et al.* (2006) 'Strategy for selection of methods for separation of bioparticles from particle mixtures', *Biotechnology and Bioengineering*, 94(4), pp. 689–709. Available at: https://doi.org/10.1002/bit.20885.

Heeres, A. (2016) *Integration of Product Recovery in Microbial Advanced Biofuel Production - Overcoming Emulsification Challenges*, *Biotechnology*.

Heeres, A.S. *et al.* (2014) 'Microbial advanced biofuels production: overcoming emulsification challenges for large-scale operation', *Trends Biotechnol.*, 32(4), pp. 221–229.

Heeres, A.S. *et al.* (2015) 'Fermentation broth components influence droplet coalescence and hinder advanced biofuel recovery during fermentation', *Biotechnol. J.*, 10(8), pp. 1206–1215. Available at: https://doi.org/10.1002/biot.201400570.

Heijnen, S.J. *et al.* (1990) 'Large-scale anaerobic/aerobic treatment of complex industrial wastewater using immobilized biomass in fluidized bed and air-lift suspension reactors', *Chemical Engineering & Technology - CET*, 13(1), pp. 202–208. Available at: https://doi.org/10.1002/ceat.270130127.

IEA (2021) (2021) *Renewables 2021, IEA, Paris*, *https://www.iea.org/reports/renewables-2021, License: CC BY 4.0*.

*Integrated Water & Wastewater Treatment Solutions* (2010) *https://sswm.info/sites/default/files/reference_attachments/AQWISE%202010%20New%20Integrated%20Solutions%20Brochure.pdf*.

Jackson, B.E., Hart-Wells, E.A. and Matsuda, S.P. (2003) 'Metabolic engineering to produce sesquiterpenes in yeast', *Org Lett*. 2003/05/09, 5(10), pp. 1629–1632. Available at: https://doi.org/10.1021/ol034231x.

Jonge, L.P. de *et al.* (2011) 'Scale-down of penicillin production in Penicillium chrysogenum', *Biotechnol J*, 6(8), pp. 944–958. Available at: https://doi.org/10.1002/biot.201000409.

Keijzers, L. (2016) *Integration of microbial production & recovery of sesquiterpenes*. Delft: TU Delft.

Kelly, W.J. (2008) 'Using computational fluid dynamics to characterize and improve bioreactor performance', *Biotechnology and Applied Biochemistry*, 49(4), pp. 225–238. Available at: https://doi.org/10.1042/BA20070177.

Kenneth, G.C. (2007) 'Climate change, biofuels, and global food security', *Environmental Research Letters*, 2(1), p. 11002. Available at: http://stacks.iop.org/1748-9326/2/i=1/a=011002.

Lane, J. (2013) *1000 project bioeconomy database launches, from Biofuels Digest SuperData*, *https://www.biofuelsdigest.com/bdigest/2013/06/24/1000-project-bioeconomy-database-launches-from-biofuels-digest-superdata/*.

Mainar Causape, Alfredo.J., Philippidis, G. and European Commission. Joint Research Centre. (no date) *BioSAMs 2015 : estimation and basic considerations.*

Neubauer, P. and Junne, S. (2010) 'Scale-down simulators for metabolic analysis of large-scale bioprocesses', *Current Opinion in Biotechnology*, 21(1), pp. 114–121. Available at: https://doi.org/http://dx.doi.org/10.1016/j.copbio.2010.02.001.

Noorman, H. (2011) 'An industrial perspective on bioreactor scale-down: What we can learn from combined large-scale bioprocess and model fluid studies', *Biotechnol J*, 6(8), pp. 934–943. Available at: https://doi.org/10.1002/biot.201000406.

Oosterhuis, N.M.G. and Kossen, N.W.F. (1984) *Scale-up of bioreactors: A scale-down approach*, *Biotechnology*.

Oudshoorn, A. *et al.* (2021) 'WO2021010822 - INTEGRATED SYSTEM FOR BIOCATALYTICALLY PRODUCING AND RECOVERING AN ORGANIC SUBSTANCE'. Available at: https://patentscope.wipo.int/search/en/detail.jsf?docId=WO2021010822.

P, B. (2019) *Energy outlook*. Available at: https://www.bp.com/content/dam/bp/business-sites/en/global/corporate/pdfs/energy-economics/energy-outlook/bp-energy-outlook-2019.pdf.

Pedraza de la Cuesta, S. (2019) *Product Emulsification in multiphase fermentations - the unspoken challenge in microbial production of sesquiterpenes*, *Biotechnology*.

Pedraza-de la Cuesta, S. *et al.* (2017) 'Use of solvents in the scale-up of microbial sesquiterpene production', *tbd* [Preprint].

Schmidt, F.R. (2005) 'Optimization and scale up of industrial fermentation processes', *Applied Microbiology and Biotechnology*, 68(4), pp. 425–435. Available at: https://doi.org/10.1007/s00253-005-0003-0.

Sharma, C., Malhotra, D. and Rathore, A.S. (2011) 'Review of Computational fluid dynamics applications in biotechnology processes', *Biotechnol Prog*, 27(6), pp. 1497–1510. Available at: https://doi.org/10.1002/btpr.689.

Steinbusch, K. (2016) 'How To Increase Productivity Of Oil Product Fermentation While Scaling Up?', *World BIO Biotechnology* [Preprint]. San Diego.

Tabur, P. and Dorin, G. (2012) 'Method for purifying bio-organic compounds from fermentation broth containing surfactants by temperature-induced phase inversion'. Edited by Amyris. US: Amyris Inc.

*Total and Amyris renewable jet fuel ready for use in commercial aviation* (2014) *https://totalenergies.com/media/news/press-releases/total-and-amyris-renewable-jet-fuel-ready-use-commercial-aviation*.

U.S. Department of Energy - Energy Efficiency and Renewable Energ (2023) *Renewable Gasoline*, *https://afdc.energy.gov/fuels/emerging_hydrocarbon.html*.

Velasco, J. (2014) 'Growing the future of bioeconomy', in *US Department of Energy*. Amyris. Available at: https://www.energy.gov/sites/prod/files/2014/11/f19/x_velasco_biomass_2014.pdf.

Wang, G. *et al.* (2015) 'Integration of microbial kinetics and fluid dynamics toward model-driven scale-up of industrial bioprocesses', *Engineering in Life Sciences*, 15(1), pp. 20–29. Available at: https://doi.org/10.1002/elsc.201400172.

Wang, T., Wang, J. and Jin, Y. (2006) 'A CFD–PBM coupled model for gas–liquid flows', *AIChE Journal*, 52(1), pp. 125–140. Available at: https://doi.org/10.1002/aic.10611.

Warner, E. and Schwab, A. (2017) *2016 Survey of Non-Starch Alcohol and Renewable Hydrocarbon Biofuels Producers*. 2.

Westfall, P.J. and Gardner, T.S. (2011) 'Industrial fermentation of renewable diesel fuels', *Curr. Opin. Biotech.*, 22(3), pp. 344–350. Available at: http://www.sciencedirect.com/science/article/pii/S0958166911000863.

# Chapter 2: A Mechanistic Model for Oil Recovery in a Region of High Oil Droplet Concentration from Multiphasic Fermentations.

**Abstract** Multiphasic fermentations are common in the production of several biofuels and commodity chemicals where an organic phase is spontaneously formed or when it is added for product removal. The immiscibility characteristics of the organic phase enable in-situ recovery, cell re-use and potentially decrease the amount of downstream processing steps. However, the turbulent conditions in the fermentation, and the presence of surface-active compounds (SACs) in the medium create a stable emulsion that is difficult to separate. A separation method based on gas bubble/oil droplet interactions has been proposed to break the emulsion formed during fermentation without damaging the cells. However, the mechanisms behind those interactions are not yet fully understood, hampering optimization. In this paper, we propose a mathematical model to describe oil coalescence when a gas bubble is in contact with a region of high oil droplet concentration. Model validation was performed using a synthetic emulsion of hexadecane in water stabilized with Tween80, and with an emulsion from a fermentation broth where a sesquiterpene product had been in-situ extracted with dodecane. By applying the optimal parameters predicted by the model, 75% and 39% oil recovery was reached for the synthetic emulsion and the fermentation broth, respectively. This represents a 6- and 3-times improvement when compared with non-optimized experiments with the same laboratory scale set-up. For the fermentation broth, higher oil recovery was not achieved likely due to unfavourable interfacial tension, oil fraction and viscosity. According to the model, however, oil recovery higher than 90% can be achieved by increasing the surface area to volume ratio of the recovery setup, and by increasing the oil fraction. In conclusion, the proposed mechanistic model allowed to improve oil recovery in the existing laboratory scale set-up and can be used for guiding the design of equipment for multiphasic fermentations at industrial scale aiming at low-cost production processes.

**Keywords:** Emulsion; Aggregation; Oil Recovery; Multiphasic Fermentation; Modelling;

Published as: Rita M. Da Costa Basto, Maria P. Casals, Robert F. Mudde, Luuk A.M. van der Wielen, Maria C. Cuellar,A mechanistic model for oil recovery in a region of high oil droplet concentration from multiphasic fermentations, Chemical Engineering Science: X, Volume 3, 2019, p. 100033, 2019.

## 2.1 Introduction

Over the past two decades, metabolic engineering has enabled the production of a broad range of products that form a second phase or in which solvents can be used for product extraction (Rude and Schirmer, 2009; Straathof, 2014). Examples of these products are long chain hydrocarbons, such as sesquiterpenes, which are often organic liquids at ambient conditions (Chandran et al., 2011). These products have numerous commercial applications as biofuels, cosmetics, pharmaceuticals, nutraceuticals and fine chemicals (Amyris, 2016; Cuellar and van der Wielen, 2015; Vickers et al., 2017). Some of the advantages of these components are their immiscibility in water and their low density. However, their microbial production results in a complex mixture of four phases (aqueous medium, gas, organic phase composed of or containing the product and microbial cells) inside the bioreactor. These can be also referred to as multiphasic fermentations. We refer in this paper to the said organic phase as 'oil'.

Dispersed oil droplets rise due to buoyancy forces. Ideally, when the droplets rise, they coalesce with each other and form clear, continuous oil phase that can be easily separated. During fermentation, however, surface-active-compounds (SACs) stabilize the oil droplets by decreasing the interfacial tension, increasing viscosity and inducing electrostatic repulsions (Heeres et al., 2014). Given the turbulent conditions typical of fermentation, instead of clear oil, a concentrated emulsion, also called cream, is formed. Such emulsions can also be formed when using solvents for product extraction during fermentations (Dafoe and Daugulis, 2014; Erler et al., 2003; Janssen et al., 2015).

Current processes use cost and energy intensive centrifugation steps, environmentally challenging de-emulsifiers and/or pH and temperature swings for breaking these emulsions after fermentation (Tabur and Dorin, 2012). Yet, several alternative techniques might be used to separate this oil from an emulsion during fermentation, in situ, without high costs, chemicals addition or harsh conditions. Some examples include dissolved air flotation (van Hee et al., 2006),(Al-Shamrani et al., 2002), foam fractionation (Burghoff, 2012), gravity

settling (Dolman et al., 2017), and more recently, gas enhanced oil recovery (GEOR) (Heeres et al., 2016).

During multiphasic fermentations, oil fractions and gas bubbles sizes are typically larger than the ones in systems where dissolved air flotation is applied (oil fractions below 0.1% and gas bubbles of 30-100 □m) (Rubio et al., 2002; van Hee et al., 2006). Foam fractionation has the disadvantage of low control at larger scales and low purities (Burghoff, 2012) and both dissolved air flotation and gravity settling require further downstream process to obtain a clear oil layer (Dolman et al., 2017). Because of this, GEOR has been proposed as a suitable technique to separate oil from these type of emulsions (Cuellar and Straathof, 2018). This method uses gas bubbles to promote coalescence between emulsified oil droplets in a cream phase and create a clear oil layer without any change in temperature, pH or chemical addition. Moreover, due to its mild operational conditions, it can be integrated with fermentation without hampering its performance (Pedraza-de la Cuesta et al., 2017). Previous studies from our group showed the potential of GEOR in oil recovery from hexadecane and yeast supernatant emulsions (Heeres et al., 2016), and from fermentation broth emulsions (Pedraza-de la Cuesta et al., 2017). A disadvantage of GEOR is that the relative importance of the mechanisms behind the separation method is not well understood yet. This hinders oil recovery optimization and currently does not allow it to compete with conventional methods, which have been reported to result in up to 90% oil recovery from fermentation broth (Renninger, 2010; Tabur and Dorin, 2012). Heeres et al showed that the limiting step for oil separation in an emulsion stabilized with SAC's, is the droplet coalescence after cream formation (Heeres et al., 2014). It has been showed that increasing oil fraction in the dispersed mixture did not have a large impact on oil recovery by GEOR (Heeres et al., 2016), yet there are no studies showing the impact of using gas bubbles directly in cream. Moreover, previous studies on GEOR applied to fermentation broths, showed that higher oil fractions can promote droplet coalescence and increase oil recovery (Pedraza-de la Cuesta et al., 2017).

In this paper, we propose a mathematical model that describes the interactions between gas bubbles and oil droplets in a cream in order to predict oil coalescence – and thus, oil recovery – for given emulsion and gas phase properties. Model validation is experimentally performed with a synthetic emulsion and with an emulsion from fermentation broth. Finally, the model is used to identify further improvement opportunities for the technology.

## 2.2 Model Development

### 2.2.1 Mathematical model development of GEOR in a cream region

In GEOR, the gas bubbles travel through a cream region, a mixture of water and oil droplets, under laminar conditions, enabling coalescence of some oil droplets onto clear oil on top (Figure 1). Several mathematical models from literature on oil coalescence were analysed, a summary of which can be seen in Table 1.

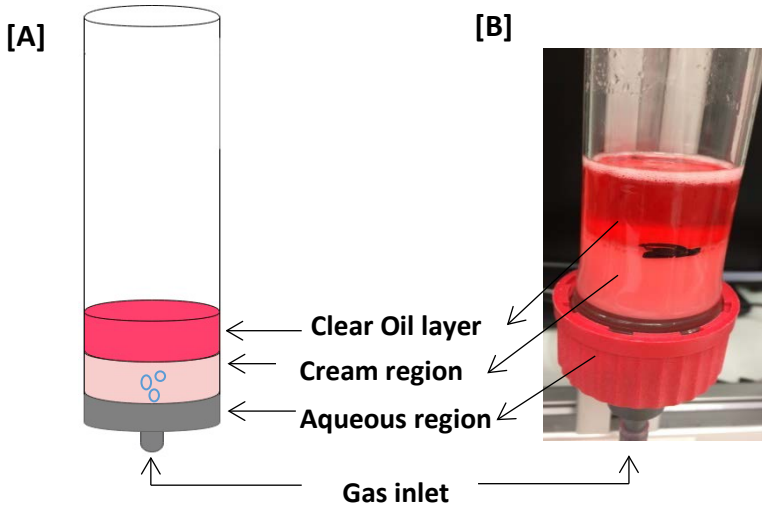


**Figure 1 -** Schematic drawing [A] and picture [B] of a laboratory column set-up with a cream region with clear oil on top.

**Table 1** - A summary of the different mechanisms depicted in literature that can describe oil droplets-gas bubble interactions.

| Mechanisms | Description | Application studied | References |
|---|---|---|---|
| **Aggregation** | Attachment of oil droplets to gas bubbles and formation of an aggregate that rises to the top and promotes coalescence. | Food industry describing the attachment of fat globules to bubbles. | (Hotrum et al., 2005; Walstra, 1993, 2003) |
| **Bursting with film layer** | Droplet coalescence is promoted by the excess of surface energy from the bursting of a bubble when passing through the interface of a thin film layer and air. | Environmental, chemical and biological industries describing the burst of a bubble passing a film layer of oil. | (Feng et al., 2016; Schlichting et al., 1960; Stewart et al., 2015) |
| **Bursting with oil layer on top** | The gas bubble when passing through the interface of a dense fluid region and the oil layer, creates a column until it breaks and promote oil droplets coalescence. | Chemical industry describing the passage of a bubble through Oil-Water interface. | (Kemiha et al., 2007; Reiter and Schwerdtfeger, 1992; Singh and Bart, 2015; Uemura et al., 2010) |
| **Flotation and Population Balance Equations** | The coalescence of oil droplets in a well-mixed, two-phase system is described by several mathematical models and experimental data defining droplet coalescence and break-up, as well as rates and efficiencies. | Mineral industry and chemical industry for particle separation and multiphasic flows studies. | (Jovanović and Miljanović, 2015; Koh and Schwarz, 2008; Ralston et al., 1999; Simon et al., 2003) |

Based on preliminary experimental studies, the aggregation model and the oil bursting model with an oil layer are the ones describing better the oil recovery by GEOR in a cream layer with oil on top. Hence, a model is proposed, integrating these two models, while preserving their main characteristics (Figure 2). In this model, a bubble goes through the cream layer (zcream) and some of the oil droplets gets attached to the hydrophobic surface of the gas bubble [A]. This event can be mathematically described by the aggregation mechanism (in food technology commonly used as flocculation). Once the gas bubble reaches the interface between the cream and the oil, a jet of cream is formed into the clear oil. The oil droplets attached to the rising bubble during aggregation are inside this cream jet [B]. With the continuous rising of the bubble, the jet gets thinner, more unstable and due to increased pressure inside the jet, some droplets are released and coalesce with the surrounding oil, described by the oil bursting mechanism [C]. The released droplets are considered to coalesce with the surrounding oil. This coalescence is possible since the surfactant prefers a hydrophobic/hydrophilic interface hence, the oil droplets released from the jet are not covered with surfactant. After the jet breakage, the bubble with the non-released oil droplets rises to the oil-air interface and is released to the surface [D]. The remaining cream and droplets, with a higher density than the surrounding oil, are back mixed to the cream layer [E].

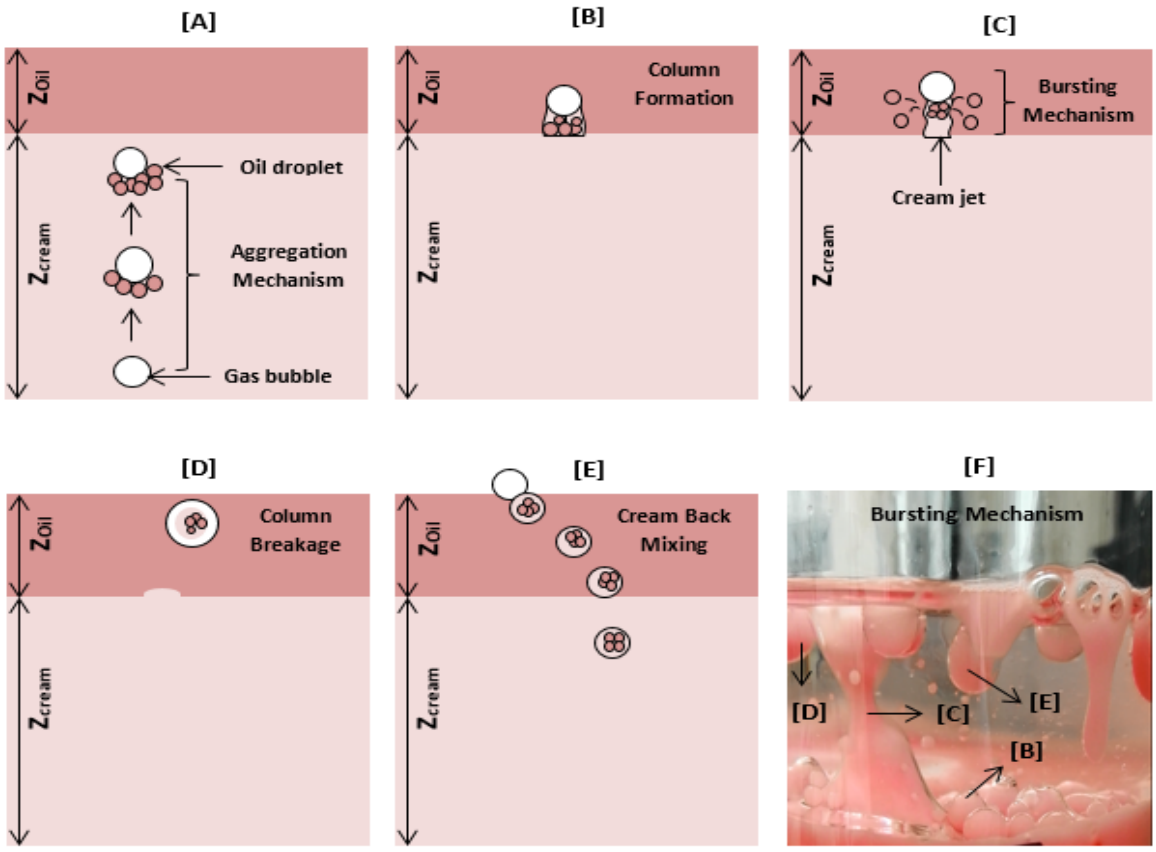


**Figure 2 -** Schematic representation of the mechanistic model describing oil recovery by GEOR in a cream layer with oil on top: [A] aggregation mechanism – rising of the gas bubble through the cream layer and attachment of oil droplets; [B] Cream jet formation with the oil droplets, previously attached, inside; [C] Rising of gas bubble through the oil layer and oil release due to pressure increase inside the cream jet; [D] Jet breakage and rising of gas bubble with remaining cream and oil; [E] Gas bubble release into the surface and back mixing of cream and oil droplets back to the cream; [F] Experimental picture of the different steps [B-E] when the gas bubbles crosses the interface between the top of the cream layer and the oil layer.

To quantify the amount of oil recovered, a mass balance in the oil layer and cream layer is made. It is assumed that bubble and droplets diameters are constant over time. In the same way, the density of both oil and cream are assumed constant, hence the model can be expressed as a volume balance.

The oil recovered is calculated by multiplying the rate of bubbles ($Q_{Nb}$ in $s^{-1}$) by the difference of the oil attached to the bubble ($V_{oil\ aggregation}$ in $m^3$), and the non-coalesced oil during bursting ($V_{oil\ bursting}$ in $m^3$) (Equation 1):

$$\frac{dV_{oil}}{dt} = Q_{N_b} \cdot \left[ V_{oil\ aggregation} - V_{oil\ bursting} \right] \quad (1)$$

**Aggregation model:**

$V_{oil\ aggregation}$ is defined by the number of droplets attached to the bubble at the top of the cream layer ($N_{b\text{-}d(zcream)}$), and by the droplet volume ($V_d$ in $m^3$):

$$V_{oil\ aggregation} = N_{b-d(zcream)} \cdot V_d \quad (2)$$

The cream height ($z_{cream}$ in m) is reduced in each time step. This height is dependent on the number of droplets in the cream ($N_d$), the droplet volume ($V_d$ in $m^3$), the cross-sectional area of the column ($A_{col}$ in $m^2$) and the oil fraction in the cream ($\varphi$), which is assumed constant (Equation 3).

$$z_{cream} = \frac{N_d \cdot V_d}{A_{col} \cdot \varphi} \quad (3)$$

For a monodisperse emulsion, the change in $N_d$ becomes:

$$\frac{dN_d \cdot V_{cream}}{dt} = \left[ - Q_{N_b} \cdot \frac{V_{oil\ aggregation} - V_{oil\ bursting}}{V_d} \right] \quad (4)$$

The bubble position in the cream was calculated from the bubble-droplet velocity ($v_{bs}$) at each time step. This velocity was obtained from a force balance on the bubble-droplets aggregate and the mass of the aggregate. In order to estimate the number of droplets attached to the bubble ($N_{b\_d}$) while travelling through the cream layer, from z=0 (base of the cream) to z=zcream (at the cream interface), ($\frac{dN_{b\_d}}{dt}$), the approach proposed by Hotrum (Hotrum et al., 2005) was used. In that approach, the attachment of droplets depends on the flow conditions ($J_{dorth}$) and the attachment efficiency (α):

$$\frac{dN_{b\_d}}{dt} = J_{dorth} \cdot \alpha \quad (5)$$

At z=0, t=0 and $N_{b\text{-}d}$ = 0. At the conditions studied in this paper, where the system is laminar and the coalescence is induced by shear, the flow in a cream layer is considered orthokinetic, which means that the bubble attachment is promoted by the turbulence created due to velocity gradients (Equation 5) (Hotrum et al., 2005). The so called orthokinetic rate ($J_{dorth}$ in 1/s) is assumed to be proportional to the volume fraction of oil (φ), the shear rate gradient (ϒ in 1/s), and the number concentration of droplets in the cream ($N_d$) (Equation 6). The shear rate (Equation 7) is directly related with the superficial gas velocity ($v_{GS}$ in m/s), cream viscosity ($\vartheta_{cream}$) and power input (P in W).

$$J_{dorth} = \frac{4}{\pi} \cdot \varphi \cdot \gamma \cdot N_d \quad (6)$$

$$\gamma = \left(\frac{P}{\vartheta_{cream} \cdot V_{cream}}\right)^{\frac{1}{2}} \quad (7)$$

The attachment efficiency at orthokinetic conditions, on the other hand, was estimated following the approach by Van de Ven and Mason, considering a Hamaker constant ($A_H$) of $10^{-20}$ J, that defines the interaction between two particles and the collision radius ($r_{coll}$), depicted as the sum of the two particles radius (Chen et al., 1998; van de Ven and Mason, 1977). From these derivations it can be seen that the aggregation mechanism is favoured by a low droplet volume and a high shear rate gradient.

**Oil bursting model:**

When the bubble rises towards the oil-air interface, a cream jet increases until the point that it breaks (Figure 2– [B] and [C]). According to Ueda, *et* al (Ueda et al., 2011), such jet breaks in three parts: the lower part, that returns to the cream region, the upper part, that gets attached to the bubble (eventually returning to the cream region) and the middle part, where part of the oil droplets coalesces into the clear oil. Hence, oil recovery due to oil bursting is calculated by the volume of the upper part of the jet formed (Figure 3). This jet was considered as an oscillating cylinder; therefore, the volume is integrated over its length ($l_b$ in m) (Equation 8). The diameter of the cream jet changes in space with an oscillating function, where $A$ is the amplitude of the wave and y the phase. The $r_{jet}$ was defined by the minimum radius that the cream jet could achieve.

$$V_{\text{oil bursting}} = \int_0^{lb} \frac{\pi}{4} \cdot [2 \cdot (r_{jet} + A + A \cdot \sin\left(2 \cdot \frac{\pi}{\lambda} \cdot z_{jet} + \frac{\pi}{2}\right))]^2 dz_{jet} \quad (8)$$

The length of the upper part of the cream jet ($l_b$) is defined by Equation 9. This parameter is dependent on the bubble velocity at $z_{cream}$ ($v_b$ in m/s) (at the cream interface), Reynolds number (Re) and Weber number (We) of the aggregate, amplitude of the cream jet (Ɛ in m) and jet radius ($r_{jet}$ in m) (Ueda et al., 2011).

$$l_b = 2 \cdot r_{jet} \cdot \ln\left(\frac{r_{jet}}{\varepsilon}\right) \cdot \left(\sqrt{We} + 3 \cdot \frac{We}{Re}\right) \quad (9)$$

$$\varepsilon = \frac{r_{jet}}{Mo \cdot C} \quad (10)$$

The jet radius ($r_{jet}$) and a constant (C) were both fitted from preliminary experiments with synthetic emulsion at varying gas flows and bubble diameters (see section 2.4.1). The $r_{jet}$ is a parameter dependent on bubble diameter and should not be larger than the bubble diameter (Ueda et al., 2011). The amplitude of the cream column (Ɛ) (Equation 10) was linked to the properties of the cream through the Morton number (Mo), as reported by Ghabache and Seon (Ghabache and Séon, 2016). A sensitivity analysis was performed (Section 2.4.2) to understand the impact of the empirical parameters in the modelled oil recovery. In general terms, it can be deduced from the above equations that oil bursting is favoured by a large bubble size and/or a low aggregate velocity.

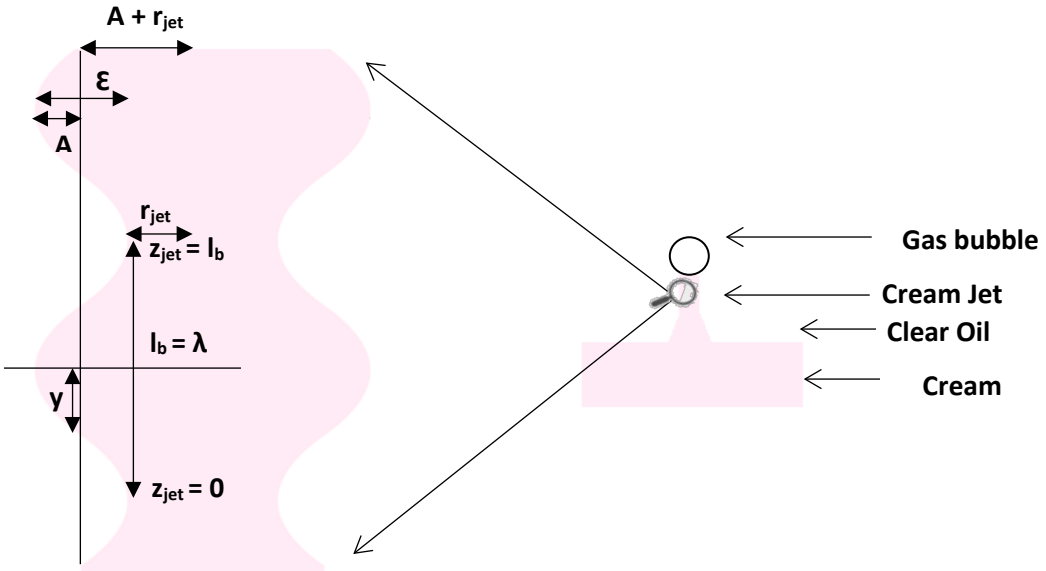


**Figure 3 -** Scheme of the upper part of the cream jet compared with the oscillation function adapted from Ueda, Y. et al [37]. Where A is the wave amplitude, y the phase, λ the period, Ɛ the amplitude of the cream jet, rjet is the radius of the cream jet and lb the length of the jet.

### 2.2.2 Model implementation

The mathematical model described in **Error! Reference source not found.** (Equation 1 to 10) was implemented in MATLAB R2015b for academic users. For a given emulsion (Section 2.3.2) and gas properties, the model calculated the oil recovery. The bubble diameter is an input parameter dependent on the nozzle size. The input time was considered the time taken during an experimental run (3600 s). This oil recovery was normalized by the number of bubbles for comparison between different $v_{GS}$ (Figure 4).

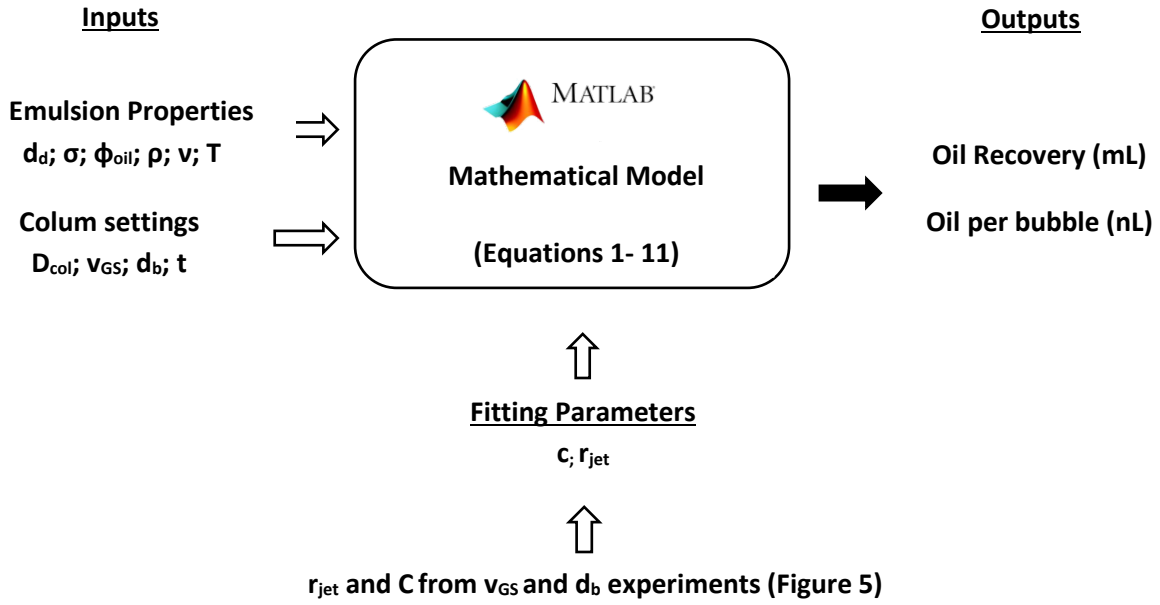


**Figure 4 -** Inputs, outputs and fitting parameters implemented in the mathematical model described in section 2.2.1.

## 2.3 Materials and Methods

### 2.3.1 Materials

Separation experiments were performed with two mixtures: a synthetic emulsion and fermentation broth from a sesquiterpene fermentation operating with in-situ solvent extraction of the sesquiterpene product. The synthetic emulsion was prepared using MilliQ water (18.2 MΩ, Millipore systems), a non-ionic surfactant, Tween80 (Sigma Aldrich, Premium) and hexadecane (Sigma Aldrich, Reagent Plus) coloured with Oil Red O dye (Sigma Aldrich). The second phase added to the fermentation broth was dodecane (Sigma Aldrich, Reagent Grade) also coloured with Oil Red O dye.

### 2.3.2 Emulsion Preparation

#### 2.3.2.1 Synthetic Emulsion

The synthetic emulsion was prepared by adding 1.5 L volume of MilliQ water, 0.01 mg/g of Tween80 and 0.1 v/v of coloured hexadecane to a 2 L stirred vessel with a six bladed rushton turbine (diameter of 45 mm) and two baffles (inner diameter of 120 mm) with in-situ monitoring of droplet size (see Section 2.3.4.1). The mixture was stirred for two hours at a rate of 1200 rpm, corresponding to a power input of 6.8 kW/m$^3$, and room temperature (18-20 °C).

#### 2.3.2.2 Emulsion from Fermentation Broth

The fermentation broth used in this work was obtained from a fermentation performed with a recombinant, sesquiterpene producing *E. coli* BL21(DE3) strain. The microorganism was cultivated aerobically at 30 °C in fed-batch mode in a medium containing glycerol as carbon source. The fermentation conditions and general composition at the time of harvest are summarised in Table 2.

**Table 2 -** Fermentation conditions for the fermentation broth used during separation column experiments.

| | |
|---|---|
| **Time of harvest[1] (h)** | 63.0 |
| **Fermenter Volume (L)** | 7 |
| **Power Input (rpm)** | 470 |
| **Average Power Input (kW/m$^3$)** | 2.27 |
| **Cell density ($g_X/kg_{broth}$)** | 25.0 |
| **Dodecane (%w/w)** | 9.07 |

[1]Being time 0 the start of the batch phase.

### 2.3.3 Separation Experiments

Separation experiments were performed either using the whole mixture prepared as described in section 2.3.2 (bulk experiments) or using a concentrated mixture (cream experiments). The latter was obtained by transferring the whole mixture to a 2 L glass decanter and harvesting the concentrated oil after one hour.

Cream experiments were performed for parameter fitting and model validation. Bulk experiments were done to study the effect of bulk in oil recovery, to compare it with previous experimental data (Heeres et al., 2016) and, to understand which settings could be used to optimize oil recovery when using fermentation broth.

#### 2.3.3.1 Parameter fitting Experiments

For the parameter fitting, cream experiments with synthetic emulsion were executed as shown in Figure 1 using a similar set-up and protocol as described by Heeres *et al*, 2016 (Heeres et al., 2016). All the experiments were performed in duplicate, originated from different mixtures. Gas sparging was generated by single orifice nozzles with varying diameters ($d_{nozzle}$: 0.05, 0.1, 0.3 and 1 mm). The superficial gas velocity varied between 0.05, 0.1, 0.5 and 1 cm/s. The air supply pressure was set at 3 bar and monitored using a

manometer. An extra manometer was added between the mass flow controller and the column to warn in case of nozzle blockage. 15 mL of the decanted aqueous solution was added to the bottom of the glass columns to account for the non-visible volume of the glass column. To the top of this liquid, 2.5 cm of cream was added. A clear oil layer, with a volume 10 times the measured bubble Sauter mean diameter (see section 2.3.4.2), was set on top of it. The oil height was maintained during the experiment by removing the oil when it reached 2.4 cm oil height (corresponding to approximately 5% increase in the oil layer). After 1h sparging, the gas flow was stopped, the mixture was let to phase-separate and the volume of clear oil recovered was determined.

#### 2.3.3.2 Model Validation Experiments (S1 and S3)

Model validation experiments were performed with synthetic emulsions. Experiments followed the previous protocol (section 2.3.3.1). An oil layer, with a volume of 5 or 10 times the measured bubble Sauter mean diameter, was set on top of the cream. The oil height was maintained during the experiment by removing the oil when it reached 2 or 2.4 cm height, respectively. Each separation experiment was performed in duplicate, originated from the same mixture. The control experiment S1, was replicated 7 times from independent mixtures and for each independent mixture, duplicates were performed (total of 14 experiments). Experiment S3, was replicated two times from independent mixtures, each performed in duplicates. Different process parameters were used for the optimization experiments and can be found in Table 3.

**Cream Experiments (S2)**

For the cream experiments, a single orifice nozzle with 0.3 mm diameter and superficial gas velocity of 0.2 cm/s ($d_b$: 0.38 cm) were set.

**Bulk Experiments (S4 and S5)**

Bulk experiments contained 150 mL of the whole mixture instead of the 15 mL aqueous solution. A nozzle with 0.1 mm diameter was used. Two different experiments were performed: 1 or 5 nozzle orifices and a superficial gas velocity of 0.1 cm/s ($d_b$: 0.23 cm) and 0.12 cm/s ($d_b$: 0.39 cm) were employed.

**Table 3** - Experimental conditions during separation column experiments for the control (S1) and optimization (S2, S4,) columns at lab scale ($D_{col}$=3.6 cm) for a synthetic emulsion with a Sauter mean droplet diameter of 40 μm.

| | **S1** | **S2** | **S3[1]** | **S4** | **S5[1]** |
|---|---|---|---|---|---|
| **Aqueous solution or Bulk volume (mL)** | 15 | 15 | 150 | 150 | 300 |
| **Cream layer height (cm)** | 2.5 | 4 | 2.5 | 2.5 | - |
| **Nozzle (mm)** | 0.1 | 0.3 | 0.1 | 0.1 | 0.1 |
| **#Holes** | 1 | 1 | 1 | 5 | 1 |
| **Oil Layer/$d_b$ (cm)** | 10 | 5 | 10 | 5 | - |
| **Bubble Sauter mean diameter (cm)** | 0.23 | 0.38 | 0.23 | 0.39 | 0.23 |
| **Superficial gas velocity (cm/s)** | 0.1 | 0.2 | 0.1 | 0.12 | 0.1 |

[1]S3 and S5 settings were not used for model validation. Only used for oil recovery comparison.

#### 2.3.3.3 Experiments with Emulsion from Fermentation Broth

When using fermentation broth, two different experiments were performed: bulk experiment ( B1b and B1c), with oil set on top of the bulk phase, since there was not enough cream generated to perform all experiments, and cream experiments (B1d) with 25 mL cream and oil on top. To ensure mixture homogeneity from the reactor to the columns, the broth was first transferred to a smaller vessel which, was manually agitated before pouring into the columns. The same protocol as the previous sections (section 2.3.3, 2.3.3.1 and 2.3.3.2) was performed. The experiments were performed in duplicates originated from the same fermentation broth. The settings for the separation experiments with emulsion from fermentation broth, can be seen below (Table 4).

**Table 4 -** Experimental conditions during separation column experiments for the broth of a 7 liter fermentation (B1) in a column of 3.6 cm diameter. Where B1a uses the same settings as S3 but no oil on top, B1b uses the same settings as S3, B1c uses the optimized settings from S4 experiment and B1d uses the same settings as S2 but with a 2.5 cm cream layer.

| Type of mixture | B1a[1] | B1b | B1c | B1d |
|---|---|---|---|---|
| **Volume (mL)** | 200 | 150 | 150 | 25 |
| **Nozzle (mm)** | 0.1 | 0.1 | 0.1 | 0.3 |
| **n° nozzles** | 1 | 1 | 5 | 1 |
| **Superficial gas velocity (cm/s)** | 0.1 | 0.1 | 0.12 | 0.2 |
| **Oil layer on top (cm)** | no | 2.2 | 2 | 1.9 |
| **Bubble diameter (cm)** | 0.23 | 0.23 | 0.39 | 0.38 |

[1]B1a experiment was only used for oil recovery comparison.

## 2.3.4 Analytic Tools

### 2.3.4.1 Droplet Size Measurements

The droplet size during synthetic emulsion preparation was monitored using an optical probe (SOPAT Gmbh – detection range from 15 µm to 1000 µm) (Maaß et al., 2012). The probe was set in the emulsion preparation vessel as presented in Heeres *et al* (Heeres et al., 2015). During the two hours of stirring, 1200 pictures (30 pictures every 3 minutes) were taken in-situ. Particle detection was obtained using the SOPAT software. To minimize the particle selection and avoid false particles detection such as gas bubbles, a threshold higher than 0.8 was set. The number of pictures taken were such that it was possible for the software to obtain at least 1 000 particles of interest. The detected particles were then analysed in the SOPAT result analyser resulting in a Sauter mean diameter of 40 ± 4 µm.

#### 2.3.4.2 Bubble Size Measurements

The gas bubble size distribution in the separation columns was determined for all nozzles and gas flows used by image analysis of a 40% ethanol solution in MilliQ water. Pictures were taken every 5 min with a digital camera (Canon 100D and a 18-55 mm lens) in a dark room. Behind the columns a white LED (Dell, model R2412Hb, full brightness and standard colour settings) was placed. The camera was set at a height of 108 cm of the floor and a distance of 85 cm of the columns. The pictures were processed with an image analyser software (ImageJ 1.47) considering the bubbles as ellipsoids and manually marking their minimum and maximum diameters.

The Sauter mean diameter was later determined using the ellipsoid bubble volume but assuming a spherical shape of the bubble.

#### 2.3.4.3 Interfacial Tension Measurement in synthetic emulsion

The interfacial tension (IFT) of the organic phase (hexadecane) in a continuous phase (100 mg/L of Tween80 in MilliQ water) was measured using a Drop Shape Analyser (model DSA100, Krüss, ADD country). The measurement followed the pendant drop method, using a stainless steel J-Shaped Needle (NE71, $d_{needle}$= 0.487 mm, ADD supplier), where a drop of organic phase (oil phase) was submerged into a continuous phase (aqueous phase) (Science). The measurement was performed at room temperature and recorded until the IFT values of the mixture reached a plateau.

#### 2.3.4.4 Oil Fraction Measurement in synthetic emulsion

To quantify the oil fraction in the cream, 12 mL of the cream obtained, as described in section 2.3.3, were processed through a Whatman filter with a PTFE membrane of 0.45 µm pore size. The oil recovered was measured in a graduated cylinder. Two passages were necessary to achieve a clear oil. Three different set of measurements were performed. An average oil fraction of 0.7±0.05 was measured.

#### 2.3.4.5 Statistical Analysis

The statistical significance of oil recovery yield for the different separation column experiments was evaluated by a one-tailed Student's t-test, assuming a heteroscedastic population for S2 and homoscedastic population for S3, S4 and S5 at a significance level of 5%.

## 2.4 Results

### 2.4.1 Parameter Fitting and Model Validation Experiments

Two parameters of the bursting model, $r_{jet}$ and constant C, required experimental fitting. Two set of experiments were performed (see section 2.3.3.1), one at constant bubble diameter ($d_b$ = 0.23 cm) and different superficial gas velocities ($v_{GS}$ = 0.05 – 1 cm/s) (Figure 5 - A) and other at constant superficial gas velocity ($v_{GS}$ = 0.1 cm/s) and different bubble diameters ($d_b$ = 0.16 – 0.55 cm) (Figure 5 - B). From the graphic representations of Yoshiaki *et al* (Ueda et al., 2011), it is observed that the cream jet formation (Figure 3) is dependent on the gas bubble, hence the $r_{jet}$ is also a function of the bubble diameter. For our system, it was found that the $r_{jet}$ dependence on bubble diameter follows a power equation given by the following empirical Equation 11.

$$r_{jet}\,(m) = 1.2 \times 10^{-6}.\,(d_b(m))^{-1.22} \qquad (11)$$

The amplitude of the cream jet is linked with the cream properties and the jet radius. However, their relation is also no yet reported in literature. For that reason, a constant, C, with a value of $9.2 \times 10^{7}$, needed to be experimentally fitted with the experimental data. Although these two parameters can be related to each other as one constant (see Equation 10), the two are kept separate to avoid inconsistencies in the cream jet geometry.

For both experiments it is observed that lower superficial gas velocities and larger bubble diameters resulted in higher oil recovery per bubble. However, the maximal experimental oil recovery achieved was 36%, for a superficial gas velocity of 0.1 cm/s and a bubble diameter of 0.23 cm, calculated as the percentage of oil recovered relative to the total oil initially present in the cream.

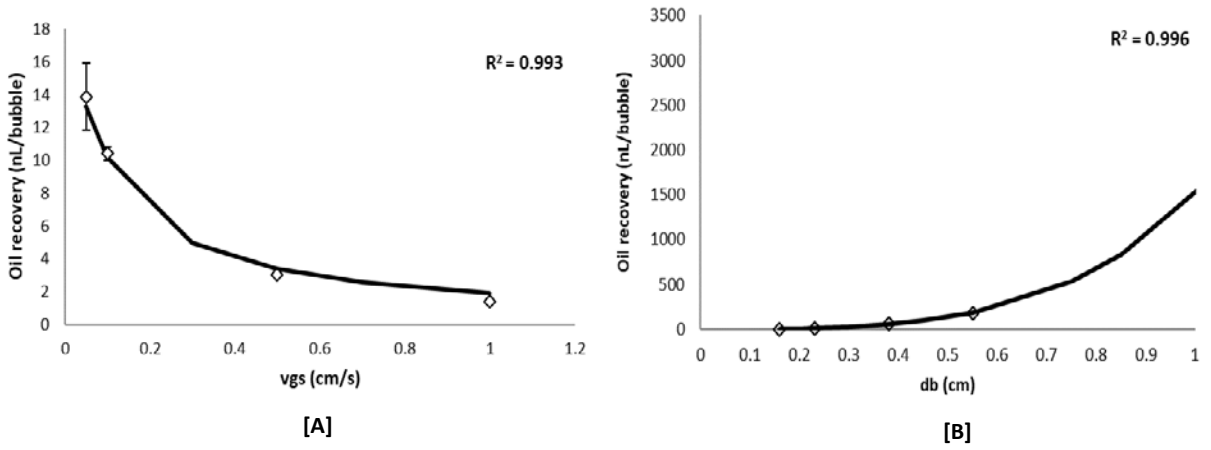


**Figure 5 -** Oil recovery normalized per number of bubbles experiments for (A) parameter fitting at different $v_{Gs}$ and $d_b$ = 0.23 cm; (B) parameter fitting at different bubble Sauter mean diameters and $v_{Gs}$ = 0.1 cm/s . For $d_b$ smaller than $r_{jet}$ it was assumed the recovery was 0. Solid line represents the model fitting for (A) 7 different $v_{Gs}$ and for (B) 12 different $d_b$. White markers represent the experimental data.

The fitting parameters were then used to predict the best parameters ($v_{GS}$, $d_b$, $D_{col}$) required to reach an oil recovery higher than 90%. Two different systems were evaluated for the lab scale set-up ($D_{col}$ = 3.6 cm): a cream layer with clear oil on top, and a bulk phase with a cream layer and oil on top. A range of 0.1 - 1 cm for bubble diameter and superficial gas velocities was simulated (Figure 6). For bubble diameters lower than 0.2 cm the oil recovery was considered 0 since the $r_{jet}$ was smaller than the bubble diameter. Other parameters, such as droplet size, were not implemented to predict oil recovery since they only have a negligible influence in the model estimations (see section 2.4.2).

An oil recovery percentage of 74% and 84% was observed for $d_b$ = 1 cm and $v_{GS}$ = 0.1 cm/s (Figure 6) when using a cream layer of 2.5 cm and 4 cm (results not shown), respectively. For both cream heights the same trend is perceived. Higher superficial gas velocities and smaller bubble diameters lead to lower oil recovery (as shown in Figure 5). Moreover, the model showed that oil recovery has the tendency to become constant regardless the increase of superficial gas velocities or bubble size (e.g.: $d_b$ = 0.6 cm and $v_{GS}$ = 0.6 cm/s). For a constant superficial gas velocity and increasing bubble diameter the number of bubbles in the system decreases, and so does the oil recovery. On the other hand, if the superficial gas velocity increases, the number of bubbles in the system increases and there is a decrease in oil recovery efficiency per bubble (Figure 5). Hence, to reach higher oil recovery, there must be a trade-off between number of bubbles in the system and superficial gas velocities. This can

be confirmed by the fact that at higher superficial gas velocities and lower bubble diameters ($d_b$ = 0.3 cm and $v_{GS}$ = 0.6 cm/s) the oil recovery become equal or even larger than for bubble diameters of 0.4 cm.

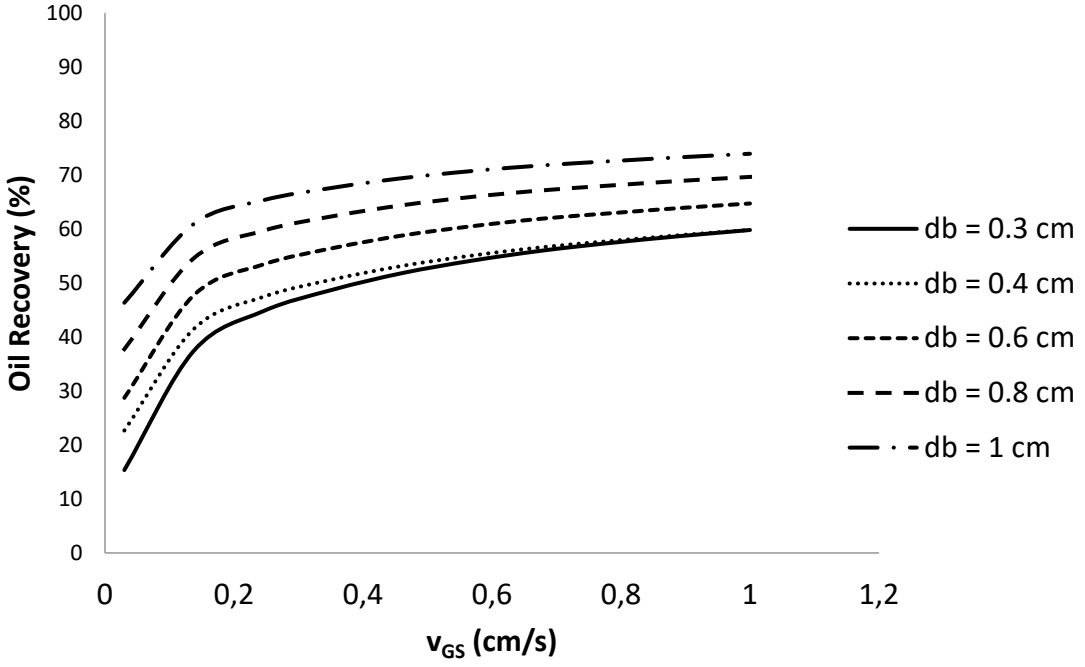


**Figure 6** - Total oil recovery (%) as a function of gas velocities and bubble diameter for a synthetic emulsion cream layer of 2.5 cm and $D_{col}$ 3.6 cm. For $d_b$ lower than 0.2 cm it was assumed that the oil recovery was zero since $r_{jet}$ was smaller than $d_b$.

A parameter that was not taken into account for model development (Section 2.2.1) was the foam formation at higher $v_{GS}$ and larger $d_b$. Based on experimental results and to avoid errors in oil recovery optimization, a foam region was identified at $v_{GS}$ higher than 0.5 cm/s and $d_b$ larger than 0.6 cm. Taking this into account, at this scale a maximal oil recovery percentage of only 59% and 74% can be predicted for a cream layer of 2.5 cm and 4 cm, respectively.

This mathematical model is a lab-scale methodology, that allows for pilot and commercial scale predictive use. Moreover, for these diameters, a cream volume between 0.5 and 2.5 L would be necessary per experiment, requiring a reactor of at least 10 L per column experiment to obtain the emulsions. Given this perspective, a model-based analysis was implemented to assess the impact of column diameter on the predicted oil recovery (Figure 7). It can be seen that recovery larger than 90% can be achieved for column diameters 5x larger than the laboratory scale column ($D_{col}$ = 3.6 cm). By changing the column diameters,

the number of bubbles ($Q_{NB}$) and the number of droplets in the cream layer ($N_d$) will increase, enhancing the recovery of oil (Hotrum et al., 2005). Interestingly, by expanding the column diameters, the effect of changing superficial gas velocity and bubble diameters, in the range studied, becomes negligible, which allows a more robust operation at larger scales.

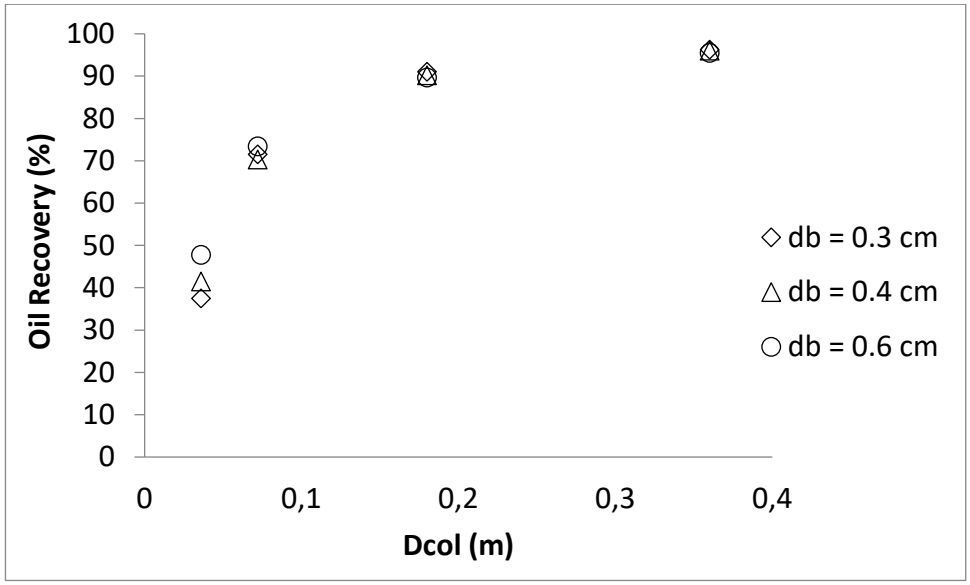


**[A]**

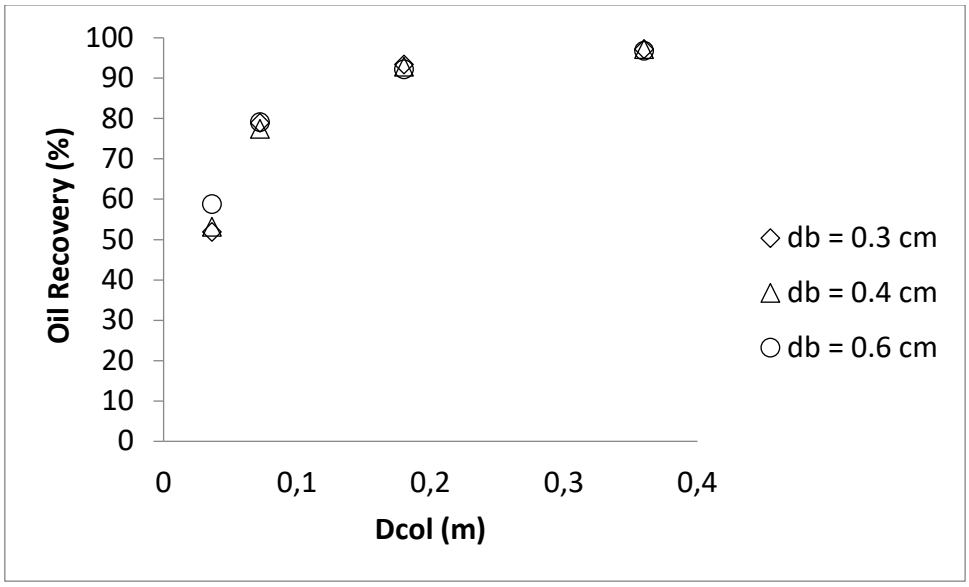


**[B]**

**Figure 7 -** Estimated total oil recovery (%) for an increase of 2X, 5X and 10X of the lab scale column diameter ($D_{col}$=3.6 cm) for different bubble diameters and two different superficial gas velocities: A) $v_{GS}$: 0.14 cm/s $v_{GS}$; B) $v_{GS}$: 0.46 cm/s for a synthetic emulsion cream layer of 2.5 cm.

### 2.4.2 Sensitivity analysis

During the course of model development, three major assumptions were made: a) bubble size was assumed equal to that measured in a 40% ethanol solution; b) constant droplet size throughout the experiment (40 μm); and c) use of empirical parameters - C and $r_{jet}$. Moreover, physical parameters, such as, interfacial tension and oil viscosity are known for the mimic emulsion. However, if a different emulsion is used where these parameters are not known or are not easily determined (e.g.: fermentation broth), then to understand their effect in oil recovery is of utmost importance. Therefore, sensitivity analysis was performed to these parameters to evaluate their effect in the oil recovery prediction by the model. The $r_{jet}$ parameter was not studied by sensitivity analysis since his value is given by a power equation (Equation 11) which is dependent on the bubble diameter. In this context, the above-mentioned parameters were varied. The constant C was increased and decreased by one order of magnitude to understand if there was any impact on the model results. The oil viscosity extremes were defined by the model boundaries. For oil viscosities outside this range, the model does not work. The interfacial tension and droplet diameter were varied taking into account the range of values of a stable emulsions (low extreme) and a weaker emulsion (higher extreme). The oil fraction was varied between the minimum and maximum values that can be found in a multiphasic fermentation. The effect of these parameters on the model results was analysed (Figure 8). For the Sauter mean bubble diameter its impact on oil recovery could already been seen in section 2.4.1. Moreover, by changing +/- 0.1 cm, using a randomized method following a Gaussian distribution, the change in bubble diameter showed a standard deviation of 0.6 mL, which follows inside the experimental error.

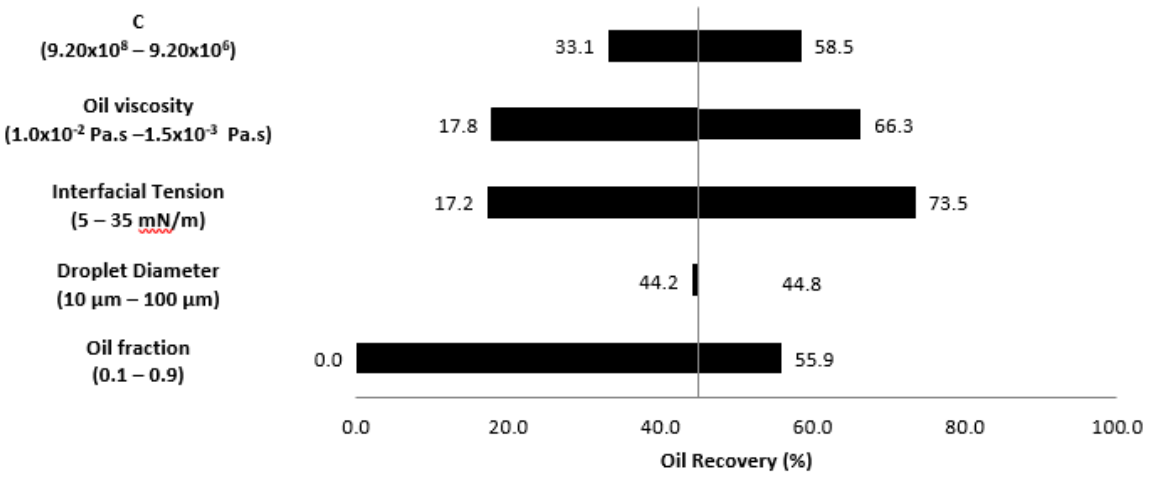


**Figure 8 -** Sensitivity analysis of the percentage of oil recovery for a common range of model parameters for a cream layer of 2.5 cm, $D_{col}$ of 3.6 cm, $d_b$ of 0.38 cm and $v_{GS}$ of 0.2 cm/s.

It is observed that the oil recovery is highly influenced by the change in oil fraction and interfacial tension. Where higher oil recovery is achieved for higher oil fraction, systems with higher interfacial tension (35 mN/m) and lower oil viscosity ($1.5x10^{-3}$ Pa.s). This shows that for each emulsion, these parameters should be always quantified previously to model predictions. Moreover, for a new emulsion a new $r_{jet}$ equation should be previously fitted. Although this might seem counterintuitive, the parameter with less influence in the oil recovery is the droplet diameter.

The same parameters were changed for higher column diameters. Recovery lower than 90% were found for oil fraction below 0.3, viscosity lower than $1.5x10^{-3}$ Pa.s and droplet diameter higher than 60 µm (results not shown).

## 2.4.2 Experiments with Synthetic Emulsion Results

### 2.4.2.1 Cream and Bulk Experiments

The oil recovery percentage was measured experimentally for a synthetic emulsion using a 2.5 cm cream layer, 150 ml of bulk phase, and a fermentation broth emulsion. The settings chosen were based on the predicted model results. When comparing the experimental oil

recovery with the model predictions, it is clear that similar results were achieved for S2 and S4 (Table 5). In addition, oil recovery were larger for S2, which used a 4 cm cream layer and bubble diameter of 0.38 cm, in contrast with the standard column (S1). Comparing S4 with S3 and S5 (bulk experiments), the oil recovery was doubled. However, higher oil recovery could not be reached, because none of the current nozzles promote an increase in bubble diameter as estimated by the model (section 2.4.1).

**Table 5 –** Model prediction and experimental oil recovery with standard deviation for the cream and bulk synthetic emulsion at lab scale ($D_{col}$=3.6 cm) and 40 μm droplet size.

| | | **Oil recovered (mL)** | **% Oil recovery** |
|---|---|---|---|
| **S1** | *Model Prediction* | 5.88 | 33 |
| | *Experimental Results* | 5.5±0.5 | 31±3 |
| **S2** | *Model Prediction* | 18.6 | 65 |
| | *Experimental Results* | 18.1±1 | 64±4<br>p-value = 0.01 |
| **S3** | *Experimental Results* | 3.0±0 | 17±0<br>p-value = 0.02 |
| **S4** | *Model Prediction* | 7.0 | 40 |
| | *Experimental Results* | 8.7±0.5 | 49±2<br>p-value = 0.02 |
| **S5** | *Experimental Results* | 3.9±0.4 | 13±1<br>p-value = 0.03 |

## 2.4.3 Fermentation Broth Experiments

To assess whether the mechanisms taking place in the synthetic emulsion are comparable to those in a fermentation broth, experiments were performed using the emulsion described in Table 4. The experimental parameters, and the respective oil recovery, can be found in Table 6. The oil recovery for this specific case could not be predicted by the model, since for this type of system, the relevant parameters (such as interfacial tension, viscosity, density, droplet size and fraction of the oil in the cream) could not be measured. Four different experiments

were performed: B1a, B1b and B1c – with oil on top; and B1d – only with cream and oil on top. Although the oil recovery is still low, B1b, B1c and B1d show an increase of 100 % in comparison to B1a, suggesting that the two mechanisms described above are also present on a fermentation broth emulsion. The percentage of oil recovery for experiment B1d, could not be attained, since the oil fraction in the cream is not known.

**Table 6 -** Oil recovery and experimental error from the broth of a 7 liter fermentation (B1) performed at a power input of 2.78kW/m$^3$ (one column per condition) in a column at lab scale ($D_{col}$=3.6 cm).

| Type of mixture | B1a | B1b | B1c | B1d |
|---|---|---|---|---|
| **Oil recovery (mL)** | 2.8±1 | 4.7±1 | 5.3±1 | 4.8±1 |
| **Oil recovery (%)** | 15±4 | 35±4 | 39±4 | - |

## 2.5 Discussion

### 2.5.1 Improving oil recovery by scale-up

A mathematical model based on two different mechanisms, aggregation and oil bursting, was proposed in order to explain the gas bubble interaction with oil droplets in a cream layer with oil on top. A systematic approach was taken to validate the model, using a synthetic emulsion with exactly the same characteristics throughout the whole research. The normalized oil recovery, predicted by the model, was shown to fit the experimental results at varying superficial gas velocities and gas bubble Sauter mean diameters. However, experimental results showed that recovery higher than 74% could not be reached at laboratory scale. Regardless, it can be seen that an increase in the column diameter is beneficial for enhancing oil recovery. This benefit with scale increase was also predicted by Pedraza-de la Cuesta *et al* (Pedraza-de la Cuesta et al., 2017). On the one hand, the number of droplets in the column increases, increasing the orthokinetic flux of oil droplets to the bubble (Equation 6) in the aggregation mechanism. On the other hand, because the time for the aggregate to reach the cream interface is lower at larger scale than at smaller scale, the number of droplets attached

to the bubble when reaching the interface decreases. When passing the interface, the bubble is slightly lighter than at smaller scale, which creates a shorter cream jet attached to the bubble after bursting, thus increasing the oil recovery. These results shows that, although the bursting mechanism still has an influence, the aggregation mechanism is the one governing oil recovery and is the first one to be optimized to achieve larger oil recovery.

### 2.5.2 Parameter effect in oil recovery

Sensitivity analysis shows that, in the range studied, droplet diameter and C would not have an impact on the oil recovery expected by the model. Oil viscosity has a bigger impact in oil recovery than the previous parameters. When using higher oil viscosities, it was observed that recovery was hindered. This is expected since with higher viscosity the drag force during the aggregation mechanism increases. Additionally, the Morton number in the bursting mechanism increases by the power four (Ghabache and Séon, 2016) hence the amplitude of the cream jet (Equation 10) is reduced in such a way that there are almost no oscillations thus, the oil is trapped inside the jet. Therefore, lower viscosities promote oil recovery in a cream layer with oil on top.

The other two parameters that have a bigger influence in oil recovery are interfacial tension and oil fraction. When the oil fraction in the cream is decreased, there is a decrease in the oil recovery. By decreasing the oil fraction, there are less possibilities for the oil to be captured by the gas bubble, decreasing the aggregation efficiency. Despite that, with increased oil fraction the oil recovery is not much higher than the base case. Increasing the oil fraction will increase the number of droplets attached to the bubble hence, the bubble velocity will decrease due to the weight increase and consequently, hamper the bursting mechanism and hinder oil recovery. The change in interfacial tension has a similar effect in oil recovery as the one of viscosity. For lower values of interfacial tension, there is an increase in the Weber number, increasing the length of the cream jet (Equation 9) and hindering oil recovery. Moreover, the impact of Morton number (Ghabache and Séon, 2016) is larger and, by decreasing the interfacial tension, the Morton number increases, and as previously described, the cream jet amplitude decreases. Thus, higher interfacial tensions result in higher oil recovery.

Droplet size show to have only a small influence in oil recovery. Nevertheless, previous experiments shown that droplet size also have an impact on the creaming behaviour of the emulsion. On one hand, for larger droplets sizes (100 μm), emulsions cream faster and oil is better recovered with GEOR (Heeres et al., 2016). On the other hand, smaller droplets size (10 μm) can take much more time to cream or not even cream (Pedraza-de la Cuesta et al., 2017), reducing the oil fraction in the system and hampering the aggregation mechanism.

Moreover, one has to consider that for lower $r_{jet}$ values, present for larger bubble diameters, there will be an increase of pressure inside the cream jet, which leads to higher amount of oil released hence, larger oil recovery, as observed in Figure 5-B. For higher $r_{jet}$ values, a thicker jet is formed, and more oil is kept inside and further back mixed to the cream (see Figure 2-[D] and [E]). This fitting parameter is highly dependent on the emulsion properties and bubble diameter and is not a measurable or tuneable parameter. Therefore, if the model is used on a different type of emulsion, to achieve reliable results, it is necessary to fit once more this parameter against new experimental data.

### 2.5.3 Can aggregation and oil bursting mechanisms improve oil recovery in synthetic emulsions?

The experimental results for the synthetic emulsion S1, S2 and S4 show that the model could predict quite well the oil recovery obtained by GEOR. This confirms that the model describes well the recovery of oil from a synthetic emulsion. Comparing the recovery between the standard column (S1) and the column using optimal settings from the model (S2), an increase in oil recovery was observed. For the bulk experiments (S3 and S4), the experiment with larger bubble diameter (S4) showed a 100% increase in recovery in relation to S3. Nonetheless, when comparing bulk experiments with cream experiments, lower recovery were achieved. The current results are consistent with published data (Heeres et al., 2016), where Heeres *et al* concluded that bigger bubbles and lower velocities would lead to higher oil recovery. Moreover, the authors stated that in zones with increased oil fraction, oil recovery was increased. The reported oil recovery for a supernatant emulsion was 66% at the same settings as S2, which are in the same range of values as the ones reported in this paper.

### 2.5.4 Are the aggregation and oil bursting mechanisms also present in fermentation broth?

To understand if the same mechanisms described before (Section 2.2) are present during oil recovery from fermentation broth emulsion, both systems were compared. For fermentation broth there was no data available of important empirical parameters such as droplet size or oil fraction. Moreover, there was no possibility of fitting the $r_{jet}$ parameter due to lack of reproducible material. Hence, the same optimal settings as for the synthetic emulsion (S4), were used (B1c). Based the sensitivity analysis results and assuming that the fermentation broth has lower droplet sizes (slower creaming) and lower oil fractions than in the mimic emulsion, one would expect that the oil recovery would be similar or lower. By comparing the oil recovery obtained by the column B1a, with no cream or oil on top, and column B1b, with oil on top, and B1d with only cream and oil on top, it is seen that there is an improvement in oil recovery for the last columns. This shows that the aggregation and bursting mechanism, are also present when using fermentation broth. The results shown by Pedraza-de la Cuesta *et al*, also support the existence of the two mechanisms described in this paper, since for experiments with higher oil hold-up in the top of the column, there was a higher degree of coalescence and higher oil recovery (Pedraza-de la Cuesta et al., 2017). Additionally, for the column experiment B1c, the recovery obtained was similar to the one of the synthetic emulsion column experiments at the exact same conditions. This corroborates that oil recovery using GEOR in fermentation broth can be described by the same mechanisms for both mixtures. Nevertheless, large oil recovery could not be reached. Further studies, on emulsion properties, oil fraction and $r_{jet}$, would allow a better use of the present mathematical model to decide on the optimal parameters for achieving larger oil recovery.

## 2.6 Conclusions

A mathematical model describing oil coalescence when a gas bubble is in contact with a region of high oil droplet concentration, has been presented. This model was successfully validated with a synthetic emulsion stabilised by Tween80 and was used to improve oil recovery at laboratory scale. Overall, oil recovery is governed by the aggregation mechanism, and interfacial tension, oil fraction, and oil viscosity revealed to be the parameters with higher impact in the recovery. Owing to the lack of measurable experimental parameters, the model could not be applied for fermentation broth, but provided valuable insight for parameter optimization. When using these parameters, oil recovery was enhanced by 50% over the base case for the columns with oil on top, demonstrating the significant impact of aggregation and bursting mechanisms. The model suggests that oil recovery above 90% could be achieved by increasing the surface area to volume ration of the recovery setup. Yet, relevant parameters such as viscosity, interfacial tension, oil fraction in cream and bubble diameter should be studied and optimized during fermentation to achieve higher oil recovery. In general, the results of this research shed new light on the mechanisms occurring during oil separation by gas-enhanced oil recovery and on the parameters, such as column design and fermentation broth properties, that can be adjusted to optimize the separation and recovery methods at large scale and help to reduce costs in production processes.

## 2.7 Acknowledgements

This work was carried out within the BE-Basic R&D Program, which was granted a FES subsidy as well as a TKI-BBE grant (TKI-AMBIC-program TKIBE-01003) from the Dutch Ministry of Economic affairs. The authors would like to thank Dr. Christian Picioreanu for his contribution in implementing the model in Matlab. To Carla Prat for performing the fermentations and Marcelo Silva and Joana Carvalho Pereira for providing a critical discussion of this work.

## 2.8 References

Al-Shamrani, A.A., James, A., Xiao, H., 2002. Destabilisation of oil-water emulsions and separation by dissolved air flotation. Water Research 36, 1503-1512.

Amyris, 2016. https://amyris.com/innovation/biofene/.

Burghoff, B., 2012. Foam fractionation applications. Journal of Biotechnology 161, 126-137.

Chandran, S.S., Kealey, J.T., Reeves, C.D., 2011. Microbial production of isoprenoids. Proc Biochem 46, 8-8.

Chen, L., Serad, G., Carbonell, R., 1998. Effect of mixing conditions on flocculation kinetics of wastewaters containing proteins and other biological compounds using fibrous materials and polyelectrolytes. Brazilian Journal of Chemical Engineering 15, 358-368.

Cuellar, M.C., Straathof, A.J.J., 2018. CHAPTER 4 Improving Fermentation by Product Removal, Intensification of Biobased Processes. The Royal Society of Chemistry, pp. 86-108.

Cuellar, M.C., van der Wielen, L.A.M., 2015. Recent advances in the microbial production and recovery of apolar molecules. Current Opinion in Biotechnology 33, 39-45.

Dafoe, J.T., Daugulis, A.J., 2014. In situ product removal in fermentation systems: improved process performance and rational extractant selection. Biotechnol. Lett. 36, 443-460.

Dolman, B.M., Kaisermann, C., Martin, P.J., Winterburn, J.B., 2017. Integrated sophorolipid production and gravity separation. Process Biochem. 54, 162-171.

Erler, S., Nienow, A., Pacek, A., 2003. Oil/water and pre-emulsified oil/water (PIT) dispersions in a stirred vessel: Implications for fermentations. Biotechnology and Bioengineering 82, 543-551.

Feng, J., Muradoglu, M., Kim, H., Ault, J.T., Stone, H.A., 2016. Dynamics of a bubble bouncing at a liquid/liquid/gas interface. Journal of Fluid Mechanics 807, 324-352.

Ghabache, E., Séon, T., 2016. Size of the top jet drop produced by bubble bursting. Physical Review Fluids 1, 051901.

Heeres, A.S., Heijnen, J.J., van der Wielen, L.A.M., Cuellar, M.C., 2016. Gas bubble induced oil recovery from emulsions stabilised by yeast components. Chem. Eng. Sci. 145, 31-44.

Heeres, A.S., Picone, C.S.F., van der Wielen, L.A.M., Cunha, R.L., Cuellar, M.C., 2014. Microbial advanced biofuels production: overcoming emulsification challenges for large-scale operation. Trends Biotechnol. 32, 221-229.

Heeres, A.S., Schroen, K., Heijnen, J.J., van der Wielen, L.A.M., Cuellar, M.C., 2015. Fermentation broth components influence droplet coalescence and hinder advanced biofuel recovery during fermentation. Biotechnol J 10, 1206-1215.

Hotrum, N.E., Stuart, M.A.C., Vliet, T.v., Avino, S.F., van Aken, G.A., 2005. Elucidating the relationship between the spreading coefficient, surface-mediated partial coalescence and the whipping time of artificial cream. Colloids and Surfaces A: Physicochemical and Engineering Aspects 260, 71-78.

Janssen, A.C.J.M., Kierkels, J.G.T., Lentzen, G.F., 2015. Two-phase fermentation process for the production of an organic compound WO 2015002528 A1 2015. Isobionics B.V.

Jovanović, I., Miljanović, I., 2015. Modelling Of Flotation Processes By Classical Mathematical Methods – A Review.

Kemiha, M., Olmos, E., Fei, W., Poncin, S., Li, H.Z., 2007. Passage of a Gas Bubble through a Liquid−Liquid Interface. Industrial & Engineering Chemistry Research 46, 6099-6104.

Koh, P.T.L., Schwarz, M.P., 2008. Modelling attachment rates of multi-sized bubbles with particles in a flotation cell. Minerals Engineering 21, 989-993.

Maaß, S., Rojahn, J., Hänsch, R., Kraume, M., 2012. Automated drop detection using image analysis for online particle size monitoring in multiphase systems. Comput. Chem. Eng. 45, 27-37.

Pedraza-de la Cuesta, S., Keijzers, L., van der Wielen, L.A.M., Cuellar, M.C., 2017. Integration of Gas Enhanced Oil Recovery in multiphasic fermentations for the microbial production of fuels and chemicals. tbd.

Ralston, J., Fornasiero, D., Hayes, R., 1999. Bubble–particle attachment and detachment in flotation. International Journal of Mineral Processing 56, 133-164.

Reiter, G., Schwerdtfeger, K., 1992. Characteristics of Entrainment at Liquid/Liquid Interfaces due to Rising Bubbles. ISIJ International 32, 57-65.

Renninger, N., 2010. Scale-up and Mobilization of Renewable Diesel and Chemical Production from Farnesene using US-based Fermentable Sugar Feedstocks, in: Review, D.I.B. (Ed.).

Rubio, J., Souza, M.L., Smith, R.W., 2002. Overview of flotation as a wastewater treatment technique. Minerals Engineering 15, 139-155.

Rude, M.A., Schirmer, A., 2009. New microbial fuels: a biotech perspective. Curr. Opin. Microbiol. 12, 274-281.

Schlichting, H., Gersten, K., Krause, E., Oertel, H., Mayes, K., 1960. Boundary-layer theory. Springer.

Science, K.A.y.s., Pendant Drop.

Simon, M., Schmidt, S.A., Bart, H.J., 2003. The Droplet Population Balance Model – Estimation of Breakage and Coalescence. Chemical Engineering & Technology 26, 745-750.

Singh, K.K., Bart, H.-J., 2015. Passage of a Single Bubble through a Liquid–Liquid Interface. Industrial & Engineering Chemistry Research 54, 9478-9493.

Stewart, Peter S., Feng, J., Kimpton, Laura S., Griffiths, Ian M., Stone, Howard A., 2015. Stability of a bi-layer free film: simultaneous or individual rupture events? Journal of Fluid Mechanics 777, 27-49.

Straathof, A.J.J., 2014. Transformation of Biomass into Commodity Chemicals Using Enzymes or Cells. Chem. Rev. 114, 1871-1908.

Tabur, P., Dorin, G., 2012. Method for purifying bio-organic compounds from fermentation broth containing surfactants by temperature-induced phase inversion, in: Amyris (Ed.). Amyris Inc., US.

Ueda, Y., Kochi, N., Uemura, T., Ishii, T., Iguchi, M., 2011. Numerical Observation of Flow Field around the Water Column behind a Rising Bubble through an Oil/Water Interface. ISIJ International 51, 1940-1942.

Uemura, T., Ueda, Y., Iguchi, M., 2010. Ripples on a rising bubble through an immiscible two-liquid interface generate numerous micro droplets. EPL (Europhysics Letters) 92, 34004.

van de Ven, T.G.M., Mason, S.G., 1977. The microrheology of colloidal dispersions VII. Orthokinetic doublet formation of spheres. Colloid and Polymer Science 255, 468-479.

van Hee, P., Elumbaring, A.C.M.R., van der Lans, R.G.J.M., Van der Wielen, L.A.M., 2006. Selective recovery of polyhydroxyalkanoate inclusion bodies from fermentation broth by dissolved-air flotation. Journal of Colloid and Interface Science 297, 595-606.

Vickers, C.E., Williams, T.C., Peng, B., Cherry, J., 2017. Recent advances in synthetic biology for engineering isoprenoid production in yeast. Current Opinion in Chemical Biology 40, 47-56.

Walstra, P., 1993. Principles of emulsion formation. Chem. Eng. Sci. 48, 333-349.

Walstra, P., 2003. Physical Chemistry of Foods. Dekker

# Chapter 3: Impact of flocculant addition in oil recovery from multiphasic fermentations

**Abstract** Emulsion formation is a major concern when dealing with multiphasic fermentations. Flocculants can be used together with other demulsification techniques to improve oil recovery in multiphasic fermentations. In this paper, the impact of adding flocculants during a multiphasic fermentation with 10 wt% dodecane, to destabilize the broth emulsion, improve creaming formation and enhance oil recovery is studied. Flocculants, $CaCl_2$ and $(NH_4)_2SO_4$ were shown to be the most promising flocculants. Flocculant addition, their time of addition, and its impact on multiphasic fermentations has been evaluated by comparing fermentation performance against reference fermentations and three oil recovery methods: gravity settling, gas enhanced oil recovery and centrifugation. When adding 75 mM of $(NH_4)_2SO_4$ during fermentation, the creaming rate during gravity settling increased 3-fold and the oil recovery by gas enhanced oil recovery was 35%, without altering fermentation performance. Addition of $CaCl_2$ during fermentation resulted in 88% and 67% oil recovery for early and late addition, which is a 4 and 3-fold increase in comparison with the reference. Yet, $CaCl_2$ deviated from standard fermentation performance when added immediately after second phase addition. In conclusion, flocculant addition during multiphasic fermentation can be used to destabilize microbial emulsions and potentially improve in-situ oil recovery.

**Keywords:** Multiphasic Fermentation; Emulsion; Flocculation; Proteins; Oil Recovery;

Published as: R.M. Da Costa Basto, M. Jiménez, R.F. Mudde, L.A.M. van der Wielen, M.C. Cuellar, Impact of flocculant addition in oil recovery from multiphasic fermentations, Food and Bioproducts Processing, Volume 123, 2020, Pages 150-163

## 3.1 Introduction

Multiphasic fermentations, where an organic product phase is spontaneously formed or when an organic solvent is added for product removal, have been of investigated for the production of bio-based commodity compounds (Straathof 2014) as well as speciality products, such as sesquiterpenes (Beller et al., 2015; Straathof and Cuellar, 2019). Sesquiterpenes are hydrocarbons with the chemical formula $C_{15}H_{24}$ that are produced via the terpenoid pathway in plants and microorganisms. The recent advances in microbial engineering have promoted the production of these compounds via fermentation. Products, such as, ß-farnesene, artemisinin and squalene, are already being produced at industrial scale (Benjamin et al., 2016; Kung et al., 2018) for applications ranging from fuels and lubricants, to pharmaceuticals, flavors and fragances.

The hydrophobicity of the organic phase creates an opportunity for in-situ product removal (ISPR) at industrial scale, by integrating fermentation with a low cost recovery method improving its productivity, avoiding product degradation and/or product toxicity, and reducing downstream costs (Cuellar and Straathof, 2018; Dafoe and Daugulis, 2014). For simplicity, we refer to all these compounds as “oils” in this work. Unfortunately, during the fermentation, stirring and surface-active components (SAC’s) present in the fermentation broth often create an oil-water (O-W) emulsion, instead of coalescence to separate phases (Heeres et al., 2014). Emulsion formation can lead to fermentations with higher viscosity and less efficient stirring and, consequently, lower mass transfer. Moreover, it can hinder product recovery after fermentation (Cuellar and Straathof, 2018). This will directly affect process costs and product price. A way to overcome this problem is to promote coalescence inside the bioreactor.

Emulsion stability is dependent on different factors such as stirring, droplet size, viscosity and the type of SACs (e.g.: salts, lipopeptides, phospholipids, glycolipids, proteins, cells and cells debris). From these, proteins are known to have a large impact in droplet stabilization (Delahaije et al., 2015; Furtado et al., 2015; Heeres et al., 2015; Singh and Ye, 2020). Proteins have three type of stabilization mechanisms: surface cohesion, steric and hydrostatic repulsion, and molecular flexibility. These mechanisms cause proteins to reshape their ternary structure, in order to maximize the number of interactions with their neighbouring

proteins (e.g.: hydrogen bonds, electrostatic bond, etc) (Damodaran, 2005; McClements, 2004). An increase in the number of interactions equals to a more stabilized droplet interface and, consequently, higher emulsion stability.

Demulsification techniques, such as mechanical processes (e.g: centrifugation, membranes, hydrocyclones) (Furtado et al., 2015; Heeres et al., 2014; Nylander et al., 2019; Tabur and Dorin, 2012), chemical methods (e.g.: addition of chemical de-emulsifiers, change in temperature, change in pH, addition of flocculants) (Dickinson, 2019; Heeres et al., 2014; Li et al., 2017; Setiowati et al., 2017; Van Hamme et al., 2006), biological transformation and additives (e.g.: decrease of cell content, type of substrate and nitrogen source and culture age, enzyme addition) (Liu et al., 2016; Nadarajah et al., 2002; Rocha E Silva et al., 2017), electrical methods and microwave irradiation (Cañizares et al., 2007; Zolfaghari et al., 2016) are widely reported for uses in food, petrochemical, waste water and pharmaceutical industries (International, 2015). Large scale production of bio-based products commonly use centrifugation, de-emulsifiers and temperature or pH swings to break microbial emulsions (Huang et al., 2001; Renninger and McPhee, 2010; Renninger et al., 2011; Tabur and Dorin, 2012). Yet, most of these techniques cannot be integrated into fermentation, restricting ISPR, and can compromise product purity, which will infer in further purification steps.

Low-cost and mild alternatives for oil recovery during fermentation, such as gravity separation and gas enhanced oil recovery (GEOR), have recently been proposed and successfully tested in-line with a bioreactor at laboratory (Dolman et al., 2017; Heeres et al., 2016; Pedraza-de la Cuesta et al., 2017) and at pilot scale (Steinbusch, 2019). The in-line gravity separator proposed by Dolman et al. 2017 makes use of the density difference between product and medium to create a concentrated emulsion. By adding this separator during fermentation, there was a decrease in the bioreactor volumes and in fermentation time (Dolman et al., 2017). Still, this technology requires additional steps to recover the oil as a single phase, potentially incurring into higher costs. GEOR, on the other hand, relies on the affinity between oil droplets and gas bubbles and aims to generate a single oil layer (Heeres, 2016). Previous studies showed that one of the key factors for the oil separation is the creaming (defined as the rising of oil droplets against gravity)(Damodaran, 2005). It was observed that when an emulsion had the capacity to cream, oil recovery by GEOR could be achieved. However, the oil recovery achieved during the fermentation process is generally

low (10% - 30% oil recovery) due to small oil droplet size, back-mixing and SACs (Da Costa Basto et al., 2019b; Pedraza-de la Cuesta et al., 2017). In contrast, mechanical methods combined with de-emulsifiers and temperature swings, such as centrifugation, have been reported to recover 90% of the oil in fermentation broth emulsion (Tabur and Dorin, 2012). However, the use of centrifugation is more energy intensive, more costly and cannot be incorporated into a single equipment.

The use of flocculants to destabilize protein emulsions has been widely studied in literature. If protein interactions are weakened, droplet to droplet interactions can be increased and droplets can aggregate creating the phenomena known as flocculation (McClements, 2004; Tadros, 2013). This phenomenon allows to generate droplets aggregates, which rise easier to the top, promoting oil separation but also to promote coalescence of the oil droplets into a single phase. There are numerous chemical compounds with flocculant properties. These compounds can be divided in different groups dependent on their destabilization mechanisms (e.g.: reduce steric repulsion, reduce molecular flexibility, shielding electrostatic repulsion) and flocculant capacity (Choi et al., 2003; Damodaran, 2005; Dickinson, 2010; Nylander et al., 2019). Moreover, flocculants have also been widely used throughout the years in wastewater treatment. These compounds promote bacterial cell flocculation to enhance solid/liquid (S/L) separation. Studies have been performed on using chitosan as flocculant agent in *E.coli* fermentations, however, most of them led to cell damage and death (e.g.: by breaking the cell walls) (Ojima et al., 2018; Rehn et al., 2013; Yang et al., 2014).

Based on a literature review, economic potential and environmental impact of each compound, it is observed that the most promising flocculants to be used during fermentation are inorganic salts. The advantage of using salts over polymers is that some of the salts with flocculant capacity are already incorporated in fermentation medium and can be easily adjusted to enhance droplet flocculation. The disadvantage is that most of the salts can be harmful to the environment. Although literature reports that di- and trivalent ions ($CaCl_2$, $CuSO_4$, $FeCl_3$) have higher flocculant capacity than monovalent ions ($(NH_4)_2SO_4$, NaCl, KCl) (McClements, 2005), NaCl, $CaCl_2$ and $(NH_4)_2SO_4$ are the ones depicting lower cost and lower environmental hazard (Table 1). A disadvantage is that in high concentrations (> 0.2 mM) (PubChem, 2019), $(NH_4)_2SO_4$ can cause eutrophication in aquatic environment. Yet, this compound is vastly used in industry and standard wastewater treatment.

In this work, the impact of adding flocculants during a sesquiterpene fermentation to destabilize the microbial emulsion, improve creaming formation and oil recovery was studied. Two flocculants, $CaCl_2$ and $(NH_4)_2SO_4$, were used. Based on literature review, preliminary tests and environmental and economic impact, two concentrations were chosen for each flocculant: 10 and 20 mM and 50, 75 mM, respectively. The use of $(NH_4)_2SO_4$ was selected, since its monovalent ion ($NH_4^+$) is already being used in the fermentation medium (15 mM) and water treatment is already in place. The oil recovery when adding flocculants was assessed by comparing three demulsification techniques (centrifugation, gravity settling and GEOR) used in microbial fermentation emulsions.

**Table 1 –** Summary of flocculants agents used to destabilize protein emulsions, their cost and environmental considerations based on the Globalized Harmonized System (GHS)(Nations, 2017).

| Type of Flocculants | Description | Compounds | Cost ($/MT) | Environmental Impact | Tested in fermentation | Tested in protein stabilized emulsions |
|---|---|---|---|---|---|---|
| **Salts** | Ionics compounds shield the charges surrounding the proteins, minimizing electrostatic repulsions. Di- or trivalent ions have the capacity of bridging proteins due to electrostatic interactions. | NaCl | 50-150 (a) | No environmental impact | (Salehizadeh et al., 2000) | (Azarikia et al., 2017; Rangsansarid and Fukada, 2007; Sarkar et al., 2016) |
| | | KCl | 220 (b) | Harmful to aquatic life | (Salehizadeh et al., 2000) | (Keowmaneechai and McClements, 2002) |
| | | $CaCl_2$ | 300 (c) | No environmental impact | (Salehizadeh et al., 2000; Stewart, 2003) | (Azarikia et al., 2017; Keowmaneechai and McClements, 2002; Sarkar et al., 2016) |
| | | $(NH_4)_2SO_4$ | 130-150 (d) | Harmful to aquatic life with long lasting effect due to excessive ammonia. | (Stratford, 1992) | (Moelbert et al., 2004) |
| | | $CuSO_4$ | 1725 (e) | Very toxic to aquatic life | (Abolhassani and Astaraie, 2010) | (Silvestre et al., 1999) |
| **Polymers and solvents** | The most common mechanisms are bridging and depletion flocculation. The first one occurs when the polymer acts as a bridge between proteins, coating the droplet. The second occurs when two | Arabic Gum | 5085 (f) | No environmental impact | - | (Dickinson, 2003) |
| | | Xantham Gum | 1100-1600 (g) | No environmental impact | - | (Krstonošić et al., 2015; Ye et al., 2004) |

| Type of Flocculants | Description | Compounds | Cost ($/MT) | Environmental Impact | Tested in fermentation | Tested in protein stabilized emulsions |
|---|---|---|---|---|---|---|
| | droplets are in proximity and due to the polymer between droplets, a gradient in osmotic pressure is formed. Solvents also have the ability of displacing molecules from the interphase by establishing interactions with proteins. | PEG10 000 | 1500 (h) | No environmental impact | - | (Losso and Nakai, 2002; Syrbe et al., 1998) |
| | | Butanol | 800-900 (i) | No environmental impact but highly flammable | (Furtado et al., 2015) | - |
| **Cross-linking Agents** | Polyfunctional molecules can create intermolecular bonds between proteins of different droplets and bridging flocculation can occur. Additionally, the creation of intermolecular bonds causes severe loss in protein flexibility which causes the droplet interface to rigidize making it more sensitive to shear. | Glutaraldehyde | 2480-2550 (j) | Highly toxic for aquatic life | (Wumpelmann and Mollgaard, 1990) | (Park et al., 2000; Sheldon, 2007) |

(a) Langfang Huinuo Fine Chemical, Co., checked at March 2019 (Alibaba)
(b) Index Mundi, commodity prices, https://www.indexmundi.com/commodities/?commodity=potassium-chloride
(c) Intratec solution, price at February 2015, www.intratec.us/chemical-markets/calcium-chloride-price
(d) Zouping Boyi chemical industry Co., checked at March 2019 (Alibaba)
(e) Kemcore, flotation reagents, https://www.kemcore.com/copper-sulphate-pentahydrate-96.html.
(f) Nanjing Gemsen International Co., checked March 2019 (Alibaba)
(g) FoodChem International Corporation, checked March 2019 (Alibaba)
(h) Zibo Aojin Chemical Co., checked March 2019 (Alibaba)
(i) ICIS
(j) Purex, focus on quality chemicals, checked March 2019 (Alibaba)

## 3.2 Materials and Methods:

### 3.2.1 Materials

The impact of flocculant addition on oil recovery was tested with two mixtures: a synthetic emulsion and a fermentation broth from a sesquiterpene fermentation operating with in-situ solvent extraction of the product. Synthetic emulsion (section 3.2.2.1) was prepared with MilliQ water (18.2 MΩ, Millipore systems), whey protein isolate (WPI) (Bulk Powders) and hexadecane (Sigma Aldrich, Reagent Plus) coloured with Oil Red O dye (Sigma Aldrich). The emulsion from fermentation broth (section 3.2.2.2) was prepared with dodecane (Sigma Aldrich, Reagent Grade) also coloured with Oil Red O dye. Flocculant stock solutions were prepared with MilliQ water and either $CaCl_2*2H_2O$ (Merck, Reagent Grade) or $(NH4)_2SO_4$ (Merck, Reagent Grade).

### 3.2.2 Emulsion Preparation

#### 3.2.2.1 Synthetic Emulsion

The synthetic emulsion, used for testing different flocculants during preliminary tests, was prepared by adding 0.18 wt.% of WPI, 10 wt% of coloured hexadecane and MilliQ water to a beaker. An external coil connected to a water bath (Eco Gold E4G, Lauda) was set around the beaker to keep a constant temperature of 30°C throughout emulsion preparation. During the first 10 minutes, the WPI was stirred with water using a magnetic stirrer (RET Basic C, IKA). After that, the coloured hexadecane was poured and stirred for 5 minutes. Finally, the mixture was homogenized with an Ultra-Turrax (IKA, Ultra-Turrax T25) at 24 000 rpm.

#### 3.2.2.2 Emulsion from Fermentation Broth

The fermentation broth used in this work was obtained from 6 fermentations performed with a recombinant, sesquiterpene producing *E. coli* strain. Pre-culture I (with 50 mL Lysogeny broth (LB) medium, 10 g $L^{-1}$ $C_6H_{12}O_6{\cdot}H_2O$ and 0.005 g $L^{-1}$ of Carbenicilin) was inoculated with 0.5 mL of stock culture in LB medium with 25% v/v glycerol and grown in a rotatory shaker (Certomat BS-1, Sartorius) at 30 °C and 250 rpm for 15 hours. After 15 hours of incubation,

Pre-culture II (with 200 mL LB medium, 10 g $L^{-1}$ $C_6H_{12}O_6 \cdot H_2O$ and 0.005 g $L^{-1}$ of Carbenicilin) was inoculated from Pre-culture I in a sufficient amount to reach an initial OD600 of 0.2 and grown in the rotatory shaker at 37 °C and 250 rpm during 6 hours. For all fermentations, the microorganisms were cultivated aerobically at 30 °C in fed-batch mode in a medium containing glycerol as carbon source and ammonium sulphate as nitrogen source. The general fermentation protocol followed the protocol described by Pedraza de la Cuesta *et al* (Pedraza-de la Cuesta et al., 2017) with an aeration rate of 1 L $min^{-1}$ and pH 6.3. The pH was controlled by adding phosphoric acid (3 M $H_3PO_4$). Foam was controlled by manual addition of 10% v/v pluronic L-81 (Sigma Aldrich). The batch medium was formed by: 1.3 g $L^{-1}$ $MgSO_4 \cdot 7H_2O$, 4.2 g $L^{-1}$ $KH_2PO_4$, 12 g $L^{-1}$ $K_2HPO_4$, 2 g $L^{-1}$ $(NH_4)_2SO_4$, 1.7 g $L^{-1}$ citric acid, 0.008 g $L^{-1}$ EDTA and 30 g $L^{-1}$ of glycerol; The feed medium was formed by: 12 g $L^{-1}$ $MgSO_4 \cdot 7H_2O$, 0.013 g $L^{-1}$ EDTA and 200 g $L^{-1}$ of glycerol. The fermentation conditions and general composition at the time of harvest are summarised in Table 2.

Once the OD600 reached a value of approximately 40, usually after 4 hours of the starting of the constant feeding rate, the temperature of the reactor was reduced to 25 °C. After 1 hour 0.1 mM of Isopropyl β-d-1-thiogalactopyranoside (IPTG) solution was added to start induction. One hour after induction, dodecane was added as second phase in the reactor to reach 15% v/v at the time of harvest. Antifoam was added in three pulses after the addition of dodecane (fermentation time: 22, 23 and 40 hours) to keep the antifoam concentration constant after feed dilution.

To assess the impact of $CaCl_2$ flocculant on the maximum growth rate and cell content during batch cultivation, a set of pre-cultures (with and without flocculant) with the compositions defined above, were grown in shake flask.

**Table 2 -** Fermentation conditions of all 6 fermentations used for testing the impact of flocculant addition on the emulsion stability.

| | |
|---|---|
| **Time of harvest[1] (h)** | 63.0 |
| **Time of addition of Dodecane[1] (h)** | 22 |
| **Fermenter Volume (L)** | 2 |
| **Power Input (rpm)** | 1200 |
| **Average Power Input (kW/m$^3$)** | 6.4 |
| **Cell density [2] ($g_X/kg_{broth}$)** | 20 |
| **Dodecane [2] (% v/v)** | 14 |
| **Air inflow (L/min)** | 1 |

[1]Being time 0 the start of the batch phase.

[2]At the time of harvest.

### 3.2.3 Flocculant addition

After preliminary tests, the selected flocculants were: 10 and 20 mM $CaCl_2$ and 50 mM and 75 mM $(NH_4)_2SO_4$; These flocculants and concentrations showed to have the highest oil recovery by centrifugation and gravity settling at smaller scale (results not shown). The flocculants were added to 4 independent fermentations and to the synthetic emulsion (see Table 3). For the fermentation, only the highest concentration of $(NH_4)_2SO_4$ was tested since there was not a great impact in the oil recovery for 50 mM of this flocculant with synthetic emulsion (see section 3.3.2.1 and 3.3.2.2). Moreover, for $(NH_4)_2SO_4$ the addition of flocculant had to be done from the beginning of the fermentation since this compound was already included in the medium recipe (see section 3.2.2.2). For $CaCl_2$, the flocculant was only added after dodecane addition since the main goal was to study the flocculant impact in oil recovery. The addition of flocculant to the fermentation broth was made as injection pulses at different fermentation times to correct for the dilution caused by the feed. The different methods of addition and respective concentration are presented in Table 3.

**Table 3 –** Flocculant addition to the fermentation broth and synthetic emulsion and their respective concentration.

| | Flocculant and method of addition | Concentration (mM) |
|---|---|---|
| | **Fermentation** | |
| F1 | Reference Fermentation[1] | - |
| F2 | Reference Fermentation[1] | - |
| F3 | Early addition of $(NH_4)_2SO_4$ at the beginning of the batch with an initial concentration of 140 mM | 75 |
| F4 | Early addition of $CaCl_2$ immediately after dodecane addition.[2] | 20 |
| F5 | Late addition of $CaCl_2$ as a pulse 1 h before harvest. | 10 |
| F6 | Late addition of $CaCl_2$ as a pulse 1 h before harvest. | 20 |
| | **Synthetic Emulsion** | |
| SE | Reference synthetic emulsion | - |
| SE1 | $CaCl_2$ | 20 |
| SE2 | $(NH_4)_2SO_4$ | 50 |

[1] With an Ammonium Sulphate concentration at the beginning of the batch of 58 ± 7 mM.

[2]Additional pulses were made to correct for the dilution by the feed.

### 3.2.4 Oil Recovery Experiments

Oil recovery experiments were performed using the different fermentation broth as described in section 3.2.2.2. Three different methods were compared: centrifugation, GEOR and gravity settling.

For the centrifugation tests, 5 mL were transferred to a glass tube and centrifuged for 15 min at 4000 rpm (Heraeus, Multifuge 1 L-R). Three samples were used for the test (Table 4). After centrifugation, pictures of every tube were taken to quantify the amount of oil released.

**Table 4 –** Fermentation samples used to test enhancement of oil recovery by centrifugation.

| Sample | Time of sample | Fermentation time |
|---|---|---|
| S1 | ≈ 16 h after dodecane addition | 38 h |
| S2 | ≈ 21 h after dodecane addition | 43 h |
| S3 | End of fermentation | 63 h |

For GEOR and gravity settling, oil recovery was only measured at the time of harvest (end of fermentation, 63h). GEOR experiments used a similar set-up and protocol as described by Heeres et al, 2016 (Heeres et al., 2016). Gas sparging was generated by single orifice nozzles with 0.1 mm diameter nozzle ($d_{nozzle}$) and a superficial gas velocity of 0.1 cm/s. The air supply pressure was set at 3 bar and monitored using a manometer. An extra manometer was added between the mass flow controller and the column to warn in case of nozzle blockage. For the 6 fermentations, 150 mL of fermentation broth was added to the glass column. To the top of the mixture, 2.2 cm of uncolored oil was added (Da Costa Basto et al., 2019b). After 2 h sparging, the gas flow was stopped, the mixture was left to phase-separate for 1 h and the volume of clear oil recovered was determined.

Gravity settling experiments were performed for the 6 fermentations by transferring 150 mL of the fermentation broth to a glass column (same column as for GEOR) and let it settle for 2 h. At the end, the concentrated oil layer formed was measured and the creaming rate (CR) could be calculated. For both GEOR and gravity settling experiments pictures were taken throughout the experiment, as described in section 3.2.5.1.

## 3.2.5 Analytic Tools and data processing

### 3.2.5.1 GEOR and gravity settling pictures

To monitor the amount of oil recovered during experiments, pictures were taken with a camera (EOS 200D, Canon) using a fixed set-up. In all cases, flash was used to preserve brightness of the pictures. Photos were taken every 1 min for the first 10 min, every 2 min for 10 minutes more, every 5 min for the next 15 minutes and after that, every 10 minutes until the end of the experiment (2 h).

#### 3.2.5.2 Creaming rate and oil recovery measurements

Oil recovery was quantified by measuring the amount of clear oil layer (i.e. oil fraction $\phi_{oil}$ = 1) formed during experiments. For each experiment, the set of pictures was analysed using the software *Image J* to measure pixel height. The conversion from pixels to cm (CF) can be done (Equation 1), since both column diameter ($d_{column}$ = 3.6 cm) and centrifuge tube diameter ($d_{tube}$ = 1.5 cm) are known. The creaming rate (CR) was estimated by equation 2. For both synthetic emulsion and fermentation broth, the cream volume ($V_{cream}$) was measured using the first picture at which the boundary between cream and broth (or water for the synthetic emulsion) was defined and the height of cream would not change in time (see Figure 1). The oil recovery was attained with the area of the column ($A_{column}$) or of the centrifuge tube ($A_{tube}$) and the oil volume recovered can be calculated by Equation 3. Where n, is column or tube and i can be oil or cream. The oil fraction ($\phi_{oil}$) for cream in fermentation broth is assumed to be 0.5 while in synthetic emulsion was measured to be 0.7 (Da Costa Basto et al., 2019a).

$$\mathrm{CF\ (px/cm)} = \frac{\mathrm{d_n(px)}}{\mathrm{d_n(cm)}} \quad (1)$$

$$\mathrm{CR\ (mL/min)} = \frac{\mathrm{V_{cream}}}{\mathrm{t_0 - t_{min}}} \quad (2)$$

$$\mathrm{V}_i\ \mathrm{(mL)} = \phi_{oil} \cdot \mathrm{H_i(px)} \cdot \frac{1}{\mathrm{CF}}\mathrm{(cm/px)} \cdot \mathrm{A_n(cm)} \quad (3)$$

The percentage of oil recovery then becomes:

$$\mathrm{Recovery\ (\%)} = \frac{\mathrm{V_{oil,recovered}(mL)}}{\mathrm{V_{oil,total}(mL)}} \cdot 100 \quad (4)$$

In case of fermentation broth, the fraction of antifoam (AF) added during fermentation was subtracted to obtain the percentage of oil recovery (Equation 5) (Da Costa Basto et al., 2019a).

$$\mathrm{Recovery\ (\%)} = \frac{\mathrm{V_{oil,recovered}(mL) - V_{AF}(mL)}}{\mathrm{V_{oil,total}(mL)}} \times 100 \quad (5)$$

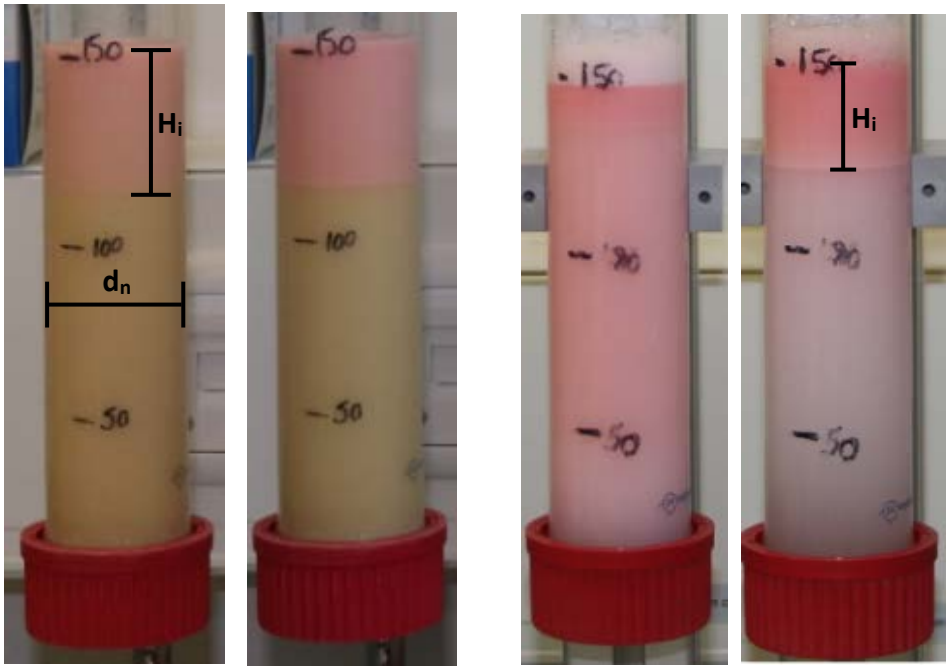


**Figure 1 –** Measuring height of the creaming rate for fermentation broth (F3) and synthetic emulsion (SE) showing the boundaries and difference in cream height change.

### 3.2.5.3 Microscopic Pictures

Microscopic pictures were taken of samples with and without oil and flocculant. In order to do that, a small drop of 10 µL was taken from homogenous broth and observed under the microscope. To take the pictures, a camera with an adaptor for the microscope (Canon G12, Carl Zeiss 42126) was used.

### 3.2.5.4 Fermentation Performance

In order to assess the effect of the flocculants in fermentation performance, two parameters were compared: biomass content ($N_X$) and $CO_2$ production during the fed-batch. The mass and carbon balances were calculated as in Pedraza *et al* (Pedraza-de la Cuesta et al., 2017). For F4 fermentation, the carbon balance could not be attained for lack of offline analysis.

#### 3.2.5.5 Online analyses

The pH, dissolved oxygen (DO) and temperature were measured with online probes (Applikon). The feed rate and base addition were continuously monitored with a scale (Meter-Toledo; Sartorius). The $CO_2$ and $O_2$ concentrations in the bioreactor were analyzed by a continuous off-gas analyzer (NGA-2000 Fischer Rosemount). All sensors, off-gas analyzer and scales were connected to a control unit (Applikon) which recorded the broth parameters in a minute basis with a Multi Fermentor Control System (MFCS)/Win 2.1 Software (Sartorius Stedim Biotech S.A.).

#### 3.2.5.6 Cell dry weight

Cell dry weight was measured by centrifuging 1.5 mL of broth at 13,000 rpm (Hearaeus, Biofuge Pico) for 5 minutes. Prior to centrifugation, the tubes with sample were weighted. After disposal of the supernatant, an additional washing step was made by adding 1 mL of MiliQ water and ressuspending the pellet, followed by another centrifugation step as prior described. This extra washing step removed the salts from the pellet allowing a better quantification of cell dry weight. The tubes with the pellet were dried in an oven (Heraeus instruments) at 105°C for 48 h. Afterwards the tubes containing the dry pellet were weighted. For fermentation F4 (see Table 3), the samples after flocculant addition could not be measured (see section 2.3.1) and cell density at the time of harvest could not be confirmed by CDW measurements.

#### 3.2.5.7 Protein analysis

A sample of 50 mL was centrifuged (Heraeus instruments, Stratos) at 17,000 rpm for 20 min and 4°C. Afterwards, 25 mL of supernatant were added in a falcon tube for total nitrogen analysis (TNM-L, Shimadzu). From the same supernatant sample, 2 mL were taken to measure ammonia by a Hagh Lange Ammonium test (LCK303, Hagh Lange) in the range of 2 - 47 mg/L $NH_4$-N and following the protocol provided by the kit. The total organic nitrogen was obtained by subtracting the value of ammonia to the total nitrogen. Using a correction factor from literature (Mariotti et al., 2008) the protein concentration can then be obtained (Equation 6).

$$C_{prot}(mg/L) = C_{N,organic} \cdot 6.25 \quad (6)$$

#### 3.2.5.8 Statistical Analysis

The statistical significance between reference and mixture with flocculant addition, was evaluated for the synthetic emulsion and fermentation broth by a one-sample student's t-test, where the mean of the reference fermentation was compared with a specified value of the fermentation with flocculant addition. The confidence interval was assumed to be 95%.

## 3.3 Results and discussion

### 3.3.1 Impact of flocculants in fermentation performance

In 5 independent fermentations, carbon balances were calculated and they closed with less than 3 % gap. In F4 cell content could not be measured by the method in section 3.2.5.4 due to cell flocculation in the cream. Without these data, balances could not be closed. Profiles, such as cell mass, $CO_2$ production (Figure 2) and dissolved oxygen (results not shown) indicate that all fermentations, excluding F4, were comparable in terms of fermentation performance.

From the six performed fermentations, only F3 has flocculant from the beginning of the batch. For this case, the maximum growth rate ($\mu_{max}$) at the beginning of the fed-batch was also tested. The results are presented in Table 5. It is observed that for F3, the addition of flocculant does not have an influence on the cell content and in the maximum growth rate of the microorganisms during batch phase. When adding $CaCl_2$, there is no statistically significant difference between the reference and the shake flask pre-culture for the biomass content (p-value=0.1>0.05) and maximum growth rate (p-value=0. 4>0.05) during batch phase.

The experimental profiles of F3 followed the same trend as the reference fermentations. Yet, for F4, the $CO_2$ production was higher than for the reference fermentation and F3. The correlation of the $CO_2$ profiles for F3 and F4 with the reference fermentation were assessed by calculating the correlation coefficient ($R^2$). For F3 and F4 the $R^2$ are 0.99 and 0.90, respectively. These results indicate that fermentation F4, although has a high correlation coefficient for the $CO_2$ profile, is influenced by the addition of flocculant, suggesting that it affected fermentation performance. This can also be observed by the increase in protein concentration (see appendix – Section 3.7). Still, fermentation F4 was used for oil recovery

comparison with the other fermentations to better understand the impact of cell flocculation and protein concentration. $(NH_4)_2SO_4$ addition to the fermentation, at the concentrations tested, do not seem to affect its performance.

**Table 5 –** Biomass present in the reactor at the beginning of the fed-batch ($N_X$ (mol)) and average maximum growth ($\mu_{max}$) between reference fermentations (F1, F2, F5 and F6) and fermentation/shake flasks with early addition of flocculants (F3 - $(NH_4)_2SO_4$ and $CaCl_2$).

| **Fermentation** | **$N_X$ (mol)** | | **$\mu_{max}$ (1/h)** | |
|---|---|---|---|---|
| Reference | 0.609 ± 0.028 | | 0.442 ± 0.015 | |
| F3 | 0.641[1] | | 0.437[1] | |
| **Shake Flasks** | **$N_X$ (mol)** | **p-value** | **$\mu_{max}$ (1/h)** | **p-value** |
| Reference | 0.0014 ± 1E-4 | | 0.459 ± 0.003 | |
| $CaCl_2$ flocculant | 0.0013 ± 0.7E-5 | 0.1 | 0.462 ± 0.009 | 0.4 |

[1] Only one fermentation performed.

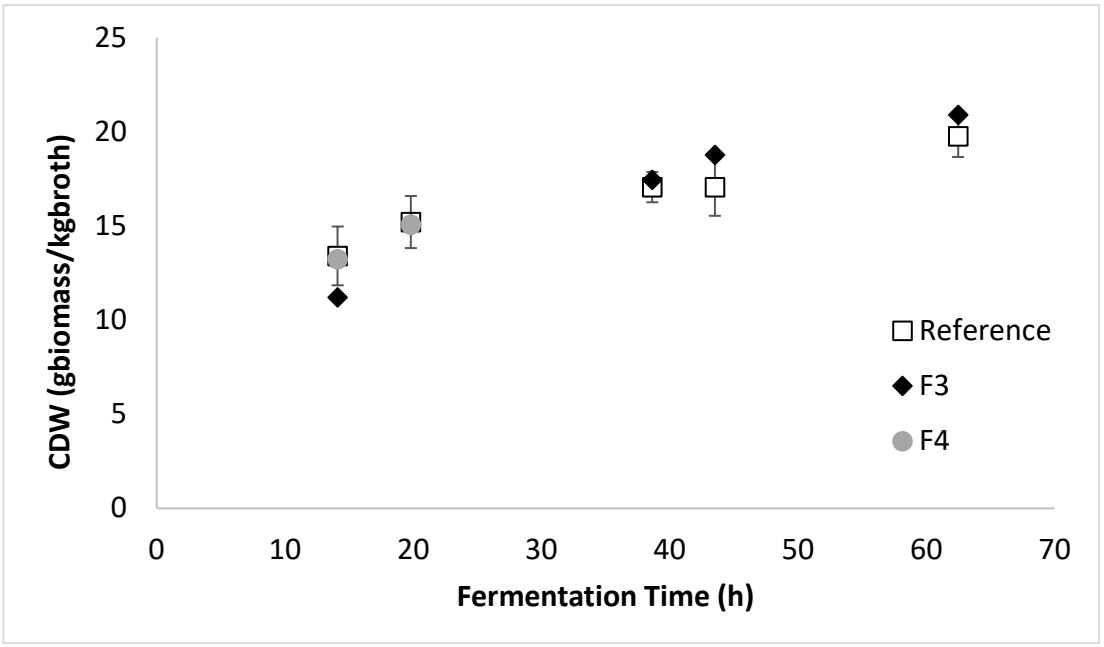


**[A]**

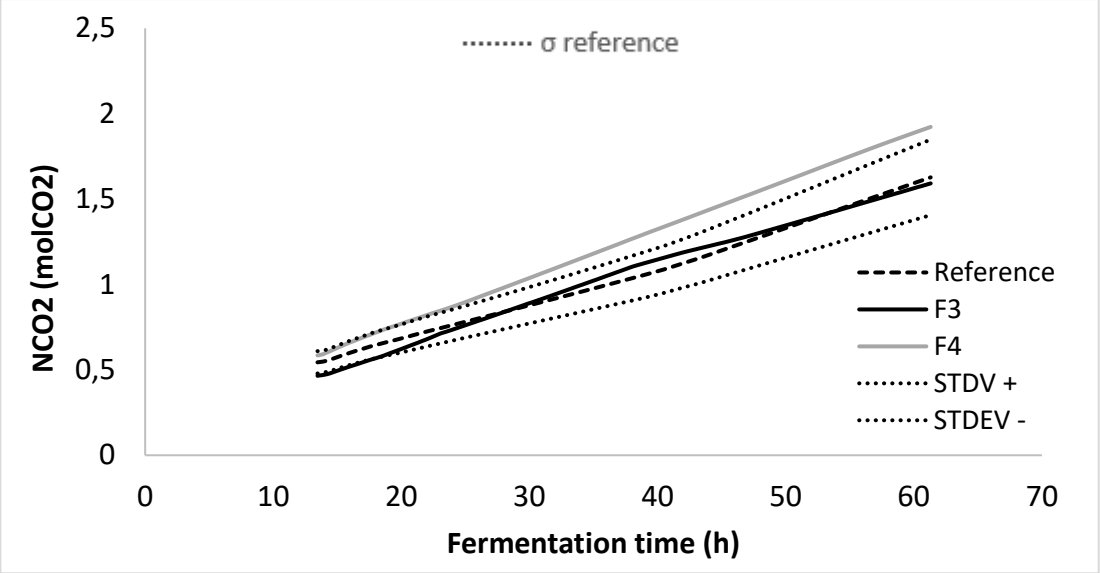


**[B]**

**Figure 2 –** [A] Total biomass in the reactor and [B] $CO_2$ production for reference fermentations and fermentation with early addition of flocculants (F3 and F4). The error bars and dotted line represent the standard deviation of the reference fermentations.

## 3.3.2 Enhancement of oil recovery by addition of flocculants

### 3.3.2.1 Impact on gravity settling

The creaming rate for the synthetic emulsion and fermentation emulsion, with and without flocculant, is depicted in Table 6.

The synthetic emulsion containing $(NH_4)_2SO_4$ (SE2) displayed a creaming rate approximately 20% higher than the reference mimic emulsion (reference SE). In contrast, for the $CaCl_2$, the creaming rate did not change yet, the time for the cream to start being formed was almost instantaneous (1 min). When looking to the fermentation broth emulsion, it was observed that fermentation F3, where 75 mM $(NH_4)_2SO_4$ was used, displayed a creaming rate 3 times higher than the reference fermentation. Moreover, the time that it took for a cream layer to start being formed was almost doubled in the reference fermentation compared to F3. This shows the potential of using $(NH_4)_2SO_4$ to enhance oil recovery by gravity settling. For fermentation broths where $CaCl_2$ was added (F4, F5 and F6), the creaming rate could not be quantified. When adding the flocculant, there was no apparent difference between the broth inside the fermenter for the reference fermentation and the fermentation with flocculant.

However, upon gravity settling, both broths behaved differently (see Figure 3). For the reference fermentation, the cream started being formed at the top of column and increased with time. For the emulsion with $CaCl_2$, an emulsion de-watering was observed, where the cream layer also containing cells, started being formed at the bottom of the column and moved upwards. Although this change in behaviour might not be beneficial for oil recovery by gravity settling, it shows that the $CaCl_2$ promotes cell flocculation.

When comparing fermentation broth emulsion with the synthetic emulsion, the creaming rate of the reference fermentation is higher than for the synthetic emulsion. This can be explained by the fact that the synthetic emulsion takes more time to form than the fermentation broth (see Figure 1). However, in the synthetic emulsion, the only stabilizer are proteins whereas in fermentation broth there are other type of stabilizers components (Heeres et al., 2014). In the synthetic emulsion, more droplets rise to the top, taking more time to reach the final cream layer. Hence, the oil fraction in the final cream layer of the synthetic emulsion is higher. When $(NH_4)_2SO_4$ is added to the synthetic emulsion, it would decrease the electrostatic repulsion created by the proteins around the droplet and enable droplet coalescence and flocculation. However, in fermentation broth, the flocculant is not only interacting with the proteins but also with the other stabilizers around the droplets, which implies a larger change in creaming rate and time of cream formation.

**Table 6 –** Creaming rate and standard deviation of fermentation broth with (F3) and without (F1 and F2) flocculant and synthetic emulsion with (SE1 and SE2) and without addition of flocculants. For fermentations where $CaCl_2$ was used (F4, F5 and F6), the creaming rates could not be measured.

| Experiment | Time for cream formation (min) | Creaming rate [mL/min] | p-value |
|---|---|---|---|
| Reference | 22 | 0.732 ± 0.07 | |
| F3 | 14 | 2.8 | - |
| Reference SE | 60 | 0.509 ± 0.002 | |
| SE1 | 60 | 0.513 ± 0.008 | 0.187 |
| SE2 | 60 | 0.621 ± 0.003 | 0.016 |

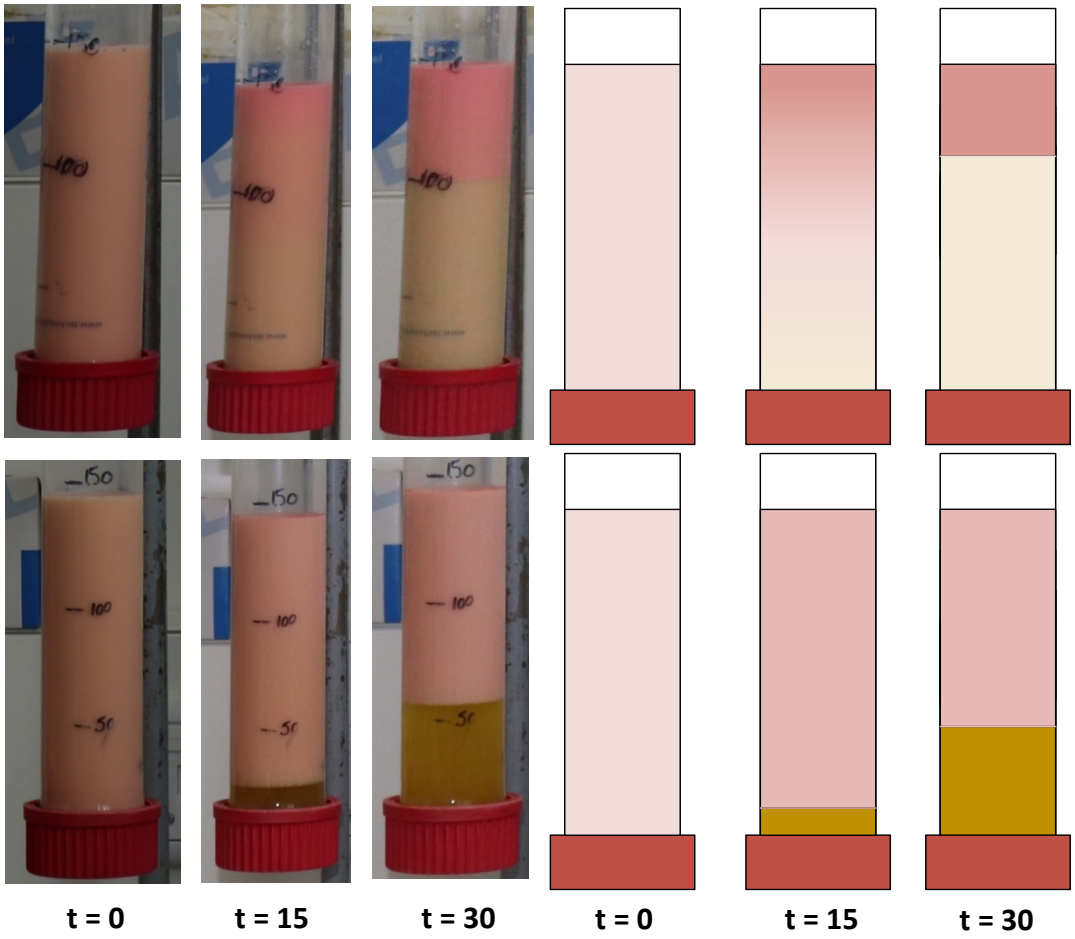


**Figure 3 –** Picture and schematic drawing of the creaming behaviour of a reference fermentation (F2) (top line) and a fermentation with late addition of $CaCl_2$ (F6) (bottom line) at different gravity settling times.

### 3.3.2.2 Impact of flocculants in oil recovery by GEOR

The impact of flocculants in enhancing oil recovery by GEOR was assessed in the aforementioned fermentations and synthetic emulsion. The reproducibility of fermentations allows to exclude important parameters, such as oil fraction and biomass concentration, that can influence GEOR's performance and results (Heeres et al., 2016; Pedraza-de la Cuesta et al., 2017). The same cannot be held for fermentation F4. The oil recovery by GEOR for the fermentations and reference synthetic emulsion and SE2 are presented in Figure 4.

During experiments with the synthetic emulsion, foam was produced and only for the experiments of reference SE and SE2, where $(NH_4)_2SO_4$ was added, the oil recovery could be quantified. The oil recovery doubled when adding the flocculant from 15% to 27%. This trend is even more clear in regard to the early addition of $(NH_4)_2SO_4$ in the fermentation broth (F3), where the oil recovery is three times larger than the reference fermentation, up to 35%. These results show that, as in the case of gravity settling, $(NH_4)_2SO_4$ has a positive impact in emulsion destabilization. When comparing these results with GEOR application in similar studies (Pedraza-de la Cuesta et al., 2017), a 3-fold higher oil recovery is reported here, showing the advantage of using flocculants for emulsion destabilization.

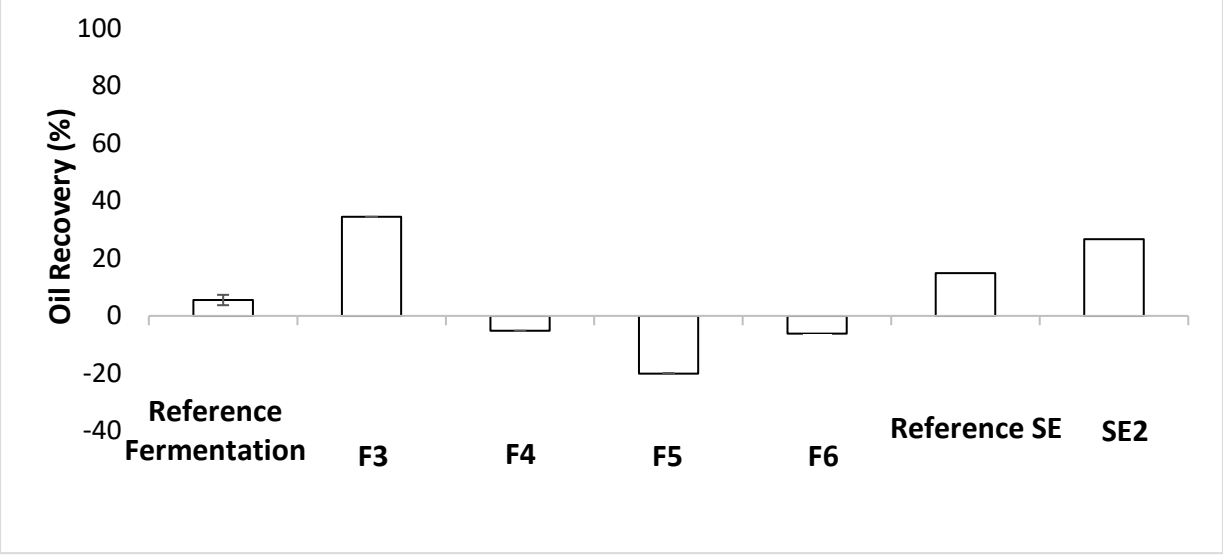


**Figure 4 –** Oil recovery percentage achieved using GEOR for reference fermentation (F1 and F2), fermentation with early addition of $(NH_4)_2SO_4$ (F3), fermentation with late addition of $CaCl_2$ (F4, f5 and F6), reference synthetic emulsion (SE), and synthetic emulsion with addition of $(NH_4)_2SO_4$ (SE2).

For the fermentations where $CaCl_2$ was added (F4, F5 and F6), the oil recovery was negative as the final oil layer measured was smaller than originally placed. This decrease can be explained by the oil back-mixing into the emulsion. Nonetheless, for fermentation F5 and F6, the color of the final layer changed from uncolored to dark red colored (see Figure 5). Only the emulsified oil is red colored (see section 3.2.4) so it appears that demulsification did take place. Yet, clearly not good enough since recovery was negative.

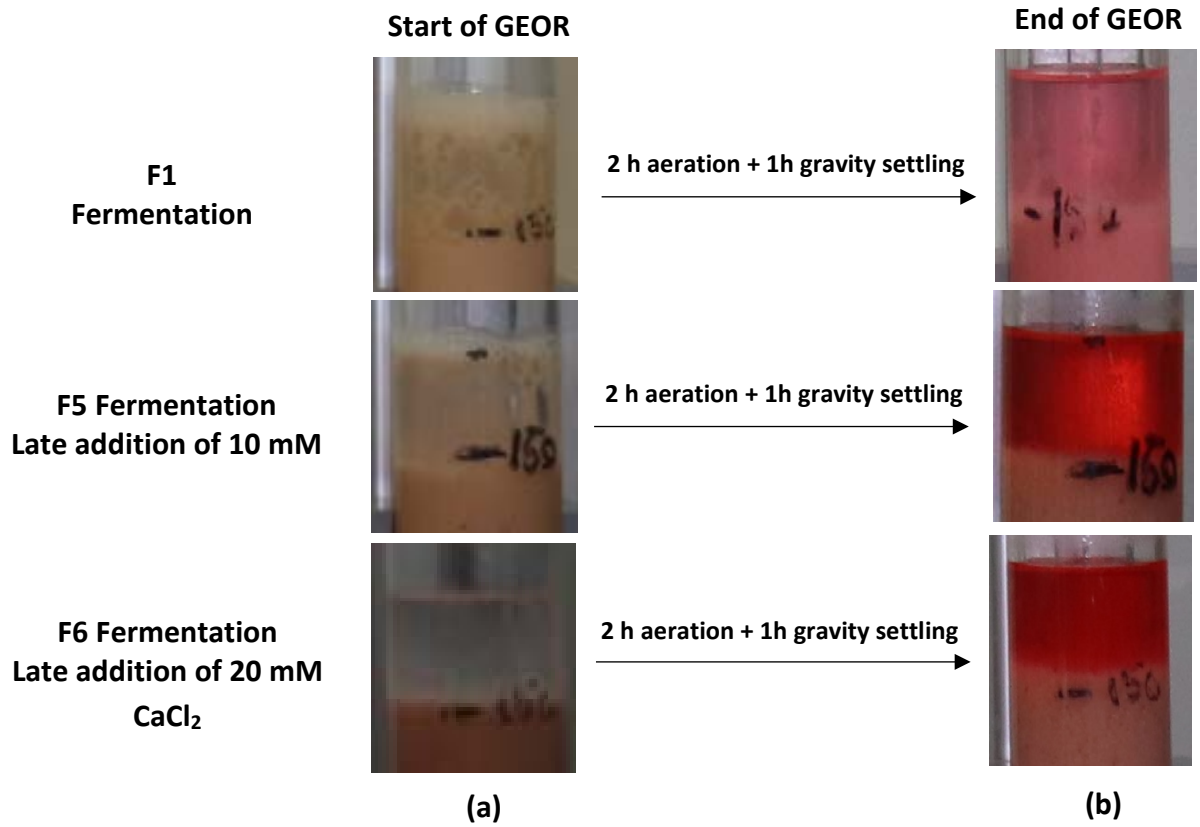


**Figure 5 –** Oil on top for the different fermentations at the start of GEOR (a) and after two hours of aeration and one hour of gravity settling (b). From top to bottom: reference fermentation (F1), fermentation with late addition of 10 mM of $CaCl_2$ (F5) and fermentation with late addition of 20 mM $CaCl_2$ (F6).

From the difference in oil layer behavior together with the results shown in the previous section (see section 3.3.2.1) it is possible to conclude that the addition of $CaCl_2$ creates an emulsion with different properties than the reference emulsions and emulsion with $(NH_4)_2SO_4$. The cream layer formed after aeration and gravity settling was denser and more

viscous, which upon stopping the aeration led to an entrapment of the uncolored oil (fresh oil with no surfactant). This increase in apparent viscosity of the emulsion, due to $CaCl_2$ addition, has already been reported for oil-water synthetic emulsions (Azarikia et al., 2017). In order to avoid back-mixing of oil droplets, lower gas flow velocities could be used.

#### 3.3.2.3 Impact of flocculants in oil recovery by Centrifugation

Centrifugation is one of the methods most commonly used to break emulsions. However, for multiphasic fermentations this method only works together with temperature swing and de-emulsifiers. The shear force applied to the emulsion is such that the oil droplets separate as a clear oil layer, coarse cream ($\phi_{oil}$ = 0.9) or as a cream layer ($\phi_{oil}$ = 0.5), depending on the emulsion stability. Figure 6 presents the clear oil layer formed after centrifugation of different fermentations with (F3, F4, F5 and F6) and without flocculant addition (reference). For the fermentation with late addition of flocculant (F5 and F6), the first two samples (S1 and S2) were used as duplos of the reference since no flocculant has yet been added to the fermenter. For fermentation F3, only one sample was used (S2) due to a technical failure. All samples were compared in terms of oil fraction, antifoam fraction and protein concentration (see Table 7).

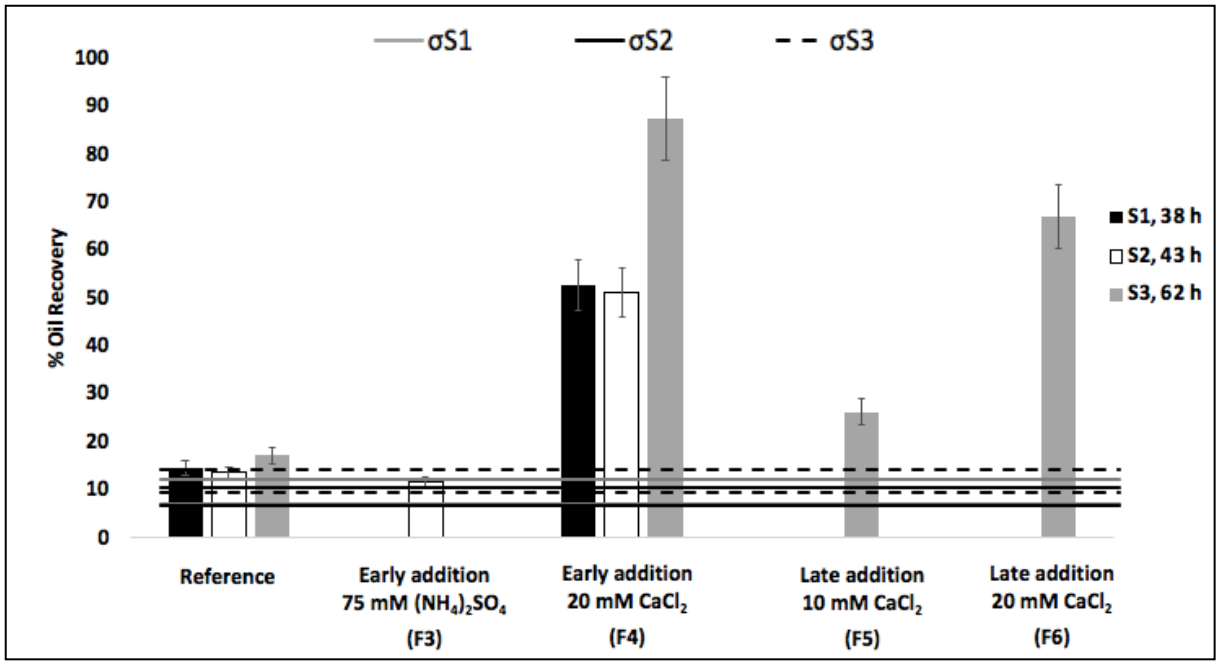


**Figure 6 –** Oil recovery after centrifugation. Where the error bars represent 10% measurement error and the lines represent the standard deviation of the reference samples obtained by the independent duplicates.

**Table 7 -** Oil fraction, antifoam fraction and protein concentration for the reference fermentations and fermentation with addition of flocculant. For fermentation with late addition of flocculant (F5 and F6) the two first samples (S1 and S2) were used as reference fermentations since no flocculant was yet added. For the references fermentation the standard deviation is presented.

| **Fermentation** | **Oil Fraction (g dodecane/g broth)** | | | **Anti-foam Fraction (% w/w)** | | | **Protein concentration (g/l)** | | |
|---|---|---|---|---|---|---|---|---|---|
| **Sample** | **S1** | **S2** | **S3** | **S1** | **S2** | **S3** | **S1** | **S2** | **S3** |
| **Reference** | 0.16 ± 0.006 | 0.16 ± 0.006 | 0.15 ± 0.001 | 0.22% ± 0.0005 | 0.22% ± 0.0005 | 0.22% ± 0.0004 | 4.18 ± 2.8 | 4.64 ± 2.9 | 2.67 ± 0.25 |
| **F3** | 0.16 | 0.16 | 0.15 | 0.19% | 0.19% | 0.18% | 3.0 | 2.66 | 4.14 |
| **F4** | 0.15 | 0.15 | 0.14 | 0.26% | 0.25% | 0.23% | 10.97 | 11.99 | 15.92 |
| **F5** | Reference | Reference | 0.14 | Reference | Reference | 0.17% | Reference | Reference | 9.43 |
| **F6** | Reference | Reference | 0.14 | Reference | Reference | 0.18% | Reference | Reference | 2.40 |

All fermentations had the same oil fraction at each sample time. However, for fermentation F1 and F4 the antifoam fraction was higher which might have an influence in emulsion stability. Comparing F1 with the other reference fermentations, it is noticeable that at this antifoam concentration the emulsion stability does not seem to be affected (shown by the small standard deviation of the reference fermentations).

The highest oil recovery was observed for F4 (88% clear oil release), yet this cannot be fairly compared against the other cases, since the early $CaCl_2$ addition had an impact on fermentation performance and oil emulsification. Surprisingly, the results showed that F4 had higher protein concentration (see Table 7), which has been reported to increase emulsion stability (Heeres et al., 2014; Heeres et al., 2015; Pedraza-de la Cuesta et al., 2017). Studies reported $CaCl_2$ as a cross linking agent (Hariyadi et al., 2014; Ye and Singh, 2000) which can promote protein bridging making the emulsion more susceptible to the shear by centrifugation and promoting oil recovery. Furthermore, the oil recovery also increased for the fermentations with late addition of $CaCl_2$ (F5 and F6). The fermentation with higher amount of flocculant added (F6 – 20 mM) resulted in a higher recovery (67 % - 3 times higher than the reference), showing that an increase in flocculant concentration is beneficial to the emulsion destabilization by centrifugation. On the contrary, the fermentation with early addition of $(NH_4)_2SO_4$ (F3), did not show any improvement in terms of oil release since the oil recovery is inside the bandwidth of the reference. These results indicate that $CaCl_2$ makes the emulsion much more sensitive to the shear applied by centrifugation. However, for the oil recovery by centrifugation, $(NH_4)_2SO_4$ is not a useful flocculant.

#### 3.3.2.4 Comparison of three enhancement oil recovery methods when using flocculants during fermentation at lab scale

In view of the results, Table 8 presents the best combination of flocculant and method of addition for the three oil recovery technologies (gravity settling, GEOR and centrifugation).

**Table 8 –** Best combination between the flocculant tested and oil recovery technologies.

| | **Gravity Settling** | **GEOR** | **Centrifugation** |
|---|---|---|---|
| **Enhancement of oil recovery** | Early addition of $(NH_4)_2SO_4$ (75 mM) | Early addition of $(NH_4)_2SO_4$ (75 mM) | Late addition of $CaCl_2$ (20 mM) |
| **Reasoning** | Quantitative improvement relative to reference and easy adjustment for fermentation broth. | | Quantitative improvement relative to reference. |
| **Drawbacks** | High concentration of ammonium which is toxic to the environment. Requirement of water treatment plants. | | Create flocs of cells, potentially hampering cell recycle. |

The early addition of $(NH_4)_2SO_4$ has shown to be the most beneficial to destabilize an emulsion from fermentation broth when using gravity settling and GEOR. Furthermore, this flocculant is very simple to apply during fermentation since it is already present in many fermentation media. In case of centrifugation, $CaCl_2$ has revealed to be the most helpful in emulsion destabilization. Its impact is closely linked with the time of addition, where early addition of this flocculant led to higher oil recovery but had an effect in fermentation performance. Clearly, follow-up research would benefit from larger data sets from fermentation with addition of flocculant. The extra data would allow to better understand the impact of flocculants into fermentation performance, to generate duplicates for gravity settling and GEOR experiments, as well as, to test different methods of flocculant addition and concentration in emulsion destabilization.

The beneficial effect in oil recovery observed by the addition of $CaCl_2$ in centrifugation and not in GEOR can be explained by the fact that the calcium ions not only shield electrostatic repulsions but can also create links between the proteins surrounding the oil droplets. The creation of flocs of biomass when using $CaCl_2$ during fermentation broth has been

demonstrated for *Saccharomyces cerevisae* (Nayyar et al., 2017; Stewart, 2018), however, no literature was found regarding *E. coli* fermentations with $CaCl_2$ flocculant. This seems to be confirmed by the microscopic pictures shown in Figure 7). Indeed, Figure 7 – [A], shows the formation of cell flocs, in contrast with Figure 7 – [B] where the cells are homogenously dispersed. When adding oil (Figure 7 – [C] and [D]), the pictures suggest that cross-linking is happening not only with cells but also with oil droplets. This interaction can explain the change in fermentation performance, emulsion rheology and the characteristic creaming observed in section 3.3.2.1. When the broth with $CaCl_2$ is under gravity settling, the cream formation retains a large fraction of the biomass present in the broth and oil cannot be separated. The same follows for GEOR, where the shear applied by the gas bubble at the conditions of this paper, helps to separate the emulsified oil but also traps the back-mixed uncolored oil into the cream. In regard with the effect of centrifugation, the extensive cross-linking reduces the molecular flexibility of proteins (Dickinson, 2019; Nylander et al., 2019). Therefore, the shear applied by centrifugation generates breaks in the droplets' protein coating, which promotes droplet coalescence.

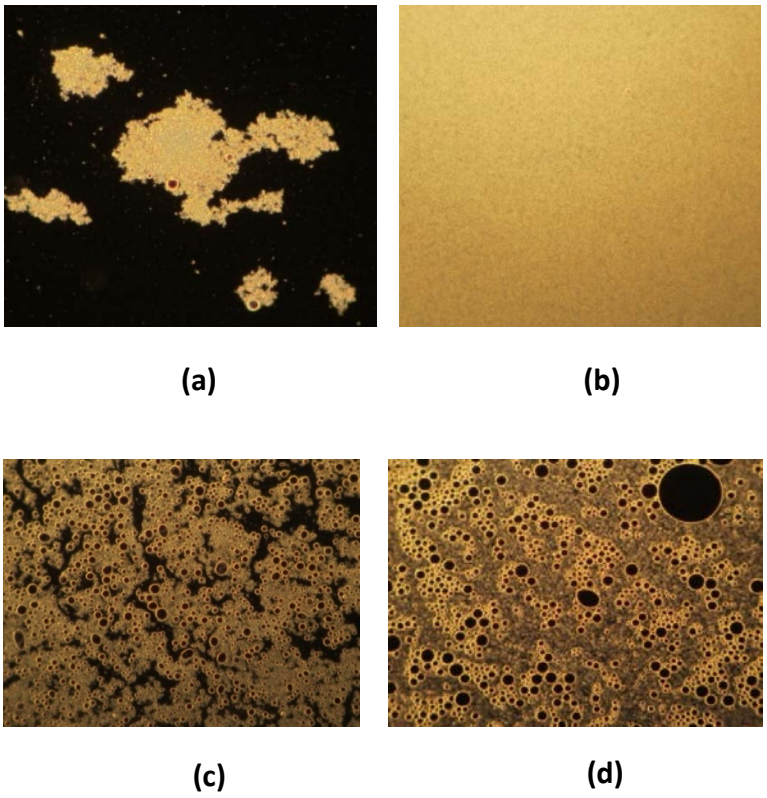


**Figure 7 –** Microscopy pictures (10x) of fermentation broth with *E. coli*. (a) Sample without cream and oil with flocculant $CaCl_2$; (b) Sample without cream and oil and without flocculant; (c) Sample of

homogeneous broth with oil and with flocculant $CaCl_2$; (d) Sample of homogeneous broth with oil and without flocculant.

Both the selected flocculants showed to have potential in terms of industrial applicability and oil recovery, not only due to their destabilization potential and fermentation compatibility, but also due to economic and environmental properties. $(NH_4)_2SO_4$ was able to improve oil recovery by gravity settling and GEOR. Moreover, it represents a great advantage for *in-situ* oil recovery since this component can be used as base addition during multiphasic fermentations and its application would only require a change in medium composition. If a more traditional method as centrifugation would be used, then late addition of $CaCl_2$ would be preferred since early addition has an effect in fermentation performance. Addition of this compound in the later stages of a fermentation could help to minimize the steps needed for downstream processing of the emulsion as well as removing the necessity of temperature swings and chemical addition. However, the creation of biomass flocs can jeopardize cell recycle and fermentation performance. Furthermore, other technologies such as mechanical coalescers (van Aken et al., 2003) or centrifugal contactor separator (McFarlane et al., 2010; Oh et al., 2012) could be implemented together with the addition of $CaCl_2$ to improve oil recovery from multiphasic fermentations.

## 3.4 Conclusion

The impact of adding flocculants ($(NH_4)_2SO_4$ (75 mM) and $CaCl_2$ (10 and 20 mM)) to multiphasic fermentation in order to destabilize the microbial emulsion formed, has been presented. The addition of the flocculants into fermentation showed that they do not affect biomass content and $CO_2$ production. However, the early addition of $CaCl_2$ forms flocs of biomass which can impact fermentation performance and cell recycle. Three techniques for oil recovery were compared: gravity settling, GEOR and centrifugation. Creaming rate and oil recovery by GEOR improved by a factor 3 compared to the reference fermentation, when adding $(NH_4)_2SO_4$. Yet, there was no impact on oil recovery by centrifugation when using this flocculant. On the other hand, when using centrifugation after late addition of $CaCl_2$, 67% of oil recovery was obtained, resulting in a 3-fold increase compared to the reference fermentation. In conclusion, the flocculant, its time of addition, and its concentration can be tuned to the recovery method to improve *in-situ* oil recovery of several technologies and by doing so, decrease production process costs.

## 3.5 Acknowledgements

This work was carried out within the BE-Basic R&D Program, which was granted a FES subsidy as well as a TKI-BBE grant (TKI-AMBIC-program TKIBE-01003) from the Dutch Ministry of Economic affairs.

## 3.6 References


Abolhassani, Z., Astaraie, A., 2010. Comparing copper sulfate, aluminum sulfate and ferric chloride in removing microbial and organic contaminations in municipal waste latex. Australian Journal of Basic and Applied Sciences 4, 887-892.

Azarikia, F., Abbasi, S., Scanlon, M.G., McClements, D.J., 2017. Emulsion stability enhancement against environmental stresses using whey protein–tragacanthin complex: Comparison of layer-by-layer and mixing methods. International Journal of Food Properties 20, 2084-2095.

Beller, H.R., Lee, T.S., Katz, L., 2015. Natural products as biofuels and bio-based chemicals: fatty acids and isoprenoids. Natural product reports 32, 1508-1526.

Benjamin, K.R., Silva, I.R., Cherubim, J.o.P., McPhee, D., Paddon, C.J., 2016. Developing Commercial Production of Semi-Synthetic Artemisinin, and of ²-Farnesene, an Isoprenoid Produced by Fermentation of Brazilian Sugar. Journal of the Brazilian Chemical Society 27, 1339-1345.

Cañizares, P., Martínez, F., Lobato, J., Rodrigo, M.A., 2007. Break-up of oil-in-water emulsions by electrochemical techniques. Journal of Hazardous Materials 145, 233-240.

Choi, O.K., Cho, K.S., Ryu, H.W., Chang, Y.K., 2003. Enhancement of phase separation by the addition of de-emulsifiers to three-phase (diesel oil/biocatalyst/aqueous phase) emulsion in diesel biodesulfurization. Biotechnology Letters 25, 73-77.

Cuellar, M.C., Straathof, A.J.J., 2018. CHAPTER 4 Improving Fermentation by Product Removal, Intensification of Biobased Processes. The Royal Society of Chemistry, pp. 86-108.

Da Costa Basto, R.M., Casals, M.P., Mudde, R.F., van der Wielen, L.A.M., Cuellar, M.C., 2019a. A Mechanistic Model for Oil Recovery in a Region of High Oil Droplet Concentration from Multiphasic Fermentations. Chemical Engineering Science: X, 100033.

Da Costa Basto, R.M., Casals, M.P., Mudde, R.F., van der Wielen, L.A.M., Cuellar, M.C., 2019b. A mechanistic model for oil recovery in a region of high oil droplet concentration from multiphasic fermentations. Chemical Engineering Science: X 3, 100033.

Dafoe, J.T., Daugulis, A.J., 2014. In situ product removal in fermentation systems: improved process performance and rational extractant selection. Biotechnol. Lett. 36, 443-460.

Damodaran, S., 2005. Protein Stabilization of Emulsions and Foams. J. Food Sci. 70, R54-R66.

Delahaije, R.J., Gruppen, H., Giuseppin, M.L., Wierenga, P.A., 2015. Towards predicting the stability of protein-stabilized emulsions. Advances in colloid and interface science 219, 1-9.

Dickinson, E., 2003. Hydrocolloids at interfaces and the influence on the properties of dispersed systems. Food hydrocolloids 17, 25-39.

Dickinson, E., 2010. Flocculation of protein-stabilized oil-in-water emulsions. Colloids and Surfaces B: Biointerfaces 81, 130-140.

Dickinson, E., 2019. Strategies to control and inhibit the flocculation of protein-stabilized oil-in-water emulsions. Food Hydrocolloids 96, 209-223.

Dolman, B.M., Kaisermann, C., Martin, P.J., Winterburn, J.B., 2017. Integrated sophorolipid production and gravity separation. Process Biochem 54, 162-171.

Furtado, G.F., Picone, C.S.F., Cuellar, M.C., Cunha, R.L., 2015. Breaking oil-in-water emulsions stabilized by yeast. Colloid Surf. B: Biointerfaces 128, 568-576.

Hariyadi, D.M., Hendradi, E., Purwanti, T., Fadil, F.D.G., Ramadani, C.N., 2014. Effect of cross linking agent and polymer on the characteristics of ovalbumin loaded alginate microspheres. International Journal of Pharmacy and pharmaceutical sciences 6, 469-474.

Heeres, A.S., 2016. Integration of Product Recovery in Microbial Advanced Biofuel Production: Overcoming Emulsification Challenges, Bioprocess Engineering. Delft University of Technology, Delft.

Heeres, A.S., Heijnen, J.J., van der Wielen, L.A.M., Cuellar, M.C., 2016. Gas bubble induced oil recovery from emulsions stabilised by yeast components. Chem. Eng. Sci. 145, 31-44.

Heeres, A.S., Picone, C.S.F., van der Wielen, L.A.M., Cunha, R.L., Cuellar, M.C., 2014. Microbial advanced biofuels production: overcoming emulsification challenges for large-scale operation. Trends Biotechnol 32, 221-229.

Heeres, A.S., Schroen, K., Heijnen, J.J., van der Wielen, L.A.M., Cuellar, M.C., 2015. Fermentation broth components influence droplet coalescence and hinder advanced biofuel recovery during fermentation. Biotechnol. J. 10, 1206-1215.

Huang, R., Christenson, P.A., Labuda, I.M., 2001. Process for the preparation of nootkatone by laccase catalysis. Google Patents.

International, S., 2015. Oil demulsification. SPE International, PetroWiki.

Keowmaneechai, E., McClements, D.J., 2002. Effect of CaCl2 and KCl on Physiochemical Properties of Model Nutritional Beverages Based on Whey Protein Stabilized Oil-in-Water Emulsions. Journal of Food Science 67, 665-671.

Krstonošić, V., Dokić, L., Nikolić, I., Milanović, M., 2015. Influence of xanthan gum on oil-in-water emulsion characteristics stabilized by OSA starch. Food Hydrocolloids 45, 9-17.

Kulmyrzaev, A.A., Schubert, H., 2004. Influence of KCl on the physicochemical properties of whey protein stabilized emulsions. Food Hydrocolloids 18, 13-19.

Kung, S.H., Lund, S., Murarka, A., McPhee, D., Paddon, C.J., 2018. Approaches and Recent Developments for the Commercial Production of Semi-synthetic Artemisinin. Front Plant Sci 9, 87-87.

Li, P., Zhang, W., Han, X., Liu, J., Liu, Y., Gasmalla, M.A.A., Yang, R., 2017. Demulsification of oil-rich emulsion and characterization of protein hydrolysates from peanut cream emulsion of aqueous extraction processing. Journal of Food Engineering 204, 64-72.

Liu, J.-j., Gasmalla, M.A.A., Li, P., Yang, R., 2016. Enzyme-assisted extraction processing from oilseeds: Principle, processing and application. Innovative Food Science & Emerging Technologies 35, 184-193.

Losso, J.N., Nakai, S., 2002. Stabilization of Oil-in-Water Emulsions by β-Lactoglobulin−Polyethylene Glycol Conjugates. Journal of Agricultural and Food Chemistry 50, 1207-1212.

Mariotti, F., Tomé, D., Mirand, P.P., 2008. Converting Nitrogen into Protein—Beyond 6.25 and Jones' Factors. Critical Reviews in Food Science and Nutrition 48, 177-184.

McClements, D.J., 2004. Protein-stabilized emulsions. Curr. Opin. Colloid In. 9, 305-313.

McClements, D.J., 2005. Food emulsions, principles, practices, and techniques, 2nd edition ed. CRC Press, Boca Raton.

McFarlane, J., Tsouris, C., Birdwell, J.F., Schuh, D.L., Jennings, H.L., Palmer Boitrago, A.M., Terpstra, S.M., 2010. Production of Biodiesel at the Kinetic Limit in a Centrifugal Reactor/Separator. Industrial & Engineering Chemistry Research 49, 3160-3169.

Moelbert, S., Normand, B., De Los Rios, P., 2004. Kosmotropes and chaotropes: modelling preferential exclusion, binding and aggregate stability. Biophysical chemistry 112, 45-57.

Nadarajah, N., Singh, A., Ward, O.P., 2002. De-emulsification of petroleum oil emulsion by a mixed bacterial culture. Process Biochemistry 37, 1135-1141.

Nations, U., 2017. Globally Harmonized System of Classifications and Labelling of Chemicals (GHS), 7th ed, New York and Geneva.

Nayyar, A., Walker, G., Wardrop, F., Adya, A.K., 2017. Flocculation in industrial strains of Saccharomyces cerevisiae: role of cell wall polysaccharides and lectin-like receptors. Journal of the Institute of Brewing 123, 211-218.

Nylander, T., Arnebrant, T., Cárdenas, M., Bos, M., Wilde, P., 2019. Protein/Emulsifier Interactions, in: Hasenhuettl, G.L., Hartel, R.W. (Eds.), Food Emulsifiers and Their Applications. Springer International Publishing, Cham, pp. 101-192.

Oh, P.P., Lau, H.L.N., Chen, J., Chong, M.F., Choo, Y.M., 2012. A review on conventional technologies and emerging process intensification (PI) methods for biodiesel production. Renewable and Sustainable Energy Reviews 16, 5131-5145.

Ojima, Y., Azuma, M., Taya, M., 2018. Inducing flocculation of non-floc-forming Escherichia coli cells. World Journal of Microbiology and Biotechnology 34, 185.

Park, S., Bae, D., Rhee, K., 2000. Soy protein biopolymers cross-linked with glutaraldehyde. Journal of the American Oil Chemists' Society 77, 879-884.

Pedraza-de la Cuesta, S., Keijzers, L., van der Wielen, L.A.M., Cuellar, M.C., 2017. Integration of Gas Enhanced Oil Recovery in multiphasic fermentations for the microbial production of fuels and chemicals. Chemicals Biotechnology Journal.

PubChem, 2019. Ammonium Sulfate (Compound) - Toxicity. U.S. National Library of Medicine, National Center for Biotechnology Information.

Rangsansarid, J., Fukada, K., 2007. Factors affecting the stability of O/W emulsion in BSA solution: Stabilization by electrically neutral protein at high ionic strength. Journal of Colloid and Interface Science 316, 779-786.

Rehn, G., Grey, C., Branneby, C., Adlercreutz, P., 2013. Chitosan flocculation: An effective method for immobilization of E. coli for biocatalytic processes. Journal of Biotechnology 165, 138-144.

Renninger, N.S., McPhee, D.J., 2010. Fuel compositions comprising farnesane and farnesene and method of making the same.

Renninger, N.S., Newman, J., Reiling, K.K., Regentin, R., Paddon, C.J., 2011. Production of isoprenoids US.

Rocha E Silva, F.C.P., Roque, B.A.C., Rocha E Silva, N.M.P., Rufino, R.D., Luna, J.M., Santos, V.A., Banat, I.M., Sarubbo, L.A., 2017. Yeasts and bacterial biosurfactants as demulsifiers for petroleum derivative in seawater emulsions. AMB Express 7, 202-202.

Salehizadeh, H., Vossoughi, M., Alemzadeh, I., 2000. Some investigations on bioflocculant producing bacteria. Biochemical engineering journal 5, 39-44.

Sarkar, A., Kamaruddin, H., Bentley, A., Wang, S., 2016. Emulsion stabilization by tomato seed protein isolate: Influence of pH, ionic strength and thermal treatment. Food Hydrocolloids 57, 160-168.

Setiowati, A.D., Saeedi, S., Wijaya, W., Van der Meeren, P., 2017. Improved heat stability of whey protein isolate stabilized emulsions via dry heat treatment of WPI and low methoxyl pectin: Effect of pectin concentration, pH, and ionic strength. Food Hydrocolloids 63, 716-726.

Sheldon, R., 2007. Cross-linked enzyme aggregates (CLEA® s): stable and recyclable biocatalysts. Portland Press Limited.

Silvestre, M.P.C., Decker, E.A., McClements, D.J., 1999. Influence of copper on the stability of whey protein stabilized emulsions. Food Hydrocolloids 13, 419-424.

Singh, H., Ye, A., 2020. Chapter 12 - Interactions and functionality of milk proteins in food emulsions, in: Boland, M., Singh, H. (Eds.), Milk Proteins (Third Edition). Academic Press, pp. 467-497.

Steinbusch, K., 2019. Successful pilot demonstration of intensified bioreactor concept FAST for low cost multiphase fermentations, in: Conference, N. (Ed.).

Stewart, G.G., 2003. BEERS | Biochemistry of Fermentation, in: Caballero, B. (Ed.), Encyclopedia of Food Sciences and Nutrition (Second Edition). Academic Press, Oxford, pp. 434-440.

Stewart, G.G., 2018. Yeast Flocculation—Sedimentation and Flotation. Fermentation 4, 28.

Straathof, A.J.J., Cuellar, M.C., 2019. Microbial Hydrocarbon Formation from Biomass, in: Wagemann, K., Tippkötter, N. (Eds.), Biorefineries. Springer International Publishing, Cham, pp. 411-425.

Stratford, M., 1992. Lectin-mediated aggregation of yeasts—yeast flocculation. Biotechnology and Genetic Engineering Reviews 10, 283-342.

Syrbe, A., Bauer, W., Klostermeyer, H., 1998. Polymer science concepts in dairy systems—an overview of milk protein and food hydrocolloid interaction. International Dairy Journal 8, 179-193.

Tabur, P., Dorin, G., 2012. Method for purifying bio-organic compounds from fermentation broth containing surfactants by temperature-induced phase inversion, in: Amyris (Ed.). Amyris Inc., US.

Tadros, T.F., 2013. Emulsion formation and stability. John Wiley & Sons.

van Aken, G., Blijdenstein, T., E Hotrum, N., 2003. Colloidal destabilisation mechanisms in protein-stabilised emulsions.

Van Hamme, J.D., Singh, A., Ward, O.P., 2006. Physiological aspects: Part 1 in a series of papers devoted to surfactants in microbiology and biotechnology. Biotechnol. Adv. 24, 604-620.

Wumpelmann, M., Mollgaard, H., 1990. Immobilization of biologically active material with glutaraldehyde and polyazaetidine. Google Patents.

Yang, Z., Degorce-Dumas, J.-R., Yang, H., Guibal, E., Li, A., Cheng, R., 2014. Flocculation of Escherichia coli Using a Quaternary Ammonium Salt Grafted Carboxymethyl Chitosan Flocculant. Environmental science & technology 48, 6867-6873.

Ye, A., Hemar, Y., Singh, H., 2004. Enhancement of coalescence by xanthan addition to oil-in-water emulsions formed with extensively hydrolysed whey proteins. Food Hydrocolloids 18, 737-746.

Ye, A., Singh, H., 2000. Influence of calcium chloride addition on the properties of emulsions stabilized by whey protein concentrate. Food Hydrocolloids 14, 337-346.

Zolfaghari, R., Fakhru'l-Razi, A., Abdullah, L.C., Elnashaie, S.S., Pendashteh, A., 2016. Demulsification techniques of water-in-oil and oil-in-water emulsions in petroleum industry. Separation and Purification Technology 170, 377-407.

# 3.7 Appendix

**Table A.1.** Oil fraction, antifoam fraction and protein concentration for the reference fermentations and fermentation with addition of flocculant. For fermentation with late addition of flocculant (F5 and F6) the two first samples (S1 and S2) were used as reference fermentations since no flocculant was yet added. For the references fermentation the standard deviation is presented.

| **Fermentation** | **Oil Fraction (g dodecane/g broth)** | | | **Anti-foam Fraction (% w/w)** | | | **Protein concentration (g/l)** | | |
|---|---|---|---|---|---|---|---|---|---|
| **Sample** | **S1** | **S2** | **S3** | **S1** | **S2** | **S3** | **S1** | **S2** | **S3** |
| **Reference** | 0.16 ± 0.006 | 0.16 ± 0.006 | 0.15 ± 0.001 | 0.22% ± 0.0005 | 0.22% ± 0.0005 | 0.22% ± 0.0004 | 4.18 ± 2.8 | 4.64 ± 2.9 | 2.67 ± 0.25 |
| **F3** | 0.16 | 0.16 | 0.15 | 0.19% | 0.19% | 0.18% | 3.0 | 2.66 | 4.14 |
| **F4** | 0.15 | 0.15 | 0.14 | 0.26% | 0.25% | 0.23% | 10.97 | 11.99 | 15.92 |
| **F5** | Reference | Reference | 0.14 | Reference | Reference | 0.17% | Reference | Reference | 9.43 |
| **F6** | Reference | Reference | 0.14 | Reference | Reference | 0.18% | Reference | Reference | 2.40 |

# Chapter 4: Hydrodynamics for the Integration of Fermentation and Separation in multiphasic fermentations

**Abstract** Important classes of phase-separating bioproducts ranging from commodity building blocks for fuels and materials to high added value flavors and fragrances, require in-situ liquid-liquid separation in advanced systems such as the integrated FAST bioreactors to improve yields and reduce capital and operational costs. Scale-up studies have hardly been published, with modelling restricted to engineering correlations and costly or absent experimental tools for scaled-up systems' hydrodynamics and overall absent data across scales. This work explores computational fluid dynamics (CFD) and experimental verification at small (2 L) and pilot (100 L) scale integrated FAST bioreactors as a modelling, analysis, and design tool for these complex reactors.

The core of the FAST bioreactor is a central downcomer where the emulsion flows into a concentric separation section. In the separation section, oil droplets should rise towards recovery while oil-less broth flows horizontally back to the fermentation compartment. Two different model systems using commercially relevant solvents (Dodecane and Oleyl Alcohol) where used to document and analyse FAST bioreactor performance.

A CFD model was developed to study the effect of emulsion inlet velocity and specific geometries for specific emulsion properties in non-coalescing systems. In general, the model predicted improved oil rise to recovery at lower velocities. Also, unfavourable development of roll cells in the separation channel was predicted when inlet velocities in the separation compartment exceeded a system dependent minimum value (Re > 250). The 'oil' recoveries can be predicted well with and with reasonable accuracy.

For the specific internal structure of the FAST bioreactor at relevant experimental (pilot) scale, the model was shown to be useful to optimize the recovery of the 'oil' phase in the critical recirculation zone. The model also predicts unfavourable 'swirls' at elevated hydraulic load that limits proper operational performance.

Our work shows that while useful for predicting trends in experimental FAST bioreactors, further work needs to be done to improve model accuracy. Key challenges especially relate to implementation of realistic coalescence models in CFD model as well as in-line measurements of droplet size (distribution) and flow phenomena within the FAST's internals.

**Keywords:** Multiphasic mixture; FAST bioreactor; Hydrodynamics; Second Phase; Oil Recovery;

## 4.1 Introduction

The increase of global warming, carbon emissions, and energy demand due to the rise of world population and industry, together with a clear need for a more sustainable world, has driven industries towards a circular bio-based economy (Straathof et al., no date) . Industries are thus becoming more aware of the necessity of developing biofuels to replace fossil fuels. As a result, the implementation of bio-based fuels on the market is growing. Several liquid biofuels, such as ethanol, biodiesel and advanced biofuels are already being produced at commercial scale using fermentative route (Renninger, 2010; Amyris, 2016; M, 2017; Vickers et al., 2017; Cuellar and Straathof, 2018a; Straathof and Cuellar, 2019). The advanced biofuels are organic compounds that resemble the current liquid fuels on the market and are drop-in fuels that can be used directly in vehicles without any engine modification. Current commercial examples have been published among others by (Total and Amyris renewable jet fuel ready for use in commercial aviation, 2014), however still with a need to lower production costs. Chemically similar compounds produced via terpenoid, and equivalent pathways also have oleofactory properties with uses in high added value flavour and fragrances markets (Soares-Castro, Soares and Santos, 2020).

Those are produced in an aerobic fermentation (Gupta, 2015), (Wen, Bond-Watts and Chang, 2013)genetically modified microorganism in an aqueous medium of sugars and nutrients. The generated hydrocarbons, which in this paper we refer to as “oil”, are excreted into the medium by the microorganisms or are added as a second phase organic solvent for product extraction. Both cases create dispersions of small oil droplets. The surface-active compounds (SAC’s) in the medium such as proteins, cells (fragments), and glycolipids stabilize the oil/water interface potentially forming a stable emulsion (Heeres *et al.*, 2014), and requiring a series of intensive steps, incurring in high costs, to separate the final product (Tabur and Dorin, 2012). Their water immiscibility and low-density properties however create an opportunity for an easy and low-cost separation.

While impressive steps to lower capital and operational expenditure have been made (Velasco, 2014; Pedraza-de la Cuesta et al., 2018), improvement of production technology remains to be a continued focus.

Bioreactor innovation for biofuels manufacturing has been limited with most of the processes being performed in conventional bioreactors such as CSTR's and batch or fed-batch systems (Cuellar and Straathof, 2018b). Promising approaches have been reported in wastewater treatment with comparably low margins in the developments of innovative processes and technologies with the aim of reducing production costs (Heijnen et al., 1990; van Benthum et al., 1999). This provides inspiration for the biofuels manufacturing industry to develop similar innovative technologies and new equipment for further cost reduction. For example, integration of fermentation and separation process in one single piece of equipment enable cell reuse and continuous product recovery, decreasing the amount of substrate needed (one of the main cost drivers in a fermentation processes) and size of fermenter while increasing productivity (Cuellar, Heijnen and van der Wielen, 2013). Also, an integrated bioreactor allows *in situ* product extraction reducing the harmful impact of the product on the microorganisms. Moreover, in situ product removal of inhibiting compounds has shown very strong effects on (volumetric) productivity (Cuellar and Straathof, 2018b).

TU Delft and its partners (Delft Advanced Biorenewables DAB BV and related organisations) developed a technology platform FAST™ (Fermentation Accelerated by Separation Technology) that incorporates fermentation and separation in a single piece of equipment enabling more efficient microbial production and separation (DAB BV, no date). In the fermentation compartment, cells produce the hydrocarbon compound that is excreted to the medium creating an emulsion while in the separation compartment these oil droplets are separated using their intrinsic buoyancy difference compared to the overall broth. The compartmentalisation allows for optimal and different conditions for each function. Broth that is depleted of organic oil droplets but includes living cells is recycled back to the fermentation compartment. If the droplets are too small and the emulsion of the oil droplets is too stable, additional techniques could be considered such as Gas Enhanced Oil Recovery (GEOR) (Heeres et al., 2016; Pedraza-de la Cuesta et al., 2017; Da Costa Basto et al., 2019).

The integration of fermentation and separation in a single vessel (Heeres et al., 2016; Pedraza-de la Cuesta et al., 2017; Da Costa Basto et al., 2019) allows potentially for a reduction in costs and an increase in efficiency for the production of advanced biofuels opening a possibility in the future to compete with the fossil fuels market. In earlier work (DAB BV, no date; Pappas and Oudshoorn, no date), we presented a novel integrated bioreactor (Figure 1) for the

integration of fermentation and separation processes to enhance productivity and reduce capital and operational costs for these and comparable products. This integrated bioreactor is denominated Fermentation And Separation Technology (FAST).

FAST bioreactor has five distinct sections which are shown in Figure 1-a and Figure 2:

Fermentation section (F) – where the organic oil droplets are produced and excreted to the liquid media;

Riser section (R) – where the liquid flows from the fermentation compartment to the separation compartment by means of the gas flow;

Downcomer section (DC) – the liquid overflows from the riser and streams down to the recirculation section. In the downcomer, the gas is separated from the mixture;

Recirculation section (RC) – the liquid re-circulates to the recirculation tube (RT) and where the oil rises to the separation section;

Separation section (S) – The oil droplets will be separated driven by density difference with the continuous phase; if necessary separation can be controlled and enhanced further by coalescences based technologies (Heeres et al., 2016; Pedraza-de la Cuesta et al., 2017; Da Costa Basto et al., 2019, 2020).

The critical step in this process is splitting and recovering the oil in the recirculation section. To understand the efficiency of this step and the impact of operational and bioreactor design parameters, such as structure of internals, physical properties and operational parameters, a hydrodynamic model is indispensable. In this work, we describe the development and use of a computational fluid dynamics (CFD) model to understand how (changes in) internals' design and operational parameters will affect oil split and can be used to optimize oil recovery. The accuracy of the predictive model was verified in a pilot scale bioreactor of 100 L with a commercially relevant model system.

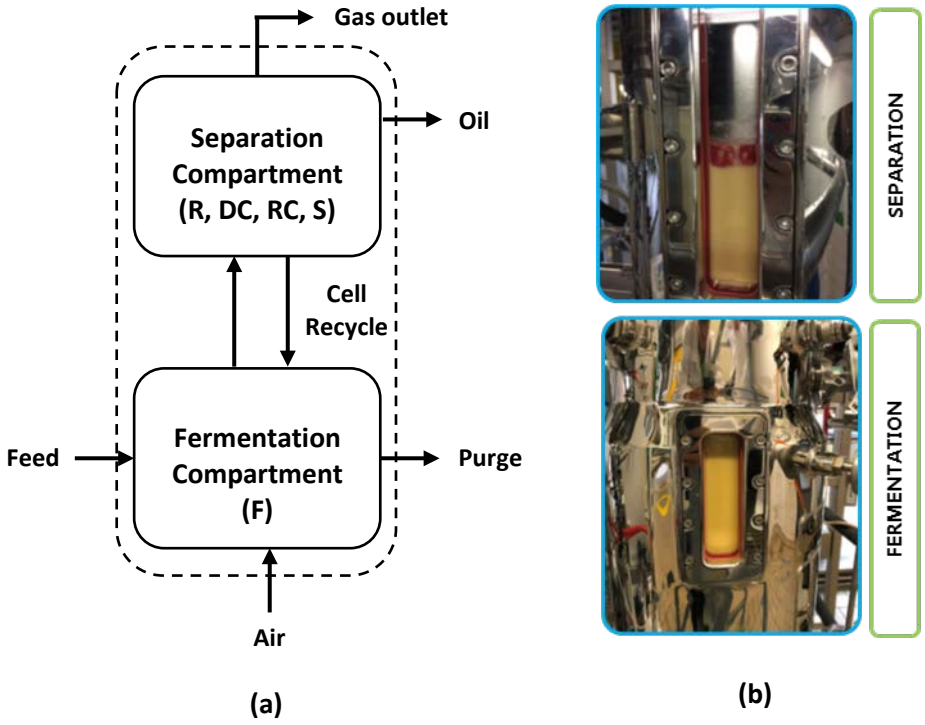


**Figure 1 –** (a) Integrated Bioreactor for the production, separation and recovery of a clear oil layer with highlights on its main functionalities (emulsion formation, oil recovery and cell recycle); (b) Pilot reactor built by DAB showing the integration of fermentation and separation and the oil separation in-situ.

## 4.2 Continuous flow system and operation of a FAST bioreactor.

One of the critical points of an integrated FAST bioreactor is the prediction and optimization of the oil split in the separation compartment. The oil recovery is dependent on the separation compartment geometry and multiphase hydrodynamics expressed as local liquid velocity, and droplet sizes and hold-up. While the study of average liquid velocity and average droplet size can be performed by using 2D models and engineering correlations, the hydrodynamics studies are limited in the real system (Appendix A. Hydrodynamic integrated bioreactor model).

For the FAST bioreactor, different functionalities are required for oil separation and recovery (Appendix B. Integrated bioreactor functionalities).

**Downcomer Design -** After the emulsified oil droplets rise and overflow into the downcomer area, the gas bubbles are separated from the liquid emulsion. To accomplish this separation, the residence time of the liquid ($\tau_{DC}$) needs to be larger than the time that takes for the gas bubbles to be separated ($\tau_{GB}$). Moreover, the time that takes for the oil droplets to start separating ($\tau_{ris,DC}$), needs be larger than the residence time of the liquid in the downcomer to avoid phase separation by creaming and therefore, suboptimal separation.

**Recirculation design (focus of this work) -** Once the liquid enters in the recirculation section, the residence time in this compartment ($\tau_{res}$) needs to be larger than the time that takes for the oil droplets to separate ($\tau_{ris,rec}$) to allow an optimal separation. To allow rising of the oil droplets, the liquid flow entering in the recirculation section needs to be as laminar as possible and turbulent flow minimized. In the FAST bioreactor, the recirculation tube is equipped with a flowmeter and a valve to monitor and control the recirculation flow entering in the fermentation compartment and improve oil separation.

Figure 2 shows a 2D a schematic overview of the FAST bioreactor's separation compartment.

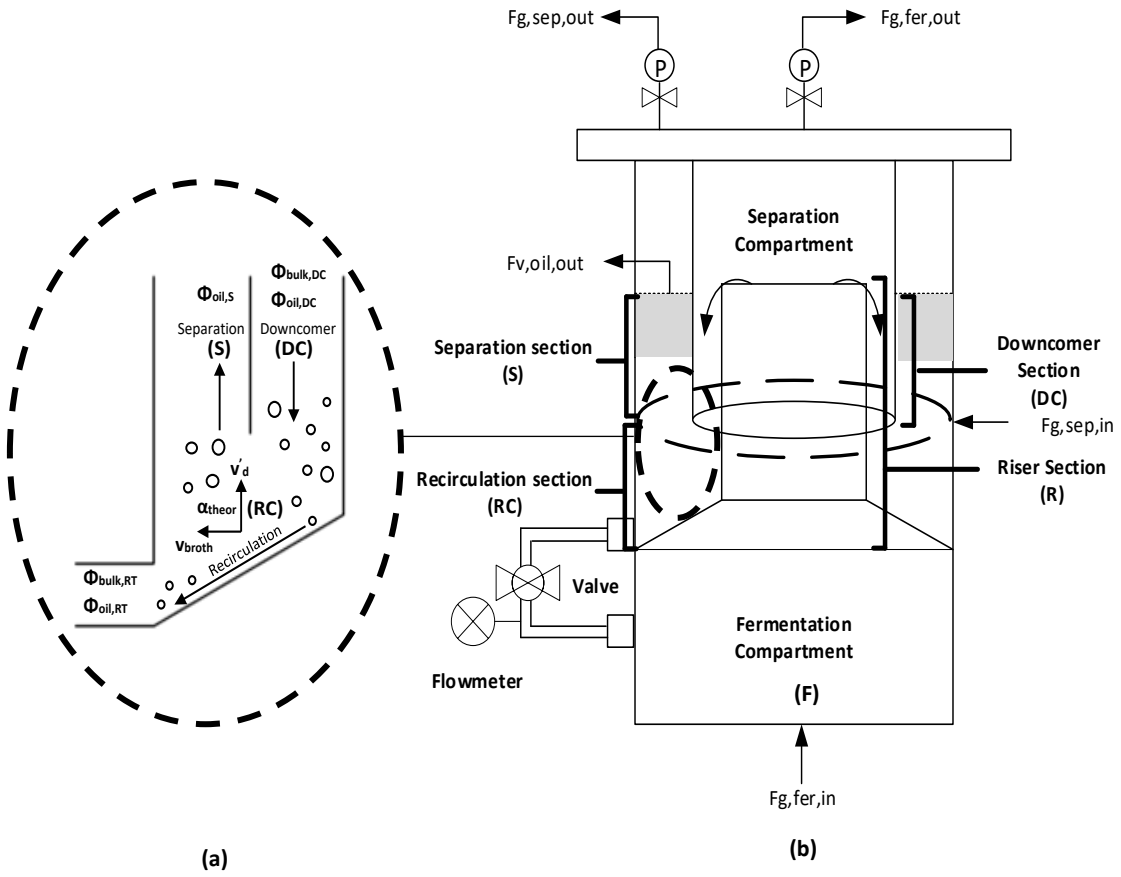


**Figure 2 –** Theoretical oil scheme of oil separation illustrating the movement of oil and bulk liquid in the downcomer and recirculation section (a) and schematic representation of the separation compartment of the integrated Fermentation And Separation Technology (FAST) bioreactor at pilot scale with the recirculation tube with valve and flow meter (b). Where Fg is the volumetric gas flow in $m^3/s$, Fv, oil, is the volumetric oil flow outside the separation compartment (Fv, oil, out is also depicted as $\phi_{oil,S}$) in $m^3/s$, $\phi_{bulk}$ is the volumetric flow of broth in the different compartments im $m^3/s$, $v_{bulk}$ the velocity of broth in m/s and $v'_d$ is the rising droplet velocity taking into account the swarm effects in m/s and $\alpha_{theor}$ is the theoretical oil split (oil droplets being separated in the separation compartment vs the oil droplets recirculating back to the fermentation compartment). This scheme was based on the work of Mandalahalli *et al*.(Mandalahalli et al., 2020).

### 4.2.1 Oil separation model

An oil separation model was developed to understand the theoretical oil split of the oil in the recirculation compartment. To achieve oil separation, the oil droplets in the recirculation section need to rise while the oil-depleted broth recirculates to the fermentation compartment via the recirculation tube.

The rising velocity of a single and small droplet ($v_d$ in m/s) can be estimated by the Stokes law (Reynolds, Richards and 2nd, 1996) (Equation 1). In a static zone, the oil droplet ($d_d$) rises to the top due to density difference between the continuous liquid phase ($\rho_c$) and disperse liquid phase ($\rho_d$) (Equation 1). This velocity depends on droplet size and liquid viscosity ($\mu$).

$$v_d\,(m/s) = \frac{(\rho_c - \rho_d)\cdot g \cdot d_d^2}{18\cdot\mu} \quad (1)$$

To account with the swarm effects of the neighbouring droplets, the Richardson and Zaki correlation (Richardson and Zaki, 1954) is used for less dense droplets systems ($\varphi_d < 0.3$):

$$v_d'\,(m/s) = v_d \cdot (1 - \varphi_d\,)^n \quad (2)$$

Where, n is a parameter dependent on the Reynolds number, droplet size and vessel diameter (Janssen and Warmoeskerken, 2006) and $\varphi_d$ is the disperse phase hold-up. For more dense systems ($\varphi_d > 0.3$), other correlations such as the Ergun correlation should be used (Crowe et al., 2011).

In a dynamic system, such as the recirculation section of the FAST bioreactor, the oil separation is also dependent on the liquid flow path and turbulence. This is directly related with the dimensions of the integrated FAST bioreactor and horizontal velocities. To promote oil separation, the turbulence intensity should be controlled, and the liquid should flow should be slow enough to allow the oil droplets to rise. Once the droplets rise from the recirculation section to the separation compartment, they are considered fully separated. Hence, the (vertical) rising velocity of oil droplets ($v_d$') should be larger than their horizontal velocity of the bulk liquid (broth and oil) ($v_{bulk}$ in m/s) in the recirculation section. At the

bottom of the recirculation section, where the bulk recirculates back to the fermentation compartment, low oil fractions are expected.

Equation 3 provides the horizontal velocity of the bulk liquid. Where $\Phi_{v,oil}$ is the inflow oil flow rate ($m^3/s$) and $A_{RC}$ is the recirculation area ($m^2$).

$$v_{bulk}(m/s) = \frac{\Phi_{v,oil}}{A_{RC}} \quad (3)$$

It is assumed no slip in the horizontal direction since the diameter of the oil droplets (µm-range) are much smaller than the dimensions of the flow channel (cm). Therefore, the oil droplet velocity is a combination of the bulk liquid velocity and the rising of the oil droplets. The actual vertical displacement ($\Delta_z$ in m) of the oil can be estimated from the time that the oil droplets are in the recirculation compartment ($t_{res}$, in s) and their slip velocity ($v_d'$ (m/s)).

$$\Delta_z\ (m) = t_{res} \cdot v_d' \quad (4)$$

The residence time of the oil droplets in the recirculation compartment can be calculated by the horizontal distance (L in m) which oil droplets will flow and their horizontal velocity.

$$t_{res}(s) = \frac{L}{v_{bulk}} \quad (5)$$

A theoretical split factor ($\alpha_{theor}$) was calculated by the ratio of vertical and horizontal oil velocities combined with the distance that they need to travel. Where H (m) is the vertical distance (height) that takes for the oil droplet at the lowest flow path position to escape into the separation zone. This height is dependent on the geometry of the integrated FAST bioreactor and the hydrodynamic of the liquid.

$$\mathrm{A}_{theor} = \frac{v_d'}{v_{bulk}} \cdot \frac{L}{H} \quad (6)$$

The oil flow separating is obtained by multiplying the split factor by the oil feed flow $\phi_{oil,DC}$ (kg/hr). It is assumed that all the oil rising to the separation section is recovered as a single liquid phase.

$$\phi_{\mathrm{oil,sep}}\left(\frac{kg}{h}\right) = \phi_{\mathrm{oil,DC}} \cdot \alpha_{theor} \quad (7)$$

The oil recovery is obtained by the ratio of the oil separating in the recirculation section and the oil entering in the downcomer (Equation 7).

$$\text{Oil Recovery } (\%) = \frac{\Phi_{\text{oil},sep}}{\Phi_{\text{oil,DC}}} \cdot 100 \quad (8)$$

The impact of oil droplet size and oil fraction of the integrated FAST bioreactor in the oil separation is studied in this document. The hydrodynamic model for liquid recirculation of the integrated FAST bioreactor and the calculation of the oil recovery are based on the work of van Benthum *et al* (van Benthum et al., 1999). The detailed model is described in appendix A.

### 4.2.2 CFD Modelling

One of the major bottlenecks of using the integrated FAST bioreactor at pilot scale is collecting accurate experimental information about hydrodynamics, flow path, local velocities, and other important variables in the recirculation section as it is internal in the reactor. Options as flowmeters, MRIs, optical or acoustic measurements are costly, too inaccurate, or unpractical to implement.

An alternative approach using biphasic CFD modelling, to predict the hydrodynamic patterns and estimate local liquid velocities in the recirculation section, was used. The biphasic CFD model could be calibrated at low local oil holdup (<5 vol%) where the bulk liquid flow is practically unaffected by the presence of the oil drops and can be predicted accurately using single phase CFD modelling. The density and viscosity of the mixture were corrected to account with the diluted dispersion. The relative motion of the segregating oil drops was estimated based on equation 7 superimposed on the calculated bulk flow field.

The liquid inlet velocity used as input in the downcomer section was obtained based on the recirculation flows achieved at different inlet gas flow. These gas flow provide the driving force of the liquid circulation within the integrated FAST bioreactor (see Appendix A. Hydrodynamic integrated bioreactor model).

## 4.3 Materials and Methods

### 4.3.1 Pilot runs

Pilot experiments were performed using the 100 L integrated FAST bioreactor (Figure 3) at the Bioprocess Pilot Facility (BPF). The 2-D description of the reactor can be seen in Figure 2. The reactor configuration are given by Oudshoorn et al patent (Oudshoorn et al., 2021) and its dimensions in Table 1. Two different experiments were performed: continuous aerobic extractive fermentation of sesquiterpene with dodecane and continuous extractive anaerobic fermentation of butanol with oleyl alcohol.

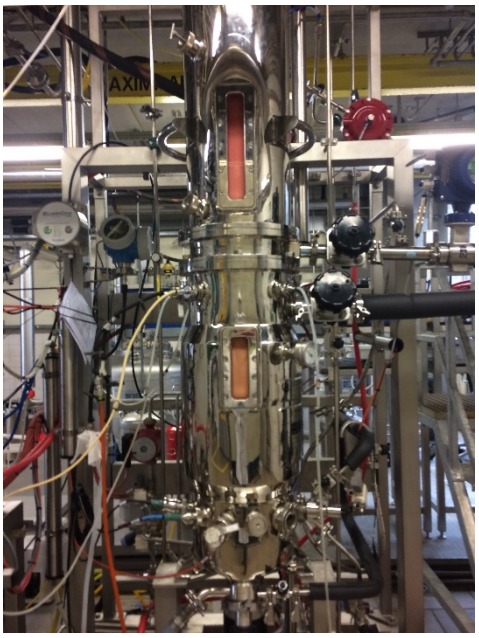

**Figure 3 –** 100 L FAST bioreactor at the BPF.

**Table 1 –** Integrate FAST bioreactor separation and recirculation dimensions.

| Section | Height (m) | Diameter (m) |
|---|---|---|
| **Recirculation** | 0.038 | 0.084 |
| **Separation** | 0.084 | 0.0374 |
| **Headspace** | 0.17 | 0.185 |

#### 4.3.1.1 Dodecane recovery in sesquiterpene producing E.coli fermentation

The first fermentation in the described integrated FAST bioreactor was performed with a recombinant sesquiterpene producing *E. coli* DP1205 strain. The fermentation protocol followed the protocol described in Da Costa Basto *et al*. (Da Costa Basto et al., 2020) with slight changes: The fed-batch duration was 5 days. The batch took approximately 11 h. The stirring speed during batch phase was 700 rpm and during fed-batch from 400-700 rpm. The air flow was 1 vvm in the fermentation compartment (47 L/min). A solution of IPTG (Isopropyl β-D-1-thiogalactopyranoside) of 0.0238 g/kg was added around 19h of fermentation together with a decrease of temperature to 25 °C when the $OD_{600}$ was approximately 30 corresponding to 0.1 kg/L of wet biomass. The second phase added was dodecane (VWR). The coloured second phase (dodecane) dosing to the reactor was started at approximately 35 h. The average feeding rate of 0.25 kg/h. The recirculation rate was started at 25 and decreased to13 L/min at approximately 60 h. The recirculation flow was measured with Jumo flow TRANS MAG H01 Magnetic flow meter DN25, see Appendix A for more detail on recirculation flow. The stirrer speed was maintained at 500 rpm.

Oil recovery measurements were performed during the runs with fermentation broth. The oil accumulated on the top of the integrated bioreactor was harvested manually and discharged into a container set on a mass balance.

#### 4.3.1.2 Oleyl alcohol recovery in butanol (ABE) producing Clostridia fermentation

The second fermentation case was performed with a *Clostridium acetobutylicum* cultivated with glucose (50% solution) as carbon source and CM2 medium according to (de Vrije and Claassen, 2018) which which contained $KH_2PO_4$ 1 g/L, $K_2HPO_4$ 0.76 g/L, $CH_3COONH_4$ 2.9 g/L (of which acetate is 2.2 g/L), $FeSO_4.7H_2O$ 6.6 mg/L, $MgSO_4.7H_2O$ 1 g, and p-aminobenzoic acid (p-ABA) 0.1 g/L), but with increased yeast extract solution (Duchefa) 42 g/kg for the seed media together with 15 g/kg glucose. Base was added as $NH_4OH$ (25% solution).Oleocetylalcoholl 80-85 (Chempri B.V.) was added as a second phase in the fermentation compartment. Glucose was adjusted to maintain a concentration of 10 g/L, because at lower concentrations fermentation performance is significantly diminished for this strain. At the end of the batch phase, oleyl alcohol was continuously added at a rate of 1 kg/h

to match the targeted butanol productivities. The solvent was separated and harvested continuously at the set dosing Solvent rate was chosen to maintain approximately 5 g/L butanol concentration in the continuous fermentation at the set glucose feeding rate. The stirrer speed was kept throughout the fermentation at 400-450 rpm. The nitrogen flow was 0.5 vvm in the fermentation compartment (35 L/min).

**Table 2 –** Overview of the two fermentation cases processed in the FAST bioreactor.

| | **FAST bioreactor** | |
|---|---|---|
| **Strain** | *E. coli* | *Clostridium* |
| **Mode** | Batch followed from fed-batch | Batch followed from fed-batch |
| **ISPR technique** | Gas Enhanced Oil recovery (GEOR) | Hybrid gas & continuous organic overlay |
| **Overall volume** | 100 L | 100 L |
| **Aqueous phase volume** | 70 L | 70 L |
| **Solvent** | Dodecane | Oleyl alcohol |
| **Temperature** | 25 $^{o}$C | 32 $^{o}$C |
| **Airflow** | 1 vvm | (**$N_2$**) 0.5 vvm |
| **Viscosity** | 0.0028 Pa.s (experimentally measured) | Considered the same as dodecane |

## 4.3.2 Methodology for the CFD model

In this paper, CFD simulations were performed in the commercial software package ANSYS FLUENT 18.2. The Euler-Euler model was used to describe the interactions between the two phases in the recirculation section: dodecane as dispersed phase ($\rho_d$ = 749.5 kg/m$^3$, $\mu_d$ = 0.00134 Pa.s), and broth as the continuous phase ($\rho_c$ = 983.8 kg/m$^3$, $\mu_c$ = 0.0028 Pa.s).

The Schiller-Naumann model was employed for the drag between the two phases. This model is described as the generally accepted model for liquid-liquid interactions (Schiller Naumann A., 1935; Sweere, Luyben and Kossen, 1987). The laminar model was selected based on Re estimations for the recirculation section and continuous phase (see Table 3). Transient simulations were run with a time step size of $\Delta t$ = 0.01 s. First order upwind discretization was used for momentum and oil fraction equations, with a first order implicit time discretization

for transient formulation. The simulation was considered converged when the absolute residuals were ≈ $10^{-5}$.

Simulations on half of the 100 L reactor were performed only for the separation compartment as 2D-axissymmetric, rotating over the x-axis crossing the centre of the riser section. The riser section was a fixed wall. The outlet was the recirculation tube. Oil separation was not depicted in the model. A tetrahedral mesh of 26k cells was used. Coarser and finer meshes were used to check mesh independency.

The input variables are: droplet diameters ($d_d$), oil hold-up ($\varphi_{oil}$) and inlet liquid velocities in the DC ($v_{DC,inlet}$).

Different values were tested to understand their impact in the hydrodynamics of the recirculation section and oil split (Table 3). The base case has a liquid velocity of 0.0032 m/s, an oil fraction of 0.1 and 20 µm droplet diameter. Moreover, the angle at the bottom of the recirculation zone was varied from 10 degrees (base case) to 22 degrees to study the impact of changing the internal geometry in the oil separation.

**Table 3 –** Input variables for the CFD model for inlet velocities in the DC different droplet diameter and volume oil fraction and Re for a droplet size of 20E-6, 40E-6 and 60E-6 m.

| Volume Oil Fraction | Velocity Inlet DC (m/s) | Re Regime |
|---|---|---|
| **0.1** | **Base case - 0.0032**<br>Case 1 - 0.0086<br>Case 2 - 0.0136 | Laminar<br>(Re < 210) |

The liquid velocities in the recirculation section were monitored by 4 virtual probes (lines). 3 virtual probes in the y-direction dividing the separation section and one line in the x-direction at the middle of the recirculation tube. The virtual probes are depicted in Figure 4.

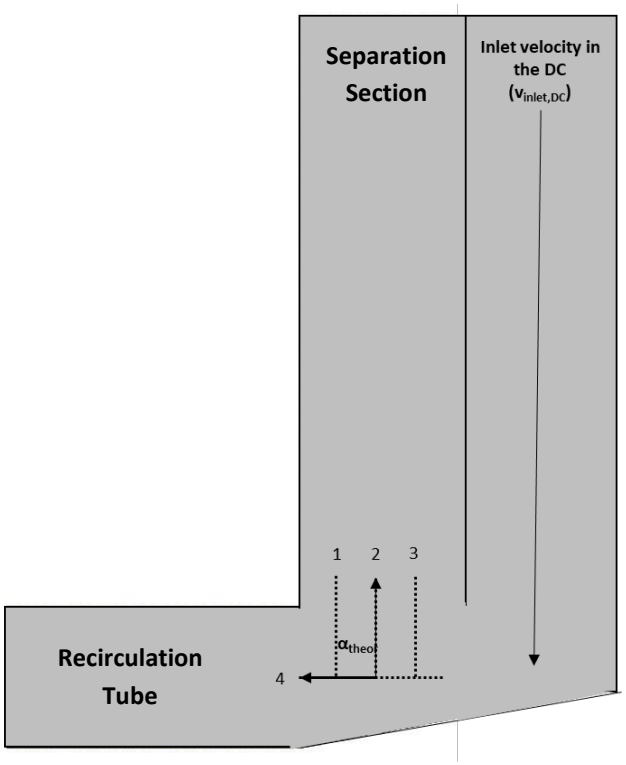


**Figure 4 –** CFD design of the recirculation section of the FAST bioreactor for the 2D axis-symmetric simulation with how the oil is separated (arrows) and the different virtual probes used to monitor the velocities (dashed lines).

#### 4.3.2.1 Experimental oil split

The experimental oil split ($\alpha_{exp}$) within separation section was obtained by the ratio between the recovered oil calculated by the harvest oil rate (total oil divided by the separation time) and the oil rate fed into the recirculation section ($\phi_{oil,DC}$). A scheme of how the oil is separated during liquid recirculation is shown in Figure 5.

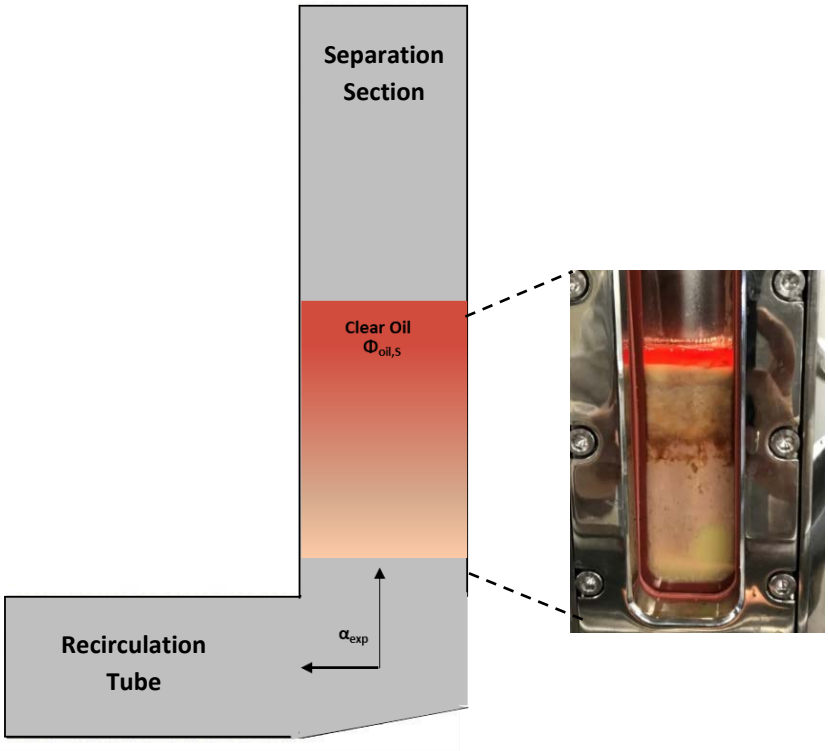


**Figure 5 –** Schematic view the oil separation based on the experimental split coefficient ($\alpha_{exp}$) in the recirculation section.

## 4.3.2 Analytics

### 4.3.3.1 Droplet size measurement of dodecane

Droplet size measurements were done using an *in-situ* optical probe (SOPAT Gmbh – detection range from 15 µm to 1000 µm) (Maaß et al., 2012; Heeres et al., 2015). However, this probe could not be used in the current integrated FAST bioreactor since no ports were available and there is no way of sterilizing the probe. Moreover, the diameter of the probe available for the measurements was 1 cm. The internal diameter of the integrated FAST bioreactor is within the same order of magnitude as the probe which, if used, could influence flow patterns. Therefore, the droplet size was estimated based on the oil rate and swarm rising velocity (Equation 1 and 2).

To confirm the method accuracy, two sets of experiments were performed to estimate the droplet size for similar matrix as used in the integrated FAST bioreactor: 20 L fermentation for

α-santalene production and FAST bioreactor run for humulene production, both with dodecane as a second phase. The droplet size was monitored using the *in-situ* optical probe.

The droplet size results obtained by the *in-situ* optical probe and by mathematical correlations (Equation 1 and 2) were both in the range of 70-80 µm.

For the FAST bioreactor run, the droplet size was estimated using the same equations (Equation 1 and 2). The average droplet size estimation in the integrated FAST bioreactor with dodecane as second phase was approximately 5 µm.

For the CFD simulations, a droplet of 20 µm was chosen. This was chosen since it is observed that for droplets in the range of 5 µm oil separation is minimal (see the following section 4.4.1). Therefore, unless coalescence techniques are added into the integrated reactor, the lower limit of droplet sizes to be used on the integrated FAST bioreactor should be higher than 20 µm. The droplet size was varied from 20-60 µm to understand what the effect of increasing droplet size in the simulations would be.

## 4.4 Results and Discussion

### 4.4.1 Oil recovery during FAST bioreactor pilot runs

Data for oil recovery in a continuous flow system (FAST) were experimentally obtained for two different systems: a sesquiterpene fermentation with a second phase addition of dodecane and a butanol (ABE) fermentation using oleyl alcohol as extractive phase. Figure 6 shows the amount of oil recovery in the separation section during each of the pilot runs of the FAST bioreactor (black circles - dodecane as second phase, white circles – oleyl alcohol as second phase).

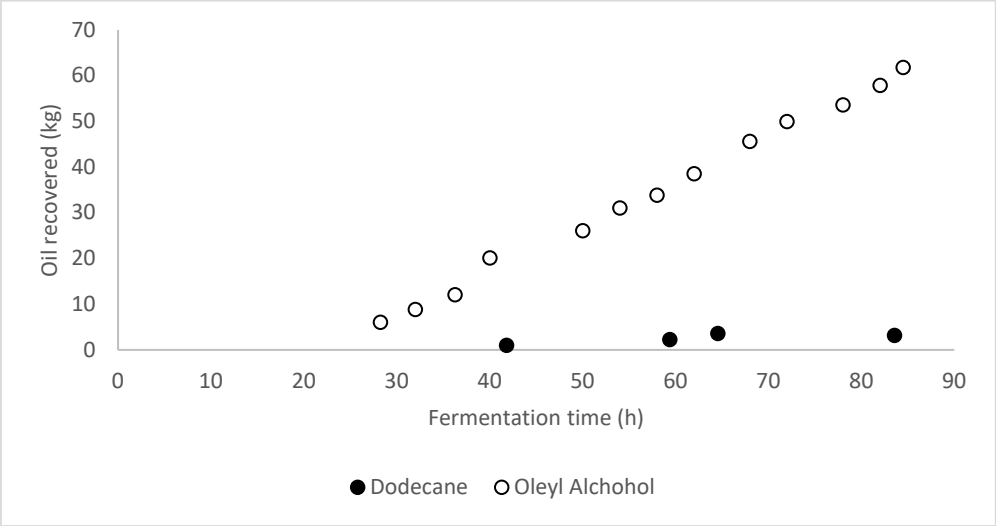


**Figure 6 –** Oil recovery in the separation compartment during the pilot runs of the FAST bioreactor with second phase addition of dodecane (black dots) and oleyl alcohol). Dodecane fermentation time was 83 h with oil feed starting at 40 h. Oleyl alcohol aided fermentation ran for 84.5 h with oil feed starting at 21h.

#### 4.4.1.1 Dodecane separation in sesquiterpene *E.coli* fermentation

For the pilot run a total of 10.8 kg of dodecane were fed to the reactor. The total oil recovery achieved after 83 h run was 3.6 kg which accounts for 33% recovery in the integrated FAST bioreactor.

The experimental oil split was estimated as 0.2% meaning that from all oil droplets entering in the separation compartment, only 0.2% were separated. The low dodecane oil separation and recovery indicate that the emulsion formed in the reactor with dodecane is highly stable and will be hard to separate within the FAST bioreactor. Emulsion stability is highly linked to the surface-active compounds, which increase during fermentation time, and droplet size (Pedraza-de la Cuesta et al., 2017; Da Costa Basto et al., 2019). This is substantiated by the small droplet size of the oil, estimated to be 5 µm. This gives an indication that for a system very low droplet size and high emulsion stability, FAST bioreactor by itself is not efficient enough to recover all the oil.

One way to optimize oil recovery in the separation section for such systems would be to make use of technologies such as GEOR (Heeres et al., 2016) or flocculant addition (Da Costa Basto et al., 2020), which would promote oil coalescence and allow a more effective separation.

To better understand what the impact of these properties, hydrodynamic studies were performed using the input variables as indicated in section 4.2.2.

#### 4.4.1.2 Oleyl alcohol separation in ABE fermentation with Clostridium

During fermentation the internal recirculation rate (see Appendix A - Hydrodynamic integrated bioreactor model) was maintained between 17-20 $L \cdot min^{-1}$. The oleyl alcohol fraction in the fermentation broth was monitored and remained constant throughout the fermentation at about 6%. With the constant oleyl alcohol hold-up, the net separation rate was thus identical to the dosing rate of extractive phase at 1 $kg \cdot h^{-1}$. Meaning that all the oil fed into the fermentation compartment was recovered via the separation compartment.

The concentration profiles of the fermentation are shown in Figure 7. The graph shows that the fermentation process remained viable throughout the fermentation and butanol toxicity was controlled adequately by means of the continuous organic phase extraction. Almost steady state butanol concentration was maintained in the aqueous broth and the extractive oleyl alcohol phase during fermentation, with the concentration of butanol much larger in the organic phase. This indicates that FAST bioreactor is capable of in-situ product recovery and butanol is kept below its inhibition limits.

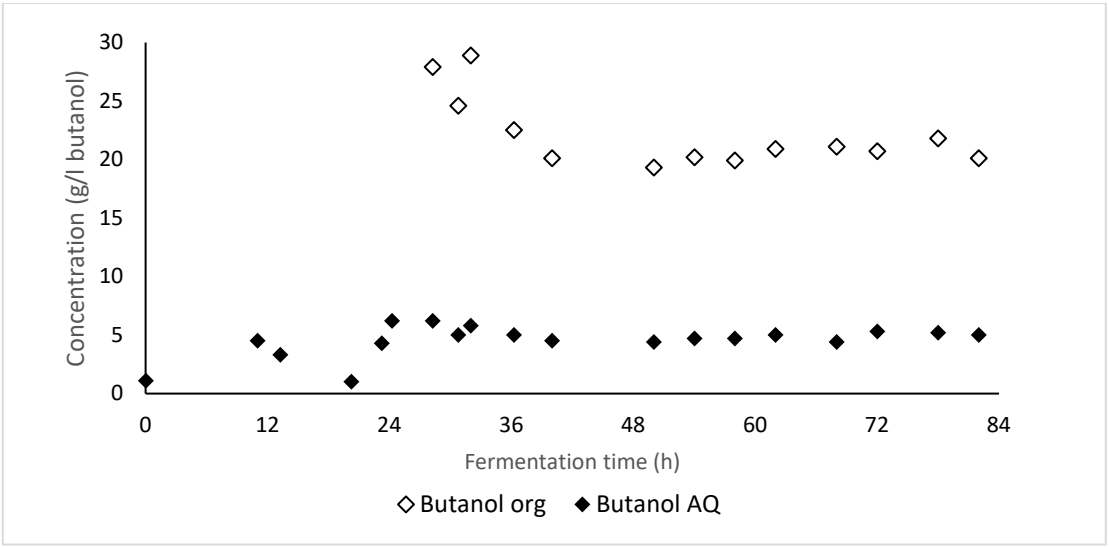


**Figure 7 –** Concentration of butanol during the fermentation run in the organic phase (white diamonds) and aqueous phase (black diamonds).

Off-line settling rate of the oleyl alcohol fermentation broth was performed by filling a glass column of 3.7 mm with 200 ml of broth and measuring the rate of oleyl alcohol formation at the top of the settling column. The observed settling rate was 450 $L \cdot m^{-2} \cdot h^{-1}$. Following the same approach as presented in section 4.3.3.1 - Droplet size measurement of dodecane, the droplet size was calculated as 90 µm.

The off-line settling tests indicates that a very high separation rate is possible. The observed constant separation rate of the FAST system follows this observation as the actual separation rate is far below the settling rate of the oleyl alcohol. The overall organic phase dosing on the system was only 62 kg of extractive phase, which is close to the total fermentation volume. The system is thus shown to be able to remove its own volume of auxiliary extractive phase during fermentation. The upper limit of the system would be, based on the settling test rate data, far higher, exceedingly far above 500 kg total removal capacity during the fermentation run. This shows that for this concrete system, when the integrated FAST bioreactor will be scaled-up, it is possible to reach higher volumes while keeping smaller areas.

### 4.4.2 Effect of velocity inlet in the FAST hydrodynamics

Figure 8 compares the different simulated patterns of oil flow and oil velocities in the recirculation section and riser tube of the FAST bioreactor for different downcomer inlet velocities for dodecane. Figure 8-[A] (Base case) shows that the oil velocity decreases close to the entrance of the recirculation section (starting velocity in the downcomer is 0.0032 m/s). The oil velocity field has a direct flow through the recirculation section and covers mainly its top part (from the middle of the recirculation tube to the top). The distance that the oil droplets need to travel from the recirculation compartment to the separation compartment can be quantified as 0.0191 m – half of the recirculation tube. At the bottom, the velocity is extremely slow and droplets in this zone will recirculate back to the fermentation compartment and will not be separated.

For case 1 and 2 (Figure 8-[B] and Figure 8- [C]), which have higher inlet velocities compared to the base case, the oil velocities are larger throughout the recirculation section. Moreover, the oil velocity field distribution becomes larger and flows through the whole recirculation section. This phenomenon is much larger in case 2, where the oil velocity field is also

distributed through the separation compartment and velocity swirls are observed. The distance for the oil to travel from the recirculation compartment to the separation compartment for both cases can be quantified as 0.0382 m (the full diameter of the recirculation tube).

This indicates that for the base case, oil separation can be enhanced due to two effects: (1) reduction of oil path to the separation compartment, and (2) reduction of turbulence and with less entrainment of oil droplets in the recirculation section. For case 2, large oil swirls in the separation compartment give an indication that separation of oil that could have been promoted via mechanisms such as GEOR (Heeres et al., 2016) is hindered. The oil can move with the swirls and again mixed with the emulsified oil reducing the oil separation capabilities. Moreover, it indicates that for these high inlet velocities a simple engineering models such as the laminar rising of oil droplets cannot correctly predict the oil separation. To be able to predict oil recoveries, an Eulerian-Lagrangian model incorporating droplet coalescence models would be more suitable.

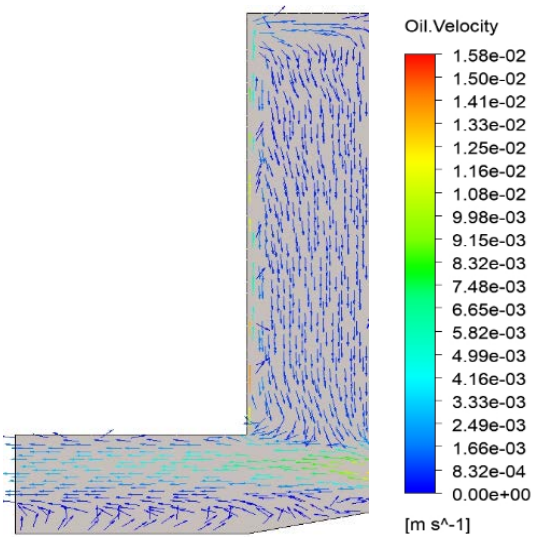


**Base case**
**($v_{DC,inlet}$ = 0.0032 m/s; $d_d$ = 20 µm; $\varphi_{oil}$ = 0.1)**

**[A]**

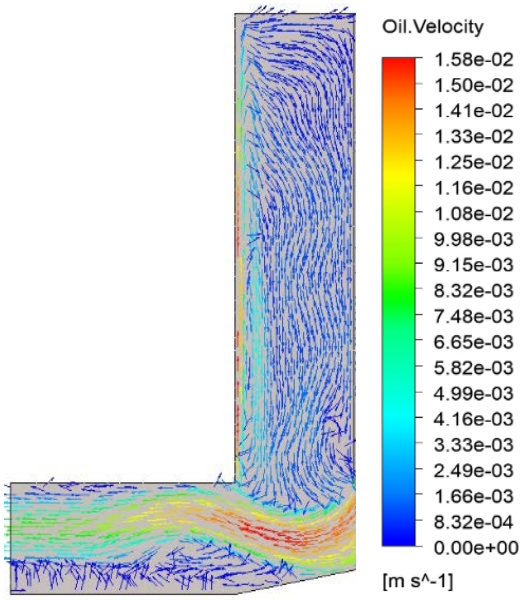


**Case 1**
**($v_{DC,inlet}$ = 0.0086 m/s; $d_d$ = 20 µm; $\varphi_{oil}$ = 0.1)**

**[B]**

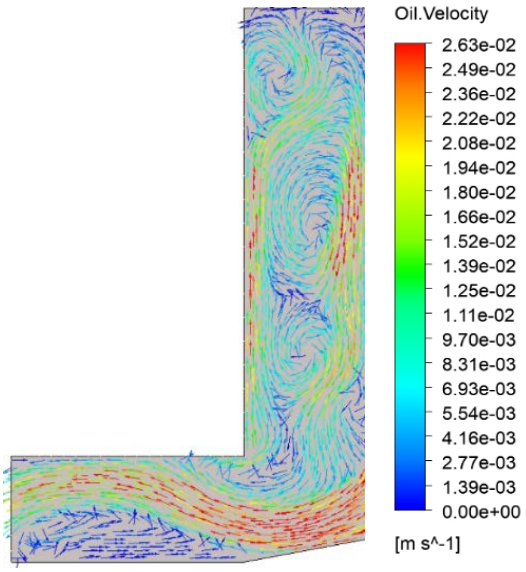


**Case 2**
**($v_{DC,inlet}$ = 0.0136 m/s; $d_d$ = 20 µm; $\varphi_{oil}$ = 0.1)**

**[C]**

**Figure 8 –** Comparison of the oil velocity vectors for different inlet velocities. [A] – Base Case, [B]- Case 1 and [C]- case 2.

### 4.4.3 Modelled oil recovery in the FAST bioreactor.

The calculated oil split was determined for different downcomer inlet velocities using Equation 5. The height H (m) that droplets need to travel in a vertical direction, during the recirculation of the liquid back to the fermentation compartment, is obtained by the CFD simulations presented in the previous section (section 4.4.2). The length L (m) which the oil droplets travel horizontally is considered to be the distance to which the velocity vectors keep on pointing towards the recirculation tube direction. The results can be seen in Table 4.

**Table 4 –** Vertical distance (H(m)) and horizontal distance (L(m)) that oil droplets flow through to separate and recirculate. The oil split and oil recovery calculated based on a droplet velocity of 1.05E-5 m/s and the flows of the CFD model for a 0.1 oil fraction and droplet size of 20 µm.

| | **Base case** | **Case 1** |
|---|---|---|
| **Vertical distance (H (m))** | 0.0191 | 0.0382 |
| **Horizontal distance (L (m))** | 0.084 | 0.084 |
| **Oil Rising Time (h)** | 0.5 | 1.0 |
| **Oil split in the separation compartment** | 0.4 | 0.06 |
| **Modelled Oil recovery (%)** | 42 | 5.8 |

The oil recovery was obtained by equation 6. The results show that for the base case, the oil recovery is 4 times higher than for case 1. The flow of oil separating for the base case is 6.4 kg/h, while for case 1 is 1.6 kg/h leading to an oil recovery of 42 and 5.8 %, respectively.

Comparing the different oil recoveries in the separation compartment for base case and case 1, it is seen that oil recovery is promoted for lower inlet velocities in the downcomer. This can be explained by two effects: lower oil velocity, which allows more time for the droplets to rise to the separation zone where they can be easily separated; and smaller rising path, which makes the droplets closer to the separation zone, taking less time (0.5 h) to reach the separation compartment before being recirculated. For case 1, it can take up to 1 h for the oil droplets to separate. This is due to the higher vertical distance required for the oil droplet to travel.

For both cases, oil recovery is low. The reason is high inlet flow in the recirculation compartment which leads to a low residence time (order of seconds) of the oil droplets in the compartment (See Appendix B - Integrated bioreactor functionalities – Table ). This implies that only the top oil droplets will be able to separate before the broth recirculates back to the fermentation compartment. One possible way to maximize oil separation is to lower the flow of oil entering in the separation compartment. However, is necessary to ensure that oxygen and substrate supply is kept so that the cells do not die.

For case two, although oil recoveries cannot be quantified, it is seen that not only the path for the oil droplets to rise in the recirculation compartment is comparable with case 1 but the high oil velocities will decrease the time of the oil droplets to rise in the recirculation compartment. Moreover, the swirls shown in Figure 8 – [C], shows that the oil droplets that

manage to rise into the separation zone, become entrapped and recirculated back not being separated. Therefore, it is observed that when inlet velocities in the recirculation zone exceed a system Re higher than 250, oil separation is hindered due to the increase of swirls.

Oil recovery prediction considering 42 h of separation run for the modelled base case and case 1 are observed in Figure 9. The oil recovery was attained based on the slip velocity of the oil droplets for oil fractions of 0.1 (Equation 2). The oil prediction obtained represent the ideal scenario for the integrated FAST bioreactor to separate oil (dodecane) based solely on hydrodynamics, oil fraction and droplet size. No emulsification or droplet coalescence are considered.

When comparing with the experimental results (Figure 9 - white circles) it is observed that the result from the simulated base case is in the same order of magnitude as the experimental oil recovery using oleyl alcohol. These results suggest two things: CFD simulations can predict with good accuracy oil recoveries (oleyl alcohol follows the same trend as the two model scenarios); and if the added dodecane has larger droplet sizes (when emulsification is hindered) and the correct inlet velocities can be tuned, dodecane separation can be optimized.

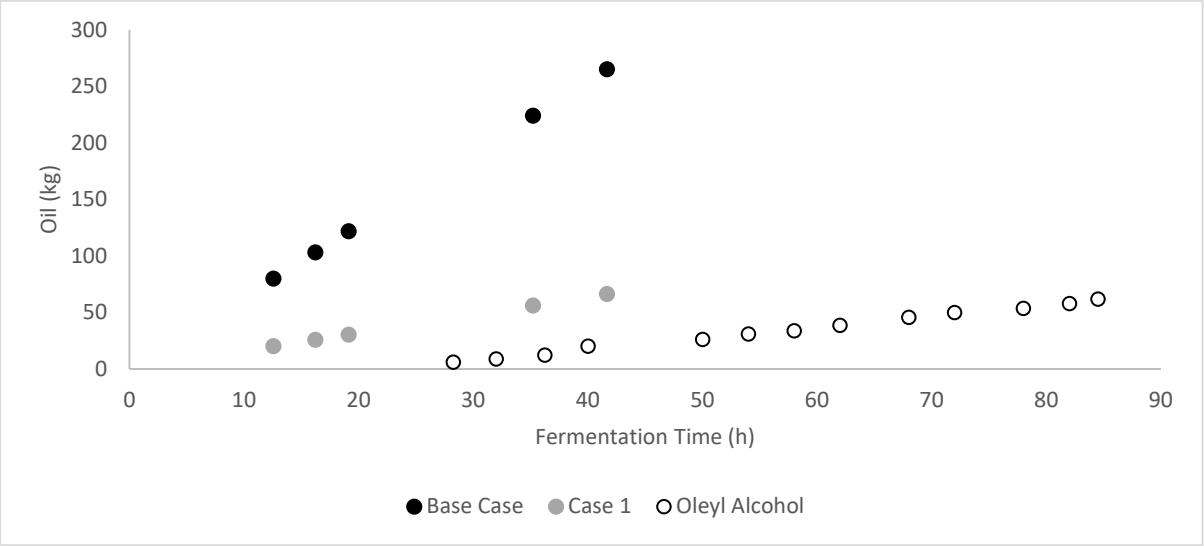


**Figure 9 –** Calculated oil recovery for dodecane considering 42 h run of the FAST bioreactor (black circles – base case and grey circles – Case 1) and experimental data for the Oleyl Alcohol separation in the FAST bioreactor (white circles).

### 4.4.4 Integrated FAST bioreactor window of operation

A window of operation could be found to promote oil recovery using the integrated FAST bioreactor. Different CFD simulations were performed by changing two different characteristics of the base case: droplet size and angle of the recirculation compartment (11$^{o}$). Their impact on the oil recirculation is discussed under this section.

In the previous sections, it was observed that (too) small oil droplets (5 μm) will hinder oil recovery. By increasing the oil droplets, oil recovery increased. Figure 10 shows that bigger droplet sizes (Figure 10-[A] – 40 μm and Figure 10-[B] – 60 μm) will lead to a decrease in the velocity flow path throughout the recirculation section and an increase in oil velocities when compared it with the base case. The vertical distance that droplets need to rise to reach to the separation compartment is 0.018 and 0.012 m for 40 and 60 μm respectively. This will lead to an increase of the oil split in the separation compartment which will promote oil recovery. For oil droplets of 40 μm, 50% of the oil entering in the recirculation compartment will be entering in the separation compartment. For 60 μm, 96% of the oil will be separated. This is expected since bigger droplets will rise faster due to higher buoyancy but also need less height to rise to the separation zone. Therefore, an emulsion with large oil droplets will lead to higher oil recoveries in the FAST bioreactor without the use of de-emulsification techniques.

Figure 11 shows how a change in one of the dimensions, such as the angle of the internal part of the separation will have an influence on the flow path. An increase in the angle of the separation zone, while maintaining all the conditions as the base case, will lead to an increase of swirls in the recirculation section and separation zone while oil velocities remain the same. When the oil flows from the downcomer, the flow path is restrained at the entrance of the recirculation section. This restriction will create the flow to deviate from a direct path into the recirculation tube creating an increase in swirls. These swirls in the flow will create oil entertainment making it difficult for oil to separate without coalescence mechanisms. A potential way of decreasing such swirls in the FAST bioreactor is by having smoother pathways. A smoother path will intrinsically allow for a more streamlined flow and the decrease of recirculation zones in the FAST bioreactor which can hinder oil recovery.

By combining all the results of this research, a window of operation can be established to stimulate the oil split in the recirculation compartment without using coalescence techniques: Oil droplets larger than 40 µm, inlet oil velocities lower than 0.0086 m/s and recirculation angles lower than 11 degrees.

This simplified CFD model, in combination with simple engineering equations, has shown to be a useful tool to predict the hydrodynamics flows and draw a window of operation where oil separation can be enhanced in the FAST bioreactor. In particular, the use of such models can provide great insight for scaling up any type of integrated reactor where hydrodynamics is not clear. For the case of the FAST bioreactor, it is expected, that a better oil prediction would be achieved if emulsification models and coalescence models, if applicable, would be included.

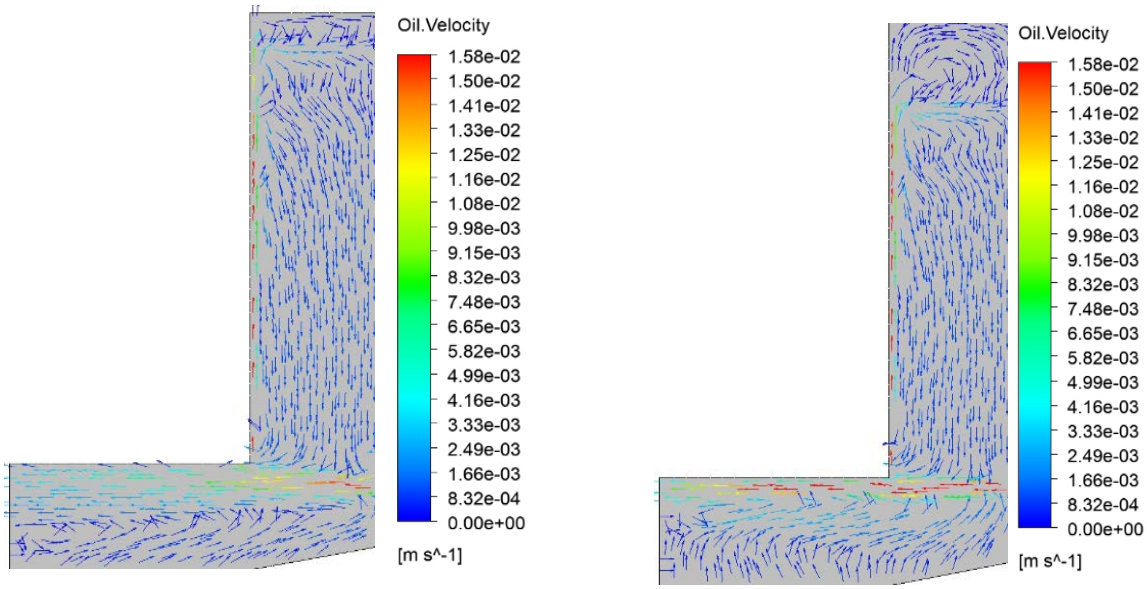


**$v_{DC,inlet}$ = 0.0032 m/s; $d_d$ = 40 µm; $\varphi_{oil}$ = 0.1**

**[A]**

**$v_{DC,inlet}$ = 0.0032 m/s; $d_d$ = 60 µm; $\varphi_{oil}$ = 0.1**

**[B]**

**Figure 10 -** Oil velocity vectors of the base case for different droplet diameter. [A] – Base Case with 40 µm droplets; [B]- Base case with 60 µm droplets.

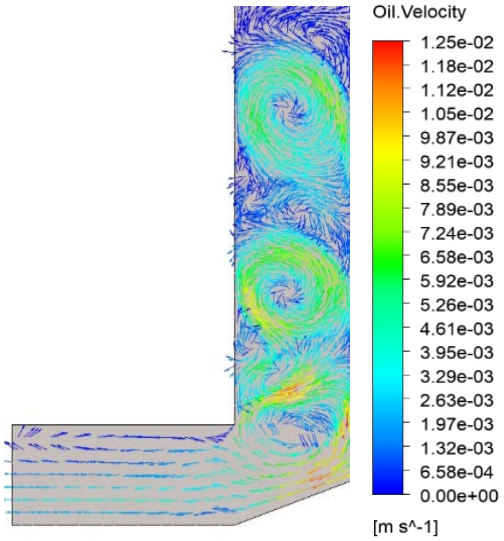


**$v_{DC,inlet}$ = 0.0032 m/s; $d_d$ = 20 µm; $\varphi_{oil}$ = 0.1**

**Figure 11 –** Oil velocity vectors for the base case with an increase angle (22 degrees) of the separation compartment.

## 4.5 Conclusion

The above results indicates that the use of an integrated FAST bioreactor to separate oil in-situ is feasible however improvements in the flow conditions and design are required to optimize oil recoveries.

CFD simulations were able to generate hydrodynamic data and be used to predict oil recoveries. Different conditions were studied to understand the window of operation and main constraints for oil separation in the integrated FAST bioreactor. Systems with larger oil droplets, lower inflow velocities in the recirculation compartment as well as smoother pathways promoted oil recoveries. Droplets that require to travel shorter distances to be separated will enhance oil recoveries. Systems where Re exceeds 250 and recirculation compartment angles are steeper will be hampered by the formation of swirls in the separation zone.

Further work is required to understand how the FAST bioreactor design and environment can be changed by keeping realistic fermentation conditions and optimize towards max oil recovery. This can be done by including (a stack of) tilted internals that will decrease droplet

travelling distance and allow smoother paths. A more detailed hydrodynamic models, with mass transfer and emulsification and coalescence models included, if applied, will be beneficial to improve accuracy.

While there are challenges in implementing realistic models and having in-line measurements to provide better droplet size and flow understanding, this work has shown that a simplified CFD model, in combination with engineering equations, can be a useful tool to predict trends in the integrated FAST bioreactor.

## 4.6 Acknowledgements

This work was carried out within the BE-Basic R&D Program, which was granted a FES subsidy as well as a TKI-BBE grant (TKI-AMBIC-program TKIBE-01003) from the Dutch Ministry of Economic affairs.

The butanol fermentation research was supported by the Dutch Ministry of Economic Affairs through the Netherlands Enterprise Agency (RvO). We thank our project partners WFBR and Biocleave for their contribution. The butanol fermentation was funded under the name DEI+FASTEST, grant number DEI2719024.

The authors would like to thank Dr. Cees Haringa for providing a critical discussion on the simulation. To Dr. Alireza for helping to set up the simulations in the Transport Phenomena server.

## 4.7 References


Amyris (2016) *https://amyris.com/innovation/biofene/*.

van Benthum, W.A.J. *et al.* (1999) 'The biofilm airlift suspension extension reactor. Part I: Design and two-phase hydrodynamics', *Chemical Engineering Science*, 54(12), pp. 1909–1924. Available at: https://doi.org/http://dx.doi.org/10.1016/S0009-2509(99)00034-2.

Da Costa Basto, R.M. *et al.* (2019) 'A Mechanistic Model for Oil Recovery in a Region of High Oil Droplet Concentration from Multiphasic Fermentations', *Chemical Engineering Science: X*, p. 100033. Available at: https://doi.org/https://doi.org/10.1016/j.cesx.2019.100033.

Da Costa Basto, R.M. *et al.* (2020) 'Impact of flocculant addition in oil recovery from multiphasic fermentations', *Food and Bioproducts Processing*, 123, pp. 150–163. Available at: https://doi.org/10.1016/j.fbp.2020.06.006.

Crowe, C.T. *et al.* (2011) *Multiphase Flows with Droplets and Particles*. second. CRC Press. Available at: https://doi.org/10.1201/b11103.

Cuellar, M.C., Heijnen, J.J. and van der Wielen, L.A.M. (2013) 'Large-scale production of diesel-like biofuels - process design as an inherent part of microorganism development', *Biotechnol. J.*, 8(6), pp. 682–689. Available at: https://doi.org/10.1002/biot.201200319.

Cuellar, M.C. and Straathof, A.J.J. (2018a) 'CHAPTER 4 Improving Fermentation by Product Removal', in *Intensification of Biobased Processes*. The Royal Society of Chemistry, pp. 86–108. Available at: https://doi.org/10.1039/9781788010320-00086.

Cuellar, M.C. and Straathof, A.J.J. (2018b) 'CHAPTER 4 Improving Fermentation by Product Removal', in *Intensification of Biobased Processes*. The Royal Society of Chemistry, pp. 86–108. Available at: https://doi.org/10.1039/9781788010320-00086.

DAB BV (no date) 'DAB.bio's revolutionary FAST$^{TM}$ biomanufacturing platform'.

Gupta, C. (2015) 'A Biotechnological Approach to Microbial Based Perfumes and Flavours', *Journal of Microbiology & Experimentation*, 2(1). Available at: https://doi.org/10.15406/jmen.2015.02.00034.

Heeres, A.S. *et al.* (2014) 'Microbial advanced biofuels production: overcoming emulsification challenges for large-scale operation', *Trends Biotechnol.*, 32(4), pp. 221–229.

Heeres, A.S. *et al.* (2015) 'Fermentation broth components influence droplet coalescence and hinder advanced biofuel recovery during fermentation', *Biotechnol. J.*, 10(8), pp. 1206–1215. Available at: https://doi.org/10.1002/biot.201400570.

Heeres, A.S. *et al.* (2016) 'Gas bubble induced oil recovery from emulsions stabilised by yeast components', *Chem. Eng. Sci.*, 145, pp. 31–44. Available at: https://doi.org/http://dx.doi.org/10.1016/j.ces.2016.02.011.

Heijnen, J.J. *et al.* (1997) 'A simple hydrodynamic model for the liquid circulation velocity in a full-scale two- and three-phase internal airlift reactor operating in the gas recirculation regime', *Chemical Engineering Science*, 52(15), pp. 2527–2540. Available at: https://doi.org/http://dx.doi.org/10.1016/S0009-2509(97)00070-5.

Heijnen, S.J. *et al.* (1990) 'Large-scale anaerobic/aerobic treatment of complex industrial wastewater using immobilized biomass in fluidized bed and air-lift suspension reactors', *Chemical Engineering & Technology - CET*, 13(1), pp. 202–208. Available at: https://doi.org/10.1002/ceat.270130127.

Janssen, L.P.B.M. and Warmoeskerken, M.M.C.G. (2006) *Transport phenomena data companion*. Delft: VSSD.

M, D.S. (2017) 'POET-DSM plans on-site enzyme manufacturing facility at Project Liberty'.

Maaß, S. *et al.* (2012) 'Automated drop detection using image analysis for online particle size monitoring in multiphase systems', *Comput. Chem. Eng.*, 45, pp. 27–37. Available at: https://doi.org/http://dx.doi.org/10.1016/j.compchemeng.2012.05.014.

Mandalahalli, M.M. *et al.* (no date) 'Electrolyte effects on recirculating dense bubbly flow: An experimental study using X-ray imaging', *AIChE Journal*, 0(0), p. e16696. Available at: https://doi.org/10.1002/aic.16696.

Oudshoorn, A. *et al.* (2021) 'WO2021010822 - INTEGRATED SYSTEM FOR BIOCATALYTICALLY PRODUCING AND RECOVERING AN ORGANIC SUBSTANCE'. Available at: https://patentscope.wipo.int/search/en/detail.jsf?docId=WO2021010822.

Pappas, T. and Oudshoorn, A. (no date) *ENABLING COST EFFECTIVE BUTANOL PRODUCTION WITH DAB.bio's UNIQUE BIOREACTOR TECHNOLOGY*. Available at: https://cdn.sanity.io/files/vpc725g9/production/95f6149c86c4a784825ec0b215d77207850e4b38.pdf (Accessed: 11 September 2023).

Pedraza-de la Cuesta, S. *et al.* (2017) 'Integration of Gas Enhanced Oil Recovery in multiphasic fermentations for the microbial production of fuels and chemicals', *Chemicals biotechnology Journal* [Preprint].

Pedraza-de la Cuesta, S. *et al.* (2018) *Techno-economic assessment of the use of solvents in the scale-up of microbial sesquiterpene production for fuels and fine chemicals*. Available at: https://doi.org/10.1002/bbb.1949.

Renninger, N. (2010) 'Scale-up and Mobilization of Renewable Diesel and Chemical Production from Farnesene using US-based Fermentable Sugar Feedstocks'. Edited by D.O.E.I.B. Review.

Reynolds, T.D., Richards, P.A. and 2nd (1996) 'Sedimentation', in *Unit operations and processes in environmental engineering*. CL Engineering, pp. 219–283.

Richardson, J.F. and Zaki, W.N. (1954) 'The sedimentation of a suspension of uniform spheres under conditions of viscous flow', *Chemical Engineering Science*, 3(2), pp. 65–73. Available at: https://doi.org/https://doi.org/10.1016/0009-2509(54)85015-9.

Schiller Naumann A., L. (1935) 'A drag coefficient correlation', *Z. Ver. Deutsch. Ing*, 77, pp. 318–320.

Soares-Castro, P., Soares, F. and Santos, P.M. (2020) 'Current Advances in the Bacterial Toolbox for the Biotechnological Production of Monoterpene-Based Aroma Compounds.', *Molecules (Basel, Switzerland)*, 26(1). Available at: https://doi.org/10.3390/molecules26010091.

Straathof, A.J.J. *et al.* (no date) 'Grand Research Challenges for Sustainable Industrial Biotechnology', *Trends in biotechnology* [Preprint]. Available at: https://doi.org/10.1016/j.tibtech.2019.04.002.

Straathof, A.J.J. and Cuellar, M.C. (2019) 'Microbial Hydrocarbon Formation from Biomass', in K. Wagemann and N. Tippkötter (eds) *Biorefineries*. Cham: Springer International Publishing, pp. 411–425. Available at: https://doi.org/10.1007/10_2016_62.

Sweere, A.P.J., Luyben, K.C.A.M. and Kossen, N.W.F. (1987) 'Regime analysis and scale-down: Tools to investigate the performance of bioreactors', *Enzyme and Microbial Technology*, 9(7), pp. 386–398. Available at: https://doi.org/http://dx.doi.org/10.1016/0141-0229(87)90133-5.

Tabur, P. and Dorin, G. (2012) 'Method for purifying bio-organic compounds from fermentation broth containing surfactants by temperature-induced phase inversion'. Edited by Amyris. US: Amyris Inc.

*Total and Amyris renewable jet fuel ready for use in commercial aviation* (2014) *https://totalenergies.com/media/news/press-releases/total-and-amyris-renewable-jet-fuel-ready-use-commercial-aviation*.

Velasco, J. (2014) 'Growing the future of bioeconomy', in *US Department of Energy*. Amyris. Available at: https://www.energy.gov/sites/prod/files/2014/11/f19/x_velasco_biomass_2014.pdf.

Vickers, C.E. *et al.* (2017) 'Recent advances in synthetic biology for engineering isoprenoid production in yeast', *Current Opinion in Chemical Biology*, 40, pp. 47–56. Available at: https://doi.org/https://doi.org/10.1016/j.cbpa.2017.05.017.

de Vrije, T. and Claassen, P.A.M. (2018) *Production of butanol and hydrogen by fermentation techniques using steam treated municipal solid wastes : EU BESTF2 MSWBH*. Available at: https://doi.org/10.18174/463764.

Wen, M., Bond-Watts, B.B. and Chang, M.C. (2013) 'Production of advanced biofuels in engineered E. coli', *Current Opinion in Chemical Biology*, 17(3), pp. 472–479. Available at: https://doi.org/10.1016/j.cbpa.2013.03.034.

## 4.8 Appendix A. Hydrodynamic integrated bioreactor model

In more detail, the recirculation flow of the FAST bioreactor is dependent on the pressure difference over the recirculation tube. The gas hold-up between the two compartments is the main cause of this pressure difference and it is dependent on the input of superficial gas velocity in the separation compartment. The best way to control the recirculation flow is by creating a control mechanism based on the hydrostatic pressures (van Benthum et al., 1999). As the reactor is closed, there is a creation of overpressure in the separation compartment ($\Delta P_{head,1}$). The sparger in the separation compartment introduces gas bubbles to recover the oil ($H_{sep}$) creating a gas hold-up ($\varepsilon_{sep}$). The liquid coming from the downcomer circulates towards the recirculation section and the oil droplets rise solely by gravity ($H_{circ}$).

The hydrostatic pressure in the separation compartment, $P_1$, measured just above the recirculation tube, where the flow is recirculated, is given by:

$$p_1 = g\rho_{sep}H_{sep}\left(1-\varepsilon_{sep}\right) + g\rho_{circ}H_{circ} + \Delta p_{head_1} + p^0 \quad \text{(Pa)} \qquad (1)$$

Being, $P^0$ is the atmospheric pressure (1 bar), $\rho_{sep}$ the density in the separation compartment and $\rho_{circ}$ the density of multiphasic mixture in the circulation section.

In the fermentation compartment, the gas bubbles, created by the sparger on the bottom of the reactor, are collected in the riser section generating a gas hold-up ($\varepsilon_{ris}$). These bubbles will leave through the top of the reactor, $F_{g,ferm,out}$, which is connected to a valve that can control the overpressure in the riser ($\Delta P_{head,2}$), thus the recirculation flow.

The hydrostatic pressure in the fermentation compartment, $P_2$, measured on the bottom of the riser, is given by:

$$p_2 = g\rho_{ferm}H_{ris}(1-\varepsilon_{ris}) + \Delta p_{head_2} + p^0 \qquad \text{(Pa)} \qquad (2)$$

The pressure difference through the recirculation tube can be obtained by the difference of the two hydrostatic pressures.

$$\Delta p_{tube} = p_1 - p_2 \quad \text{(Pa)} \tag{3}$$

$$\Delta p_{tube} = g\rho_{sep}H_{sep}(1-\varepsilon_{sep}) + g\rho_{circ}H_{circ} - g\rho_{ferm}H_{ris}(1-\varepsilon_{ris}) + \Delta p_{head_1} - \Delta p_{head_2} \tag{4}$$

The gas hold-up (ε) of the two compartments can be expressed by a simple correlation used for large scale internal loop air-lift reactor (Heijnen et al., 1997):

$$\varepsilon_g = \frac{v_{GS}}{0.25} \tag{5}$$

When a liquid flows passes through the tube, there is a pressure drop created by friction losses of the tube ($K_{f,tube}$) that can be described by the Bernoulli's equation.

$$\frac{\Delta p_{tube}}{\rho_{circ}} = K_{f\,tube}\left(\frac{1}{2}\right)v_{circ}^2 \tag{6}$$

Where $v_{circ}$ is the liquid velocity through the holes and $\rho_{circ}$ is the liquid velocity. This liquid velocity is dependent on the volumetric oil fraction in the circulation flow.

$$\rho_{circ} = (1-\varphi_{oil,circ})\rho_w + \varphi_{oil,circ}\rho_{oil} \tag{7}$$

The frictional loss coefficient can be correlated with the geometry of the reactor by taking into account the reactor geometry and the phenomena that occurs when the liquid flows through the recirculated tube: contraction and expansion (Janssen and Warmoeskerken, 2006). The friction losses caused by contraction are given by:

$$K_{f\,cont} = 0.45\left(1 - \frac{A_{circ}}{A_{sep}}\right) \tag{8}$$

Where the $A_{circ}$ is the cross-section area of the slit from where the recirculated liquid flows and $A_{sep}$ is the cross-sectional area from the separation compartment. For the friction losses due to expansion a similar expression can be obtained.

$$K_{f\,exp} = \left(\frac{A_{total}}{A_{circ}} - 1\right)^2 \tag{9}$$

This coefficient considers the circulation area in the tube and the total sectional area of the reactor, $A_{total}$. The overall friction coefficient can be obtained by the two former expressions.

$$K_{f\,tube} = 0.45\left(1 - \frac{A_{circ}}{A_{sep}}\right)\left(\frac{A_{sep}}{A_{circ}}\right)^2 + \left(\frac{A_{total}}{A_{circ}} - 1\right)^2\left(\frac{A_{sep}}{A}\right)^2 \tag{10}$$

The circulation velocity can now be determined and correlated with the circulation flow by means of the circulation area of the tube.

$$F_{V,circ} = v_{circ}A_{circ} \quad (\text{m}^3/\text{s}) \tag{11}$$

For a proper functioning of the integrated FAST bioreactor, the residence time of the recirculation flow should be enough to allow the oil droplets to rise and separate. However, small oil droplets have a higher residence time to rise to the top so they will recirculate via the tube and coalesce with the oil droplets being formed in fermentation compartment.

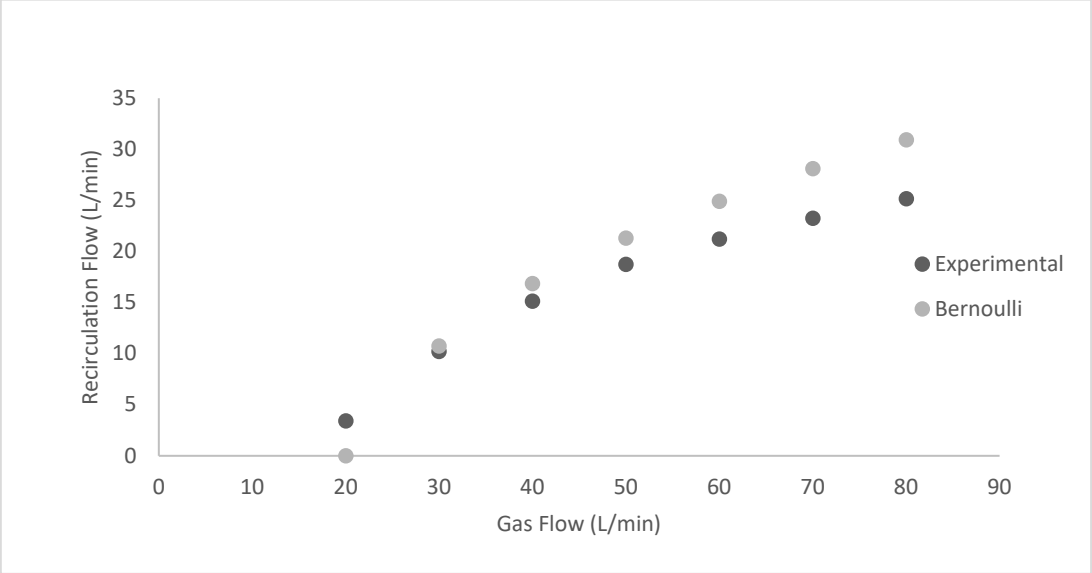


**Figure A-1 –** Recirculation flows over the tube as function of the gas flows introduced in the fermentation compartment.

In Figure A-1, water experiments were performed at different gas flow velocities and the recirculation flows measured in the tube were compared with the recirculation flow given by

the recirculation model (Bernoulli). It is observed that for higher gas flows the model overestimates the recirculation flow. This divergency can be explained by an under estimation of the friction coefficient or an under estimation of the gas hold up used in the model which was calculated using the correlation by the Heijnen et al (Heijnen et al., 1997) which might not be the ideal correlation to use in the FAST bioreactor. For the studied ranges of this article (30 – 50 L/min) an error of maximum 13.7% was found between experimental and model predictions. Therefore, the recirculation flows were used to calculate the inlet velocity of the liquid in the downcomer used in the CFD model.

## 4.9 Appendix B. Integrated FAST bioreactor functionalities

**Table B.1 –** Characteristic times for the different functionalities of the separation compartment of the integrated FAST bioreactor.

| Studies | How to study (Tests and functionalities) | Sections |
|---|---|---|
| **Cells viability during liquid recirculation** | Oxygen depletion<br>$\tau_{OD} > t_{dc} + t_{res}$[1] | Downcomer and recirculation section |
| **Separation compartment functionalities** | Prevent gas bubble circulation<br>$t_{dc} > \tau_{GB}$ | Down-comer |
| | Prevent creaming in the down-comer<br>$\tau_{ris,DC} > t_{dc}$ | Down-comer |
| | Proper residence time for droplet rise<br>$\tau_{res} > \tau_{ris,rec}$ | Recirculation section |
| | Promote rising of oil droplets<br>**Laminar Flow** | Recirculation section |

[1] Merely an indication since it is not known which is the actual effect of this limitation in the cells.

**Residence time in the downcomer:**

The residence time in the downcomer can be calculated by the ration between the height and liquid velocity of the down-comer.

$$t_{dc} = \frac{H_{dc}}{v_{dc}} \text{ (s)} \quad (1)$$

The liquid velocity in that region, which can be obtained from the cross-sectional area in the down-comer and the circulation flow, is presented below.

$$v_{dc} = \frac{F_{circ}}{A_{dc}} \text{ (m/s)} \quad (2)$$

**Characteristic time for the rise of gas bubbles:**

The characteristic times of the gas bubbles indicates the time necessary for a bubble, in a certain liquid volume, to rise and leave through the top of the reactor without entering in the separation compartment. Considering that the gas bubbles in the bubble column have 5 mm, the rising velocity of these bubbles is 0.25 m/s.

$$\tau_{GB} = \frac{H_{dc}}{v_{GB}} \text{ (s)} \quad (3)$$

**Oxygen depletion by the cells**

However not the focus of this work, one characteristic time that can be included for bioreactor design is the time that take for the cells to change metabolism in an environment with no oxygen or substrate supply.

For cell viability, a relation with the characteristic time for oxygen depletion was made to understand if the cells (wild type, experimental GMO and theoretical GMO) are viable during the recirculation flow in the separation compartment.

The cells entering in the separation compartment consume a certain amount of oxygen to keep producing hydrocarbons. There is no addition of a gas or nutrients flow due to the attempt of reaching a compartment as stagnant as possible, thus the oxygen available for the cells is the one dissolved into the liquid at the moment of entering in the downcomer (assumed to be 65% of $O_2$ dissolved). Thus, the time to reach oxygen depletion by the cells ($\tau_{OD}$) must be larger than the time that takes the cells to go from the downcomer($t_{dc}$) and to the recirculation tube ($t_{res}$) where they will be recirculated into the fermentation compartment.

Microbial metabolism is dependent on the oxygen and substrate availability. Because substrate can be added without having a big influence on the oil separation, the study of the characteristic time for oxygen depletion in the separation compartment was chosen to be the principal factor in terms of cell viability.

Assumption:

The fermentation compartment and the riser section are presumed to be well mixed, thus the concentration of cells is the same in both sections.

At feed-phase the concentration of cells ($C_X$) in the reactor is 3.13 mol/L (77 g/L), thus the number of cells can be achieved for each by the equation below.

$$N_X = C_X \times V \quad \text{(molX)} \tag{4}$$

Where V is the volume for each section (section 1 – down-comer and section 2 – effective volume).

The only oxygen consumed by the cells is the one dissolved in the liquid. The requirement of oxygen by the cells needs to be calculated so that the time for oxygen depletion can be attained. Having the number of cells in the two compartments and knowing at which rate one cell consumes oxygen, the consumption rate ($R_{O2}$) can be achieved.

$$R_{O2} = -q_{O2} \times N_X \quad \text{(molO}_2\text{/h)} \tag{5}$$

Thus, the characteristic time for oxygen depletion can be written as follows:

$$\tau_{OD} = \frac{DO \times V}{R_{O2}} \quad \text{(s)} \tag{6}$$

Where the DO is the concentration of dissolved oxygen in the liquid when entering in the down-comer section (30% - 0.139 mol/m$^3$).

The results of the characteristic times for the separation compartment at different reactor scales are presented in the table below.

**Table B.2 –** Times calculated based on different volumes for the integrated FAST bioreactor at Pilot scale. The following assumptions were made: DO – 0.139 mol/m$^3$, $R_{O2}$ = -0.0298 mol oxygen/h-1.Cmol biomass (theoretical yield E. coli feed phase), bubble velocity of 0.25 m/s, droplet size of 20 µm and velocity in the downcomer of 0.0032 m/s.

| **Characteristic Times** | **FAST (s)** | |
|---|---|---|
| | **Dodecane** | **Oleyl Alcohol** |
| $\tau_{OD}$ | 4 | NA (anaerobic system) |
| $t_{dc}$ | 260 | 44 |
| $t_{res}$ | 17 | 3 |
| $\tau_{GB}$ | 3.4 | NA (anaerobic system) |
| $\tau_{ris,DC}$ | 80066 | 167 |
| $\tau_{ris,rec}$ | 2243 | 434 |

From the times calculated based on the dimensions of the integrated FAST Bioreactor it is observed that not all functionalities will be fulfilled.

**Table B.3 –**Functionalities of the integrated FAST bioreactor.

| | | |
|---|---|---|
| Oxygen depletion<br>$\tau_{OD} > t_{dc} + t_{res}$* | Not fulfilled | NA |
| Prevent gas bubble circulation<br>$t_{dc} > \tau_{GB}$ | Fulfilled | NA |
| Prevent creaming in the down-comer<br>$\tau_{ris,DC} > t_{dc}$ | Fulfilled | Fulfilled |
| Proper residence time for droplet rise<br>$\tau_{res} > \tau_{ris,rec}$ | Not fulfilled | Not fulfilled |

It is observed that the with the base case conditions, the dodecane oil does not have enough time to separate which is observed by an oil recovery of only 42% presented in section 4.4.3. When comparing both oils, the oleyl alcohol rises much faster than the dodecane. Which explains the different in oil separation in the integrated FAST bioreactor.

# Chapter 5: Conclusions and Outlook

The fermentative route of phase separating products or toxic products that require in-situ extraction in a 2nd phase such are of increasing interest in the past years. In chapter 1, the use of Fermentation Accelerated by Separation Technology (FAST) as developed by DAB BV, is introduced as a promising technology to achieve low separation costs for phase separating ('oily') products or extractive fermentations for inhibitory or instable products, using an organic solvent. We refer to the second liquid phase as O, implying 'oily product' including organic solvent. If the integrated FAST bioreactor is used, then downstream processing steps can be combined with the fermentation process in one single reactor. The "oily" phase can be recovered while the cells are recycled back to the fermentation. With the integrated, extractive FAST reactor, the organic solvent flow and residence time can be controlled, and product recovery can potentially be increased. This type of reactor will allow a decrease in CAPEX due to increased volumetric productivity, due to a decrease of unit operations and an increase in fermentation efficiency due to cell recycle and solvent extraction. However, limited experimental and modelling studies of FAST reactors have been reported and scale-up such type of reactor and optimization of product and/or oil recovery is still a challenge.

During the development of this thesis, a task-based approach was established to investigate the possible scale up of an integrated reactor encompassing different functionalities. The integrated FAST bioreactor has three main functionalities:

(1) Continuous fermentation with cell recirculation, which is a 3-phase system of gas(G)-liquid(L)-cell (S) interactions,

(2) 4 phase emulsion formation with gas, aqueous phase (L), oil or organic solvent phase (liquid phase O) and cells (S) interactions, and

(3) 3 phase oil recovery with gas (G), aqueous phase (L) and oily or organic solvent (O) interactions.

To simplify the research, each functionality was broken down into two-phase interactions (Figure 1).

In this thesis, oil recovery in the separation compartment was the central focus. Emulsion formation in the fermentation and the effect of cell recycle during fermentation were studied at

lab scale in different projects under the DIRC (Delft Integrated Reactor Column) umbrella project (Heeres, 2016a; Pedraza de la Cuesta, 2019) and not reported here.

The gas-oil interaction was the first mechanism studied. The use of gas bubbles to separate oil from a fermentative emulsion without harming the cells was investigated at lab scale (Chapter 1). From this work, a mechanistic model was developed to predict oil recovery at pilot and commercial scale. Optimal operational conditions could be defined at different conditions. While the scale-up showed to have a positive impact in the oil recovery when using gas bubbles, further studies on emulsion properties and fermentative broth are required to quantify optimal parameters for the scale-up of the integrated reactor.

The subsequent interaction to be studied was L-O interactions at lab scale to promote demulsification. The use of flocculants to destabilize microbial (Pickering) stabilization of emulsions, enhance creaming and oil recovery were assessed by comparing three different demulsification techniques (Chapter 2). Flocculant addition showed to enhance oil recovery without impacting the biomass. However, this depends highly on the timing of addition to the fermentation. Depending on the different demulsification techniques used at commercial scale, flocculation can be tuned to optimize in-situ oil recovery and reduce production process costs.

To better understand the effect of the scale-up in L-O interactions, the integrated FAST bioreactor at pilot scale was modelled (Chapter 3). CFD simulations were used to understand the effect of hydrodynamics in in-situ oil separation in a system with small oil droplets.

During this research several gaps were identified as well as the challenges towards implementation. These findings are summarized on the tables below (Table 1 and Table 2).

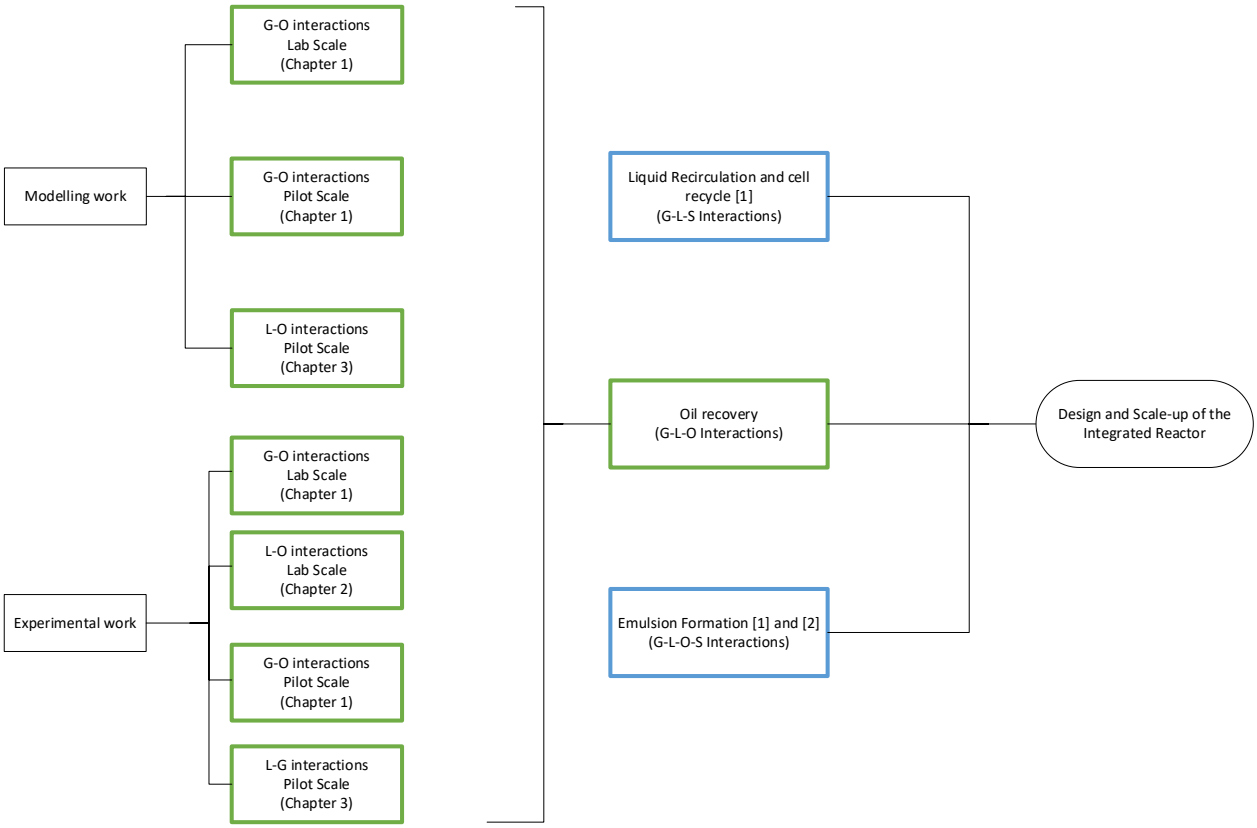


**Figure 1 –** Model based approach *studied in this study* for the design and understanding of the relevant parameters for scale up of the integrated reactor. Where G is gas (air), L is water (medium), O is organic phase (oil) and S is solids (cells). Green squares were addressed in this thesis; Blue squares not addressed in this thesis.

**Table 1 –** Gaps in this research and future work needed to allow for a better understanding of the oil separation in an integrated bioreactor.

| Gaps in this research | Future work |
|---|---|
| **Cell recycle functionality**<br><br>Cell recycle was studied at small scale by combining 2L bioreactor with oil recovery by GEOR (Pedraza-de la Cuesta *et al.*, 2017). However, large scale tests on this functionality were not made under this research.<br>Pilot runs were performed and no visible effects on cell viability were observed (Chapter 4). However, the tests focus on separating the second phase (oil) addition and not necessarily on cell performance. | • Incorporate microbial models to understand if how the cells would behave without supply of oxygen and substrate.<br><br>• Study the effect of emulsion formation throughout the pilot run to understand if cell recycle will increase cell stress leading to an increase in SAC (Surface Active Components) concentration and hampering oil separation |
| **Emulsion formation**<br><br>Several small scales studies were done on emulsion formation throughout the DIRC project (Heeres, 2016b; Pedraza de la Cuesta, 2019). During this research, the basic concepts of emulsion formation were studied: droplet stability due to SACs, Effect of interfacial tension in emulsions; Mimic emulsions were created to represent the conditions of an emulsion during fermentation by measuring droplet sizes, interfacial tension, and creaming rates (chapter 2 and 3). | • Measurement of droplet size, creaming rates, interfacial tensions and level of proteins during a fermentation at small and large scale.<br>• Study of the effect on emulsion formation by applying different conditions (e.g.: stirrer speed, oil fraction, viscosities) at small and pilot scale.<br><br>This study would allow to understand how to tune the conditions for oil separation at different times of the bioreactor run. |
| **Incorporate coalescence models in CFD simulations**<br><br>During this research, a Computational Fluid Dynamic (CFD) model has been developed considering only water and oil. Different coalescence models can be found currently in literature. Droplet and droplet interactions have been of focus in the scientific world. Within this research a coalescence model has been developed describing oil coalescence when a gas bubble is in contact with a region of high oil droplet concentration (chapter 2). | • Incorporate coalescence models into CFD models to better understand how the hydrodynamics of the integrated FAST bioreactor could have an effect in droplet coalescence and oil recovery.<br><br>• Design different separation compartments, by incorporating internal mechanisms (e.g.: trays) or using gas bubbles mechanisms such as GEOR, in a way that would promote droplet coalescence. |

| Gaps in this research | Future work |
|---|---|
| **<u>Scale-Up of the integrated FAST Bioreactor</u>**<br><br>The main goal of this research was to learn and understand how one could scale-up an integrated bioreactor such as the FAST bioreactor. Insights on how to improve oil recovery and an approach to scale-up such integrated reactors were achieved. | • Design a 1 $m^3$ and 100 $m^3$ integrated FAST Bioreactor by combining the insights gather at the small scale (Chapter 2 and 3) and the hydrodynamics model at pilot scale (chapter 4).<br><br>• Model the large-scale reactor with different velocity inlets to understand the effect on the reactor hydrodynamics and optimize oil recovery.<br><br>This design should incorporate less sharp internal edges to prevent swirls of the liquid and an increase of the surface area to volume ratio of the recovery setup. Moreover, velocities must be tuned to allow for creaming of the oil droplets in the recirculation compartment while keeping cell viability. |

**Table 2 -** Challenges during implementation of this research and toward future implementation.

| **Challenges towards implementation** | |
|---|---|
| **CFD simulations with increase geometry and complexity** | • <u>Time of simulations</u>:<br><br>One of the main challenges of this research is the long simulation time of a pilot scale reactor. Simple Euler-Euler CFD simulations, as run throughout this thesis, took approximately 3 months per simulation to run. If one would want to incorporate microbial kinetics and droplet coalescence models, especially on the recirculation compartment, different simulations such as Euler-Lagrange (Haringa *et al.*, 2016) or Latice Boltzman (Van den Akker, 2018)would be required. These simulations are more complex and follow the particle-based interaction instead of treating the fluids as interpenetrating continua and therefore become more local detailed.<br><br>• <u>Complexity of simulations</u>:<br><br>The use of the integrated FAST reactor includes four phase interactions. Literature of three and four phase modeling is scarce indicating the complexity of such simulations. Since CFD accuracy will depend highly on the models employed, an increase in phases will create a challenge on giving accurate simulated results. Therefore, this research followed a task-based approach and was divided into simulation of only two phase systems.<br><br>• <u>Large scale CFD simulations:</u><br><br>By increasing the scale of the reactor in a CFD simulation the time needed for simulations will be increased due to the increase of partial differential equations to be solved. For the pilot scale it is required to split the reactor into compartments and focus only on the recirculation compartment. For a simulation of the whole reactor or a larger scale design a stronger computer or longer times, than the time of this research, would be needed to understand oil separation of a multiphasic mixture at industrial scale. |
| **Gather of experimental data** | • <u>Lab scale:</u><br><br>The main difficulty in gathering data at lab scale is to mimic the emulsion at larger scale in a way that the data gathered is relevant for the research. Throughout this research, different emulsions were created for different studies. Interfacial tension, droplet size, viscosities were studied to be able to use that data in models. Although these mimic emulsions give a lot of insights, they are not an exact mimic of the fermentation conditions. Fermentation emulsions are always changing and are complicated to understand their characteristics. Emulsion viscosity, droplet sizes will change throughout the reactor especially at large scale. |

| Challenges towards implementation | |
|---|---|
| | • <u>Pilot scale:</u><br><br>During this research, pilot experiments were performed. However, these experiments were linked to the experiments of DAB BV. Although, several data were gathered, fermentation conditions could not be changed in name of the research. The conditions where microorganism would survive were a must and recirculation flows could not be changed just for testing. Moreover, droplet sizes are not possible to be studied *in situ* and in the moment that samples are taken the emulsion is changed and is not representative of the real system.<br>This creates challenges to verify simulated or model results. |
| **Upscaling to production scale** | The scale-up of the integrated FAST bioreactor can be studied by CFD simulations, regime analysis or engineering correlations. However, these would only give insights on how the bioreactor would perform. With this research, we gather several insights on how to optimize conditions to maximize oil recovery. Nevertheless, the actual results need to be tested at production scale and this is only possible if the timelines of building the integrated FAST bioreactor fit with the timelines of the research. |

The data collected during this research project are of importance to guide the design and scale-up of integrated bioreactors. Improved design of internals to with less sharp internals would be beneficial to improve the hydrodynamics of the system. Droplet sizes, oil fractions and recirculation flows are critical to the separation of oil from emulsions. The use of methods as GEOR and flocculant addition in large scale integrated FAST bioreactors can optimize oil recovery while allowing cell recirculation.

The integrated FAST bioreactor has shown to be able to separate a second liquid phase of oily products or organic solvent *in situ* while stably maintaining productive fermentation conditions. Based on this proof of principle, its future use and market implementation is being further developed by DAB BV.

## 5.1 References

Van den Akker, H.E. (2018) 'Lattice Boltzmann simulations for multi-scale chemical engineering', *Current Opinion in Chemical Engineering*, 21, pp. 67–75. Available at: https://doi.org/10.1016/j.coche.2018.03.003.

Haringa, C. *et al.* (2016) 'Euler-Lagrange computational fluid dynamics for (bio)reactor scale-down: an analysis of organism life-lines', *Engineering in Life Sciences* [Preprint]. Available at: https://doi.org/10.1002/elsc.201600061.

Heeres, A.S. (2016a) *Integration of Product Recovery in Microbial Advanced Biofuel Production: Overcoming Emulsification Challenges*, *Bioprocess Engineering*.

Heeres, A.S. (2016b) *Integration of Product Recovery in Microbial Advanced Biofuel Production: Overcoming Emulsification Challenges*, *Bioprocess Engineering*.

Pedraza de la Cuesta, S. (2019) *Product Emulsification in multiphase fermentations - the unspoken challenge in microbial production of sesquiterpenes*, *Biotechnology*.

Pedraza-de la Cuesta, S. *et al.* (2017) 'Integration of Gas Enhanced Oil Recovery in multiphasic fermentations for the microbial production of fuels and chemicals', *Chemicals biotechnology Journal* [Preprint].

# Transcript of Records and List of Publications

**Research-related skills**

**Journal Articles**

- Da Costa Basto, RM, Casals, MP, Mudde, RF, van der Wielen, LAM & Cuellar, MC 2019, 'A mechanistic model for oil recovery in a region of high oil droplet concentration from multiphasic fermentations' Chemical Engineering Science: X, 2019, vol. 3, 100033
- R.M. Da Costa Basto, M. Jiménez, R.F. Mudde, L.A.M. van der Wielen, M.C. Cuellar, Impact of flocculant addition in oil recovery from multiphasic fermentations, Food and Bioproducts Processing, Volume 123, 2020, Pages 150-163

**Oral presentations:**

- Hydrodynamics for the Integration of Fermentation and Separation in the Production of Diesel and Jet Biofuels , 11$^{th}$ European Symposium on Biochemical Engineering Science, 11-14 September 2016, Dublin, Ireland
- Hydrodynamics for the Integration of Fermentation and Separation in the Production of Diesel and Jet Biofuels, 10$^{th}$ World Congress of Chemical Engineering, 1-5 October 2017, Barcelona, Spain
- Hydrodynamics for the Integration of Fermentation and Separation in the Production of Diesel and Jet Biofuels, 12$^{th}$ European Symposium on Biochemical Engineering Science, 9-12 September 2018, Lisbon, Portugal

Rita Maria van Haastert Sousa Pires da Costa Basto was born on the 15th December 1986, in the city of Lisbon, Portugal. After she finished her high school education in 2004, she started her Integrated Master Education in Biological Engineering at the Instituto Superior Técnico (IST). In April 2012, she moved to Delft, Netherlands, to do an internship for her master thesis at the DSP department of DSM Food Specialities. The work was done under supervision of Dr. Jeroen Den Hollander (DSM), Dr. Guilherme Ferreira (DSM and IST) and Dr. Luís Fonseca (IST) on Expanded Bed Chromatography to purify enzymes from cells homogenates.

In September 2013, she started a Professional Doctorate program in Bioprocess Engineering at Delft University of Technology (TUDelft). She worked on the conceptual design of an integrated reactor and separator for the microbial production of diesel and jet biofuels at DAB bv with partnership of TUDelft under the supervision of Dr. Maria Cuellar, Dr. Kirsten Steinbusch and Prof. Dr. Ir. L.A.M. van der Wielen.

She started her PhD research in September 2015 at the same group (Bioprocess Engineering) with Prof. Dr. Ir. L.A.M. van der Wielen and Prof. Dr. R. F. Mudde as promotors and Dr. Maria Cuellar as supervisor. During her research, she studied the hydrodynamics for the integration and fermentation in the production of diesel and jetbiofuel, as presented in this thesis.

As of February 2020, she joined Johnson&Johnson at the Jansen Biologics department (The Netherlands) as a manufacturing process specialist. She has grown into Staff manufacturing process specialis and is currently doing an assignment at Therapeutics Development & Supply as Scientist.

LinkedIn: www.linkedin.com/in/rita-costa-basto-28859258/

# Acknowledgements

*Nothing in life is to be feared, it is only to be understood. Now is the time to understand more, so that we may fear less. — Marie Curie*

If years ago, someone would tell me that I would be finishing my PhD, I would not believe it. Yet, it did happen, and I am so happy that I had the opportunity to embrace on this journey. And what a journey it was: During these years, I met so many new people. Unfortunately, I also had to say goodbye to two of the most important people of my life. I got married and moved to a new house. Luckily, I also had the opportunity to bring two lives to this world. I found a new job that I love and met again amazing new people. I visited new countries and experienced new cultures. While I was writing this thesis, we went through a world pandemic where a new world formed around all of us, and everyone had to adapt.

As Paul Janssen said: "*Many people are capable of doing much more than they believe*" but I would not manage without the people below. So, bear with me while I thank to these people.

To my promotor **Luuk**, who has been tireless this past year. Without you, it is undoubtedly I would not manage to finish this thesis. I am truly thankful for all your efforts, guidance, advises but most of all your motivation. Every time we talked, there was no question on your side that I would finish my PhD. That energy gave me the energy to continue. Also, thank you for giving me the opportunity to visit Limerick and the amazing country which is Ireland. You opened your house to me and my family and now we will have unforgettable memories.

Thank you to **Rob**. From the moment of my interview, I had a great admiration for you and your work. Your pragmatic sense and your way of easing even the most complex subjects as fluid dynamics, was inspiring. But most of all, I will always remember a talk we had on my first year of the PhD. I was so nervous for presenting in my first conference and you just talked to me about how is normal to feel nervous and how you feel before you enter in a classroom. The way you shared your experience is something I have taken since then and I have tried to

share with others. Sometimes, the simplest act can have a great impact on someone's life. You had in mine. Thank you.

To **Maria**, and now I need to repeat the words of Susana, "Why did you do the PhD?: The easy answer is Maria. Although much more was involved in this decision, I do not think I would have embraced in this journey if she was not there by my side. Maria, thank you for opening my views, for challenging me and supporting me, thank you for believing (until the end) that I could do this. Thank you for giving me the opportunity to work with bubbles and pink droplets. I learned so much with you but most important I learned that being kind is a weapon and not a weakness. Thank you for giving me a shoulder to cry on when I needed the most and for always having the right words. Thank you for making science practical and fun (and cute with all the cat memes). I enjoyed every minute I had with you as my supervisor.

No research is done alone and for that I want to thank my students: **Lisette, Maria, Eliana, Marc, and Miguel**. I have learned so much with you and this thesis would have not been finished without all your hard work. Thank you for putting so much of you in this research but most important, thank you for showing me that supervising someone can be fun and rewarding.

This research was performed hand in hand with the DAB team. I will start with **Arjan Oudshoorn**, that just by itself should have a paragraph on his own. Thank you for so many meetings to align on ideas, discussions of FAST experiments, scale-up, butanol and discussions about everything. But special thanks for all the supervision on the last chapter and all the Wednesday meetings with children on the background. Thank you to **Kirsten, Fabienne and Rob**, for all their support. It was always great working with you. Thank you for my nice purple Minion at the beginning of the PhD. I looked as purple as him after finishing writing this thesis.

Thank you to my awesome paranymphs: **Debby, Petra, and Joana (from the side line)**. **Debby and Joana**, you were my buddies during the four years but also after the four years. You have been such a great comfort so many times during this PhD. I am so thankful for all the time you spent helping me and motivating me throughout the past years. I am so glad I was able to share this journey with you girls. Thank you for all the fun in the conferences, nights outs and days ins. To **Petra**, thank you for picking up the paranymph role in such short notice and for all your support during the organization. You are truly the sister I never had and always

wanted. Thank you for your constant support and friendship and for making my life so much fun.

To the BPE group, who was the best group I could have while doing this PhD. I thoroughly enjoyed all the moments. To **Kawieta,** which without her help any PhD would be finished. Thank you for all your nice words and constant enthusiasm. To **Adrie and Marcel**, for all your wisdom and guidance. To **Ludo**, for teaching me a bit about squash and for the nice conversations at coffee break. To **Stef, Max and Song**, which were always there to support us in and outside the lab. To what I consider the old guard PhDers: **Arjan Heeres**, you were big shoes to fill in this project, but I am so happy that I was able to still learn so much with you. To **Carlos**, for your great enthusiasm in everything you did. To **Shima**, for your nice comments. To **Susana** for being my big sister in this project and for showing me the world with different perspective. You are a well of creativity. To **Marcelo**, for being my office buddy. Thank you for your lovely taste of Portuguese Pimba. It made the days funnier. To **Silvia**, to bear with all my conversations about weddings and children and much more. To **Victor**, thank you for being my CFD partner in BPE and the person who I could ask anything on the matter. To **Chema**, for being the best companion for Biopro and to visit Copenhagen. And for being yourself at any step of the way. To **Bianca**, for all the support during the PhD and during work. I am happy to be able to work with you again at Janssen. To **Marina** (for me you are part of the old crew), thank you for being my honorary paranymph and for the great moments when you were working at DAB. You were a great office buddy. To **Paco**, for bringing so much joy to the BPE group.

Now to the newer crew: **Mariana, Joan, Tiago, Roxanne, Daphne, Monica, Marijn, Oriol, and Joana**. Thank you for binging so much energy to the BPE group as well as new ideas and experiences. Although short I really enjoyed all the moments we spent together. Specially Karaoke nights.

How lucky am I to have share so many experiences and thoughts with these amazing people?

I also need to thank to the Transport Phenomena group which embrace me as their one. Special thanks to **Cees**, for guiding me when I was setting up my CFDs simulations, to **Alireza** for helping to run the simulation in the TP server (otherwise would have taken even more

time), **Manas** and **Sid** for just brainstorming with me and to **Luis Portela** for so many meetings and guidance “na buoyancy das gotas”.

Many say that we should only thank the people involved directly on the PhD. Well, for me that is not case since the people mentioned above, although not directly related to my PhD, they were key for me to go through and finish this journey.

To my family away from home: To **Cata** for always being there. Even countries apart you were always present. To **Francisca** for being a support and example throughout the first years of my PhD and the following years. To **Rafa**, for always being there for me and sailing the Netherland world with me. And to **Dave**, for being part of this extended family. To the Portuguese crew in the Netherlands: **MJ, Diogo, Sara (and Jan), and Ana**. Thank you for bringing Portugal to the Netherlands and for all the times we cheered for Portugal. A special thanks to **MJ** for this amazing cover. I could not find a better person to do this for me. To **Noa**, for being an example of resilience and strength. Thank you for opening me the doors to the Janssen world.

Thank you also to my Janssen colleagues which always found the time to motivate me in finishing my PhD during lunch hours. To **Eric**, which spent so many Saturdays in the office with me while I finished writing this thesis. Thank you for picking my English Summary and make a better version of it in Dutch. Your support was indispensable for me to finish writing this thesis. To my cool group: **Wesley van Rijn, Corine, Tyron, Aloysius, Jurrit, Martijn, Wesley vd Berg, Floor, Marlies**. Thank you for all the support and making these last year’s so funny. To many more to come.

Ik wil mijn hartelijke dank uitspreken aan mijn lieve familie hier in Nederland: **Sjaak, Elly, Paul, Petra, Tim, Cas, René, Femke, Koen en Bart**. Jullie hebben mij zekerheid en een thuis gegeven in dit, voor mij toch een beetje, onbekende land. Jullie hebben mij met open armen en veel liefde ontvangen en altijd de steun gegeven die ik nodig had. Ik houd van jullie allemaal.

Because an emigrant always has two houses and their heart is always split now is time that I move to Portugal and change to Portuguese (yes, these acknowledgments are a journey by itself).

Às melhores amigas/os que alguém podia imaginar**: Sofia, Regi, Meggy, Pipa, Nuno, Ana, Dani, Miana, Tiago e Inês**. Tenho saudades vossas todos os dias. Obrigada por estarem sempre presentes na minha vida e por todo o apoio que me deram nestes anos. Por me ouvirem e por

estarem sempre à distância de um telefonema e sempre disponíveis para estarmos juntas quando vou a Portugal. Cada um de vocês inspirou-me a acabar este doutoramento.

À minha Família. Como se agradece a alguém que está sempre presente, que sempre estará e que é um porto seguro aconteça o que acontecer. Obrigada **Miguel** por seres o melhor irmão que podia ter, por apoiares-me sempre que precisei de desabafar e por perceberes as minhas frustrações. Obrigada **Té** por todo o apoio e por aturares o meu irmão todos os dias. Obrigada **Luisinho**, por trazer tanta felicidade a esta família. Tenho de agradecer as minhas madrinhas: **Tia Sofia e Tia Mafalda**. Obrigada por estarem sempre presentes na minha vida e por todo o suporte que têm dado.

For my **father** I will write in English because I want the whole world to understand what I am writing. My father is my example and my inspiration. He is the greatest person and professional that I ever met. He is the one guiding me, pushing me to my limit but he is also the one that does not allow me to give up. He makes me thrive for perfection and although I am very far from it, every day I work 120% so I can get a bit closer to it. He is the one who taught me that life is balance. He taught me that life is to be enjoyed and lived. And even in the worse moments, I can have the strength to keep moving forward. When people ask me: who is the person that inspires you the most? I can easily answer: **My father**. Obrigada pai por nunca desistir de mim e por acreditar que eu tinha o que era preciso para acabar o doutoramento, mesmo quando eu não acreditava em mim mesma.

To my **mum**, who is not here physically but I truly believe she is spiritually. She was my biggest lost at the beginning of the PhD, but she is also the brightest guiding star through it. What she was, is in me, and I take her in everything that I do. So, this thesis is much as mine as hers.

And to finalize I need to thank to the most important people of my life. These two girls that came to change my world and colour it a thousand times more.

**Joana e Tessa**, obrigada por serem as melhores filhas que uma mãe podia desejar. Espero que quando crescerem percebam o porquê de a mãe ter estado ausente e espero que esta tese seja uma inspiração para no futuro atingirem tudo o que mais desejam. Vocês sempre foram o melhor do meu dia. You are my love and my life, and I am so proud of my girls.

The last words of this thesis are for my husband, **Marco**. There are no words to describe how much I am thankful for having you by my side. You are the best father (and sometimes mum)

our girls could have. You were always there when I could not be, and this thesis would not have been possible without your constant support. Thank you for never giving up on me, for helping me grow as a person but most of all, thank you for giving me my first dream which allowed me to dream further.